(4)

A TRIDENT SCHOLAR PROJECT REPORT

NO. 151

THE EFFECTS OF TRANSOM GEOMETRY ON THE RESISTANCE OF LARGE SURFACE COMBATANTS

UNITED STATES NAVAL ACADEMY
ANNAPOLIS, MARYLAND

UNCLASSIFIED

SECURITY CLASSIFICATION OF THIS PAGE (When Data Entered)

REPORT DOCUMENTATION PAGE

READ INSTRUCTIONS BEFORE COMPLETING FORM

1. REPORT NUMBER: U.S.N.A. - TSPR; no. 151 (1988)

2. GOVT ACCESSION NO.

3. RECIPIENT'S CATALOG NUMBER

4. TITLE (and Subtitle): THE EFFECTS OF TRANSOM GEOMETRY ON THE RESISTANCE OF LARGE SURFACE COMBATANTS.

5. TYPE OF REPORT & PERIOD COVERED: Final 1987/88

6. PERFORMING ORG. REPORT NUMBER

7. AUTHOR(s): Thomas K. Kiss

8. CONTRACT OR GRANT NUMBER(s)

9. PERFORMING ORGANIZATION NAME AND ADDRESS: United States Naval Academy, Annapolis.

10. PROGRAM ELEMENT, PROJECT, TASK AREA & WORK UNIT NUMBERS

11. CONTROLLING OFFICE NAME AND ADDRESS: United States Naval Academy, Annapolis.

12. REPORT DATE: 10 June 1988

13. NUMBER OF PAGES: 93

14. MONITORING AGENCY NAME & ADDRESS (if different from Controlling Office)

15. SECURITY CLASS. (of this report)

15a. DECLASSIFICATION/DOWNGRADING SCHEDULE

16. DISTRIBUTION STATEMENT (of this Report)

This document has been approved for public release; its distribution is UNLIMITED.

17. DISTRIBUTION STATEMENT (of the abstract entered in Block 20, if different from Report)

18. SUPPLEMENTARY NOTES

Accepted by the U.S. Trident Scholar Committee.

19. KEY WORDS (Continue on reverse side if necessary and identify by block number)

Ship resistance
Hulls (Naval architecture)
Hydrodynamics

20. ABSTRACT (Continue on reverse side if necessary and identify by block number)

This report presents the results of an investigation into the calm water resistance characteristics of a series of transom sterned ships. The research was conducted as a Trident Scholar project at the U.S. Naval Academy. Five transom shapes and their corresponding after-bodies were designed to examine the effect of draft and beam at the transom on ship resistance. There were two draft and two beam variations from a common baseline hull. The forebody was →

(OVER)

DD FORM 1 JAN 73 1473 EDITION OF 1 NOV 68 IS OBSOLETE

S/N 0102-LF-014-6601

UNCLASSIFIED

SECURITY CLASSIFICATION OF THIS PAGE (When Data Entered)

held constant for all five designs. Each of the variations represented typical surface combatants of the frigate/destroyer family. Models were built of each hull and still water resistance tests were run in the 380 foot towing tank at the U. S. Naval Academy's Hydromechanics Laboratory. Analytical studies of each hull were performed using existing potential flow code algorithms.

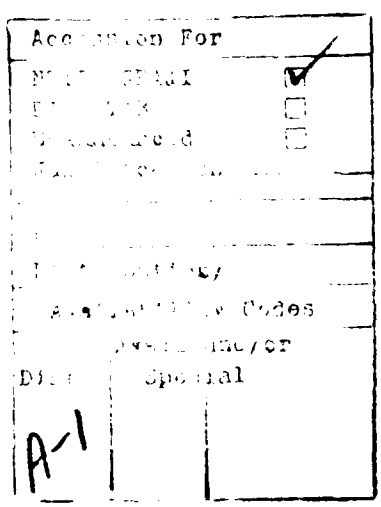

U.S.N.A. - Trident Scholar project report; no. 151 (1988)

THE EFFECTS OF TRANSOM GEOMETRY ON THE RESISTANCE OF LARGE SURFACE COMBATANTS

A Trident Scholar Project Report

by

Midshipman Thomas K. Kiss
Class of 1988

U. S. Naval Academy

Annapolis, Maryland

Roger H. Compton

Advisor: Professor Roger H. Compton
Naval Systems Engineering Dept.

Accepted for Trident Scholar Committee

Dennis F. Hasson
Chairperson

10 June 1988
Date

TABLE OF CONTENTS

LIST OF TABLES

LIST OF FIGURES

LIST OF SYMBOLS

A_T IMMERSED TRANSOM AREA (FT^2)

A_{WP} WATERPLANE AREA AT DESIGN WATERLINE (FT^2)

A_X MAXIMUM SECTION AREA (FT^2)

AP AFTER PERPENDICULAR

B_T TRANSOM BEAM AT DESIGN WATERLINE (FT)

B_X BEAM AT MAXIMUM SECTION AREA (FT)

C_B BLOCK COEFFICIENT, $\nabla/(L \times B_X \times T_X)$

C_F FRICTIONAL RESISTANCE COEFFICIENT BASED ON 1957 ITTC CORRELATION LINE, $0.075/(LOG_{10}(R_N)-2)^2$

C_{FORM} FORM DRAG COEFFICIENT

C_R RESIDUARY RESISTANCE COEFFICIENT, C_T-C_F

C_{Tm} MODEL TOTAL RESISTANCE COEFFICIENT, $R_T/(0.5x\rho xVm^2xS_m)$

C_{VP} VERTICAL PRISMATIC COEFFICIENT, $\nabla/(A_{WP} \times T_X)$

C_W WAVE RESISTANCE COEFFICIENT, C_R-C_{FORM}

C_{WP} WATERPLANE AREA COEFFICIENT, $A_{WP}/(L_{pp} \times B_X)$

C_X MAXIMUM SECTION COEFFICIENT, $A_X/(T_X \times B_X)$

DWL DESIGN WATERLINE

EHP EFFECTIVE HORSEPOWER

FP FORWARD PERPENDICULAR

F_N FROUDE NUMBER, $V/(g \times L_{WL})^{0.5}$

g ACCELERATION DUE TO GRAVITY (FT/S^2)

i_R RUN ANGLE, (DEG)

LCB	LONGITUDINAL DISTANCE FROM AMIDSHIPS TO THE CENTER OF BUOYANCY (FT)
LCF	LONGITUDINAL DISTANCE FROM AMIDSHIPS TO THE CENTER OF FLOTATION (FT)
L_{PP}	LENGTH BETWEEN PERPENDICULARS (FT)
R_F	FRICTIONAL RESISTANCE (LBS)
R_N	REYNOLDS NUMBER, $(V \times L_{WL})/\nu$
R_R	RESIDUARY RESISTANCE (LBS)
R_T	TOTAL RESISTANCE (LBS)
R_W	WAVEMAKING RESISTANCE (LBS)
S	WETTED SURFACE AREA (FT^2)
T_T	DRAFT AT TRANSOM (FT)
T_X	DRAFT AT MAXIMUM SECTION (FT)
V_m	MODEL VELOCITY (FT/S)
V_S	SHIP VELOCITY (KNOTS)
$Z_{\otimes}$	SINKAGE AT AMIDSHIPS (+ UP)
(S)	FROUDE WETTED SURFACE COEFFICIENT, $S/\nabla^{2/3}$
β_T	TRANSOM DEADRISE ANGLE AT CENTERLINE (DEG)
∇	DISPLACED VOLUME (FT^3)
Δ	DISPLACEMENT (LT)
Δ_L	DISPLACEMENT-LENGTH RATIO, $\Delta/(L^{PP}/100)^3$
τ	RUNNING TRIM ANGLE (DEG) (+ BOW UP)
ρ	DENSITY OF WATER (SLUGS/FT^3)
ν	KINEMATIC VISCOSITY (FT^2/SEC)

ABSTRACT

This report presents the results of an investigation into the calm water resistance characteristics of a series of transom sterned ships. The research was conducted as a Trident Scholar project at the U.S. Naval Academy. Five transom shapes and their corresponding afterbodies were designed to examine the effect of draft and beam at the transom on ship resistance. There were two draft and two beam variations from a common baseline hull. The forebody was held constant for all five designs. Each of the variations represented typical surface combatants of the frigate/destroyer family. Models were built of each hull and still water resistance tests were run in the 380 foot towing tank at the U.S. Naval Academy's Hydromechanics Laboratory. Analytical studies of each hull were performed using existing potential flow code algorithms.

INTRODUCTION

The transom stern is a feature found on many U.S. Navy surface combatants including all active frigates, destroyers, and cruisers. Transom sterns are characterized by an abrupt, near vertical ending to the ship's hull. Figure 1 is a sketch of a typical transom stern and another common stern type, the cruiser stern. The cruiser stern is commonly found on lower speed commercial ships and large sail powered pleasure craft. The transom stern offers several advantages over the cruiser stern for surface combatants. It facilitates internal arrangements and, because of its simple shape, is easier and cheaper to fabricate. More importantly for naval ships, it generates less resistance at high speeds than would a cruiser stern thus allowing surface combatants to attain such speeds with lower propulsive power. The reduced high speed resistance of a transom sterned ship is accompanied by a reduction in the amount of trim by the stern relative to a cruiser sterned hull. However, naval ships generally cruise for long periods of time at low to moderate speeds where there is a resistance penalty caused by the transom. The chaotic turbulent eddies which form as the fluid flows past the

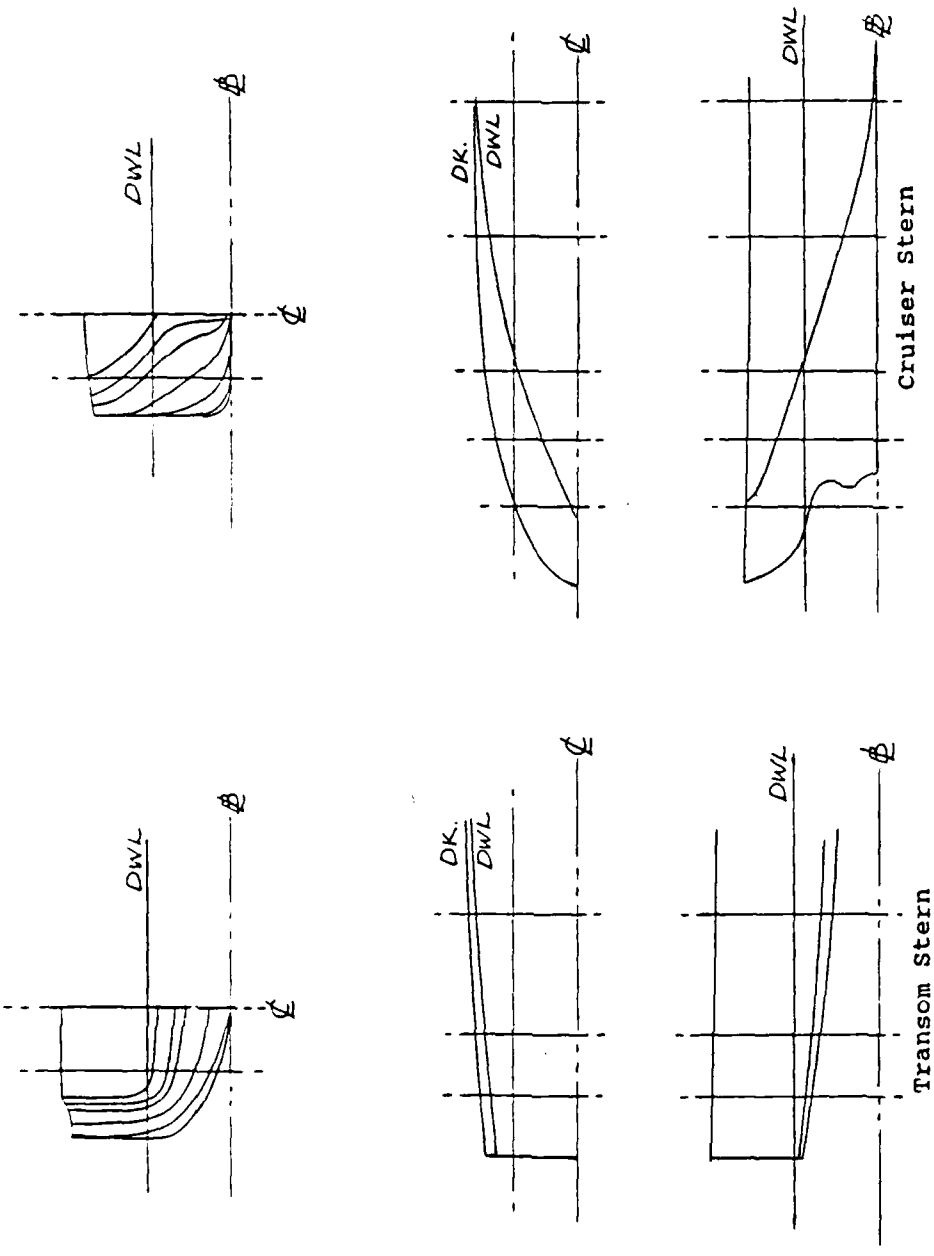

FIGURE 1: Schematic Views of Transom and Cruiser Sterns

sharp corner of the transom (i.e., flow separation) are physical manifestations of increased resistance relative to the smooth flow off a cruiser stern. It is of interest to the U.S. Navy to develop a transom type which minimizes the resistance penalty at cruising speeds (typically 14-18 knots) while still providing the desirable lower resistance characteristics at high speeds.

There has been little systematic research concerning the effect of various physical transom characteristics on ship resistance. There are several reasons for this. First, designing a systematic series of ships in order to isolate the effects of any single geometric change, transom shape in this case, is difficult. In addition, the resulting differences in model resistance for such a systematic series have been too small to be measured accurately by available dynamometry and data acquisition systems. It must also be recognized that systematic series design and testing is tedious and expensive.

Earlier investigations of the effects of transom sterns on ship resistance have resulted in a few published guidelines for the naval architect. In 1932, a report from the Experimental Model Basin (EMB)[1] described the effect of transom area and buttock line shape on resistance. It was suggested that immersed transom area

be increased for higher operating speeds and that hollow buttock lines were beneficial from a resistance standpoint. St. Denis, in a short article proposed similar guidelines. A study, conducted by Gillmer[2] in the Isherwood Hall towing tank at the U.S. Naval Academy, was undertaken to evaluate the effects of planform shapes of the transom on ship resistance using small (about five feet long) models. This report, in which relatively low speeds were studied, recommended that transom planform shape be rounded or tapered, not cut off in a straight line transversely. In his classic book, Saunders[3] summarized the earlier work regarding transom sterns and recommended that shallow transom draft resulted in lower high speed resistance and that transom ventilation speed could be computed on the basis of a Froude Number in which transom draft was the characteristic length. The most recent studies into the problem have been performed at the David Taylor Research Center (DTRC) by Wilson, Thomason, O'Dea, Jenkins, and Nagle.[4,5]

Research conducted at the U.S. Naval Academy into the comparative naval architecture of U.S. and Soviet frigates by Kinports[6], while concentrating on the seakeeping performance of current frigates, did baseline studies of the comparative still water powering of two frigates. The U.S. frigate had a conventional, relatively

narrow transom, while the Soviet stern was more beamy from amidships to the transom. The wider beamed transom form exhibited up to 5% higher resistance in the medium speed range, but about 3% lower resistance at the high end of the speed range.

Ship powering estimates for new ship designs are generally determined by several methods. During the initial design phase, ship resistance can be predicted from parametric data for existing ships of the same type. Overall hull form parameters can be used in conjunction with standard systematic series methods[6] to estimate propulsive power requirements. In the later stages of design, model testing of the exact hull shape is conducted in order to predict more accurately a specific ship's resistance. Theoretical methods for estimating ship resistance have been proposed over the years but until the advent of fast, modern computers in recent years, none of these methods were tractable. Moreover, the accuracy of the theoretical methods, as applied to the ship powering problem, remains unproven. Various mathematical approaches to solving the theoretical problem at hand have been transformed into computer algorithms called "flow codes".

Presently, there are many flow codes which purport to predict ship resistance. These flow codes employ classical inviscid, potential flow theory to calculate the energy in the wave train generated by a moving surface ship.[7] These programs run on both mini-computers and the latest super computers. At present, the best of these flow codes seems able to predict resistance trends satisfactorily for early stage design estimating purposes. It was unclear whether they were sensitive enough to discern resistance differences between small local transom shape variations. If such analytical methods can be shown to predict resistance trends accurately, they will become a increasingly valuable design tool. They could then be used to optimize hull form, at least from the standpoint of minimizing calm water resistance, quickly and efficiently before experimental testing.

The analytical work of Wilson and Thomason[5] employs one such computer algorithm - namely XYZ Free Surface (XYZFS), developed at David Taylor Research Center (DTRC) by Dawson[8]. Wilson and Thomason, assuming adequate sensitivity, used XYZFS to examine the effects of transom geometry on ship resistance. With extremely limited experimental verification, they proposed a design guide for transom stern geometry based on their flow code

analyses. Their analyses indicated that transom draft, T_T, was the most significant variable in determining calm water resistance effects attributable to the transom. Second in importance was transom beam, B_T.

The primary purpose of the present study is to quantify the effects of transom geometry on ship resistance in calm water by experimental means. A systematic series of transom shapes were designed, fabricated, and tested over a speed range corresponding to Froude numbers of 0.21 to 0.62. Because ships tend to grow heavier throughout their service life, it was decided to test the series at a second, heavier displacement. Consequently, after the design displacement for each stern was studied, the model's displacement was increased 20 percent and the test series rerun.

It is the secondary purpose of the present study to compare results of experimental testing with analytical methods such as Wilson's.

DESIGN RATIONALE

The design rationale for the systematic series was to consider realistic hull shapes and to isolate, insofar as is possible, the effects of specific local hull geometry variations on still water resistance. Based on Wilson and Thomason's report[5], transom draft and transom beam were selected as the geometric variables of primary importance. The five hulls were designed to have characteristics typical of current frigate/destroyer design practice. Table I displays a list of geometric coefficients commonly used to describe a ship's hull form and a range of values for each coefficient representing surface combatants. The selected transom geometric features of draft, beam, and sectional area were nondimensionalized using the corresponding features of the maximum hull cross section. A baseline transom was designed to approximate the average value for each of these ratios. Figure 2 is a body plan with bow and stern profiles for the baseline hull. Transom area was held constant for all five transoms in order to isolate the effects of transom beam and draft. Two transoms were designed with different waterline beams to cover the

Table I: Range of Typical Destroyer Hull Parameters

	MIN		AVG		MAX
L_{DWL}/B_X	6.76	<	8.44	<	9.64
B_X/T_X	2.816	<	3.138	<	3.466
L_{DWL}/T_X	20.26	<	26.53	<	32.49
∇	45.60	<	71.18	<	112.36
C_B	0.456	<	0.504	<	0.573
C_X	0.784	<	0.841	<	0.994
C_P	0.576	<	0.601	<	0.661
C_{WP}	0.690	<	0.747	<	0.798
(S)	6.586	<	7.428	<	8.105
B_T/B_X	0.219	<	0.444	<	0.735
T_T/T_X	0.0725	<	0.122	<	0.158
A_T/A_X	0.020	<	0.052	<	0.090
β_T	0.0	<	7.9	<	18.0

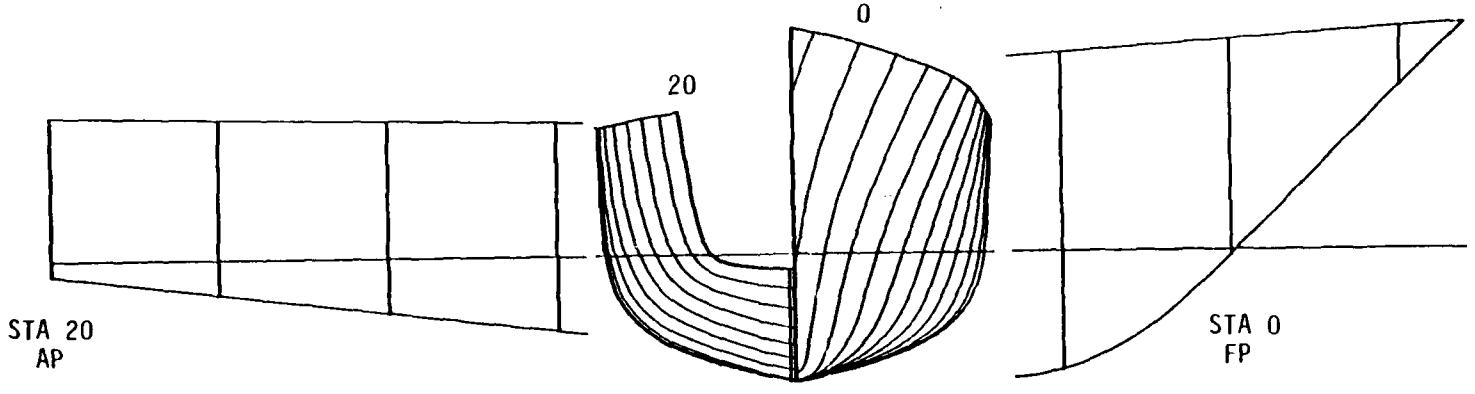

FIGURE 2: Abbreviated Lines of the Baseline Hull

range of beam ratios while maintaining the draft of the baseline transom. Similarly, the remaining two transoms were designed with varying drafts to cover the range of draft ratios while maintaining the baseline waterline beam. Figure 3 shows, in matrix form, the scope of the geometric variations studied for this project.

The effects of changing transom shape can be seen for some distance forward of the transom. It was decided to fair the entire portion of each hull from its point of maximum sectional area to the transom using currently accepted naval architectural practice. All hull forms were faired into the same maximum cross section shape. The afterbodies were all of the same length and were terminated vertically at the after perpendicular. The shape of each afterbody was designed to provide a smooth and logical transition from the common maximum section to each of the five transom shapes. Displacement, length, maximum waterline beam, draft, and longitudinal prismatic coefficient were held constant for the series and changes in other geometrical characteristics were minimized.

Figure 4 shows the common maximum cross section and the systematically varied transom cross sections for the five hulls in the series. The draft variations are drawn on the left and the beam variations are drawn on the right. Figure 5 shows the sectional area curves for the

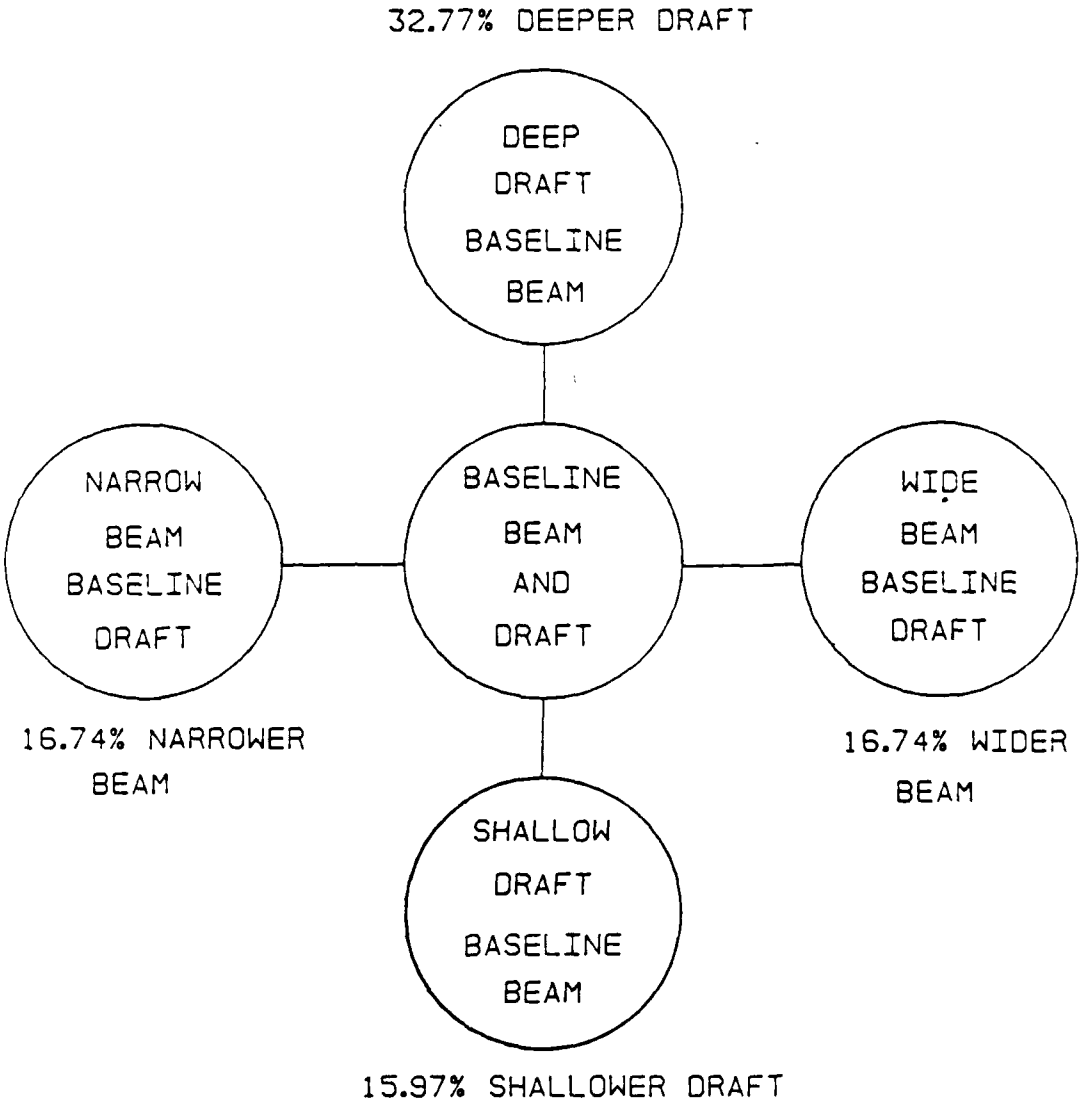

FIGURE 3: Transom Geometry Matrix

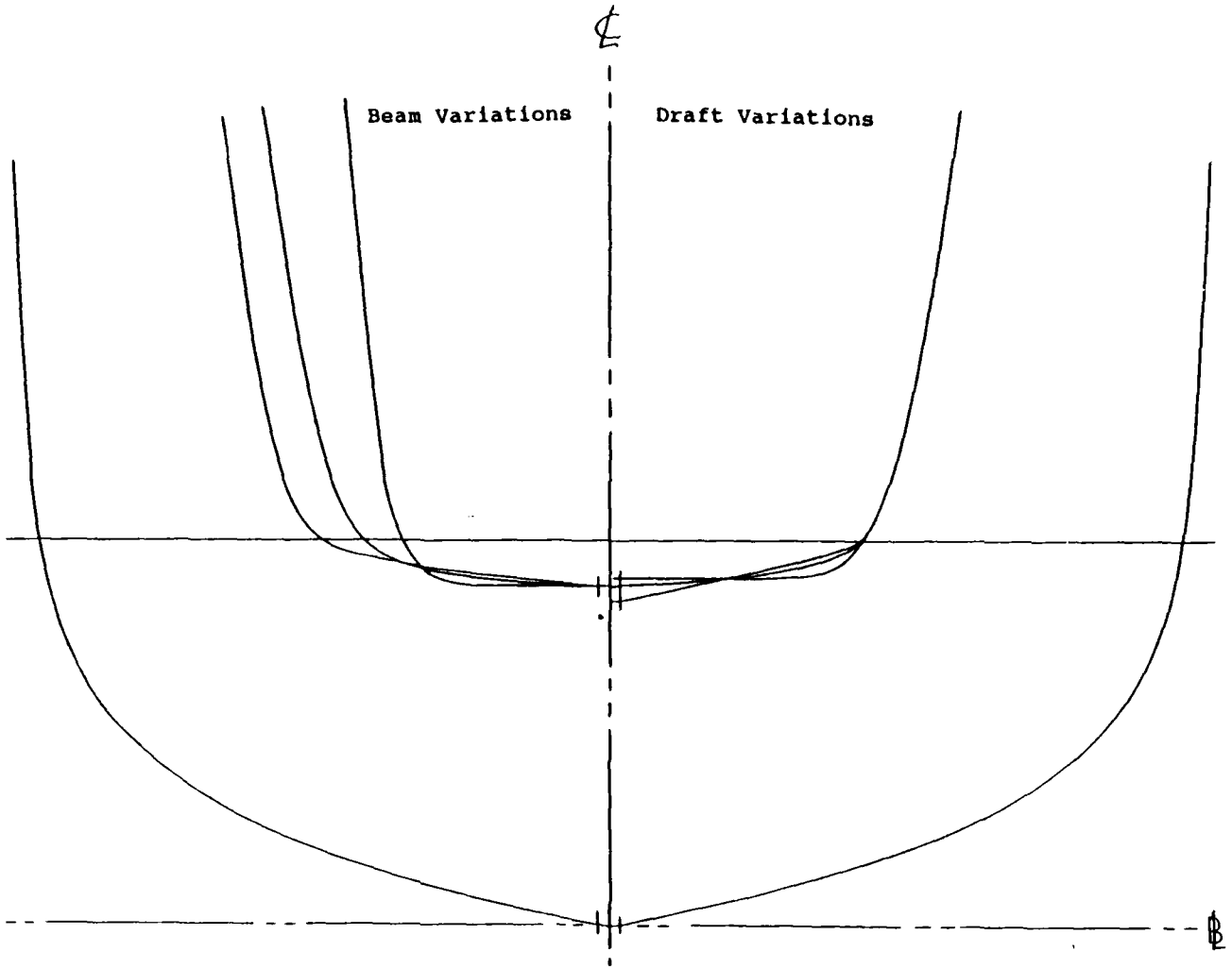

FIGURE 4: Transom Shape Variation for the Series

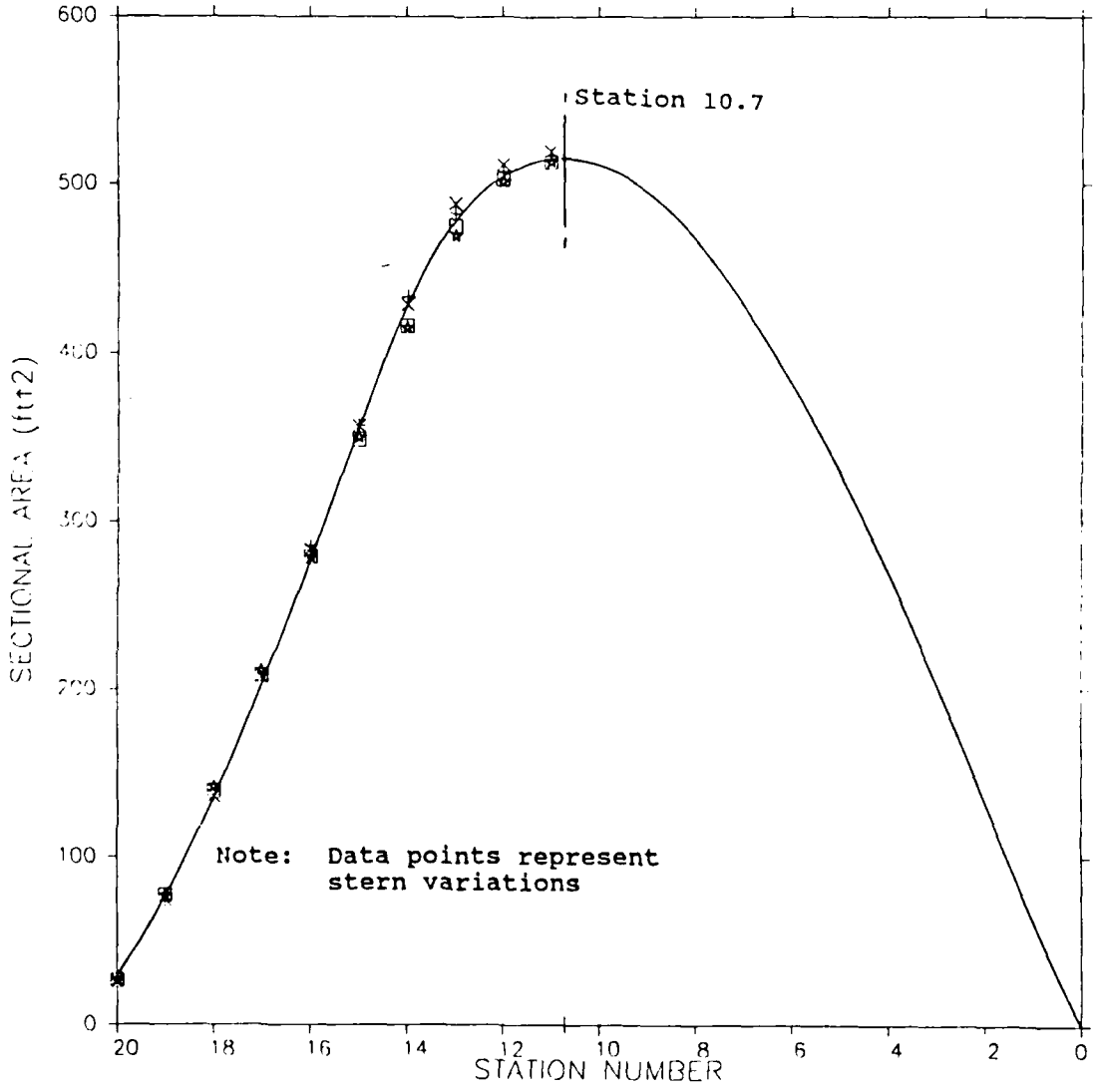

FIGURE 5: Sectional Area Curves for the Series

five hulls. It should be noted that the sectional areas for all variations are identical from the bow to the ship's maximum section where the different afterbodies were attached. The area under each of the curves is constant and represents the displaced volume, ∇, of each hull.

The forebody used for each hull was that of a modified FFG-7 class frigate. The modification was above the waterline forward of station 5 (of 20) and resulted in increased flare and stem profile rake relative to the as-built FFG-7. This hull was chosen because it represents current U.S. frigate design practice, is not fitted with a large bow mounted sonar dome, and because a model of convenient size was readily available. The model was tested at a displacement slightly heavier than that of the actual FFG-7 in order to make the ship more representative of general surface combatants. The model was cut transversely at the maximum section (station 10.7 of 20) and each afterbody was attached to the FFG-7 forebody. Table II shows the values for each of the coefficients and ratios presented in Table I for each of the five systematic hull forms at their design displacement. Table III shows these values for the five hull forms at a displacement 20% greater than the design condition.

Table II: Design Displacement Hull Parameters

CONSTANT PARAMETERS

L_{PP}/B_X= 8.95 B_X/T_X=3.04 L_{PP}/T_X= 27.2

$L^2/(B_X*T_X)$= 243.44 C_X= 0.755

INDIVIDUAL HULL PARAMETERS

	BASELINE	DEEP DRAFT	SHALLOW DRAFT	WIDE BEAM	NARROW BEAM
Δ	53.78	53.99	53.56	53.58	53.91
C_B	0.458	0.460	0.456	0.457	0.459
C_P	0.607	0.610	0.605	0.605	0.609
C_{VP}	0.640	0.640	0.638	0.633	0.645
C_{WP}	0.716	0.719	0.715	0.721	0.712
S	7.267	7.259	7.311	7.309	7.261
B_T/B_X	0.430	0.429	0.432	0.502	0.358
T_T/T_X	0.119	0.158	0.100	0.119	0.119
A_T/A_X	0.051	0.052	0.051	0.051	0.052

Table III: Design Displacement+20% Hull Parameters

INDIVIDUAL HULL PARAMETERS

	BASELINE	DEEP DRAFT	SHALLOW DRAFT	WIDE BEAM	NARROW BEAM
∇	53.78	53.99	53.56	53.58	53.91
C_B	0.458	0.460	0.456	0.457	0.459
C_P	0.607	0.610	0.605	0.605	0.609
C_{VP}	0.640	0.640	0.638	0.633	0.645
C_{WP}	0.716	0.719	0.715	0.721	0.712
S	7.267	7.259	7.311	7.309	7.261
B_T/B_X	0.430	0.429	0.432	0.502	0.358
T_T/T_X	0.119	0.158	0.100	0.119	0.119
A_T/A_X	0.110	0.111	0.109	0.121	0.099

MODEL DESIGN AND CONSTRUCTION

The five stern sections were built by the Technical Support Department of the U.S. Naval Academy over a period extending from June of 1987 to February of 1988. Each transom was designed by hand to the required dimensions. The transoms were then digitized using the FASTSHIP computer program (resident on workstations in the Hydromechanics Laboratory). FASTSHIP was used to complete the design of each stern. First, lines were faired to match the digitized transom. After each transom was faired, the rest of each stern section was faired into the transom and the common forebody. An iterative method was used to ensure that the desired geometrical properties of each hull were held constant. The hydrostatic properties of each hull were calculated using the U.S. Navy 's Ship Hull Characteristics Program (SHCP). Agreement on displacement was within 0.4 percent while agreement on wetted surface was within 0.35 percent. These numbers were independently verified by FASTSHIP output.

All of the sterns were built using high density, closed cell foam. Foam was chosen over wood because it is easier to shape and is unaffected by water intrusion. The shaped foam afterbody was coated with epoxy and a thin layer of glass cloth before final fairing and fitting to the common forebody. The first two models were laid up and faired entirely by hand using waterline lifts above the design waterline and buttock lifts below it. Figures 6 and 7 are photographs of the hand built sections in various stages of construction. An important communication link was developed in the Fall of 1987 by the staff of the Laboratory to send numerical data representing each hull form directly from the FASTSHIP program to the numerically controlled (NC) milling machine in the model shop. Using this development, the last three stern sections were laid up as were the first two, milled on the NC machine, and then finally hand faired. Figure 8 is a photograph of a model being cut on the NC milling machine. Figure 9 is a photograph of a stern section after being cut along quarter inch spaced waterlines on the NC milling machine. A related program was developed to define and cut station templates to aid in the final manual fairing process. By using the NC mill to rough cut the model, the fabrication of a stern was reduced from 35 days to 21 days.

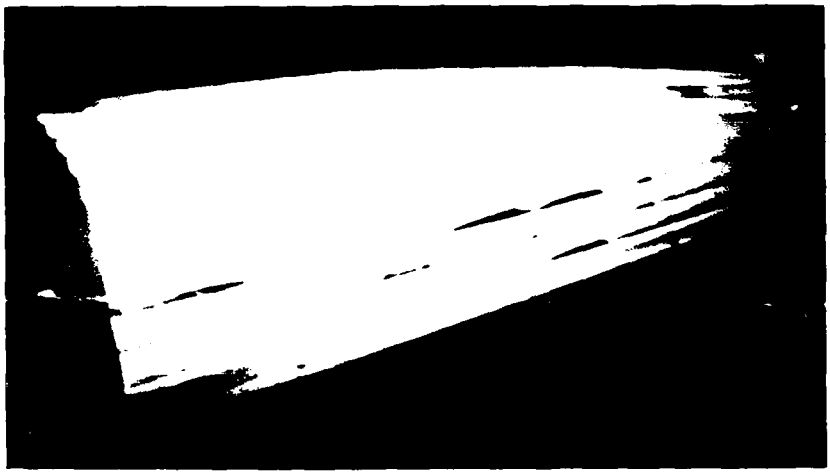

FIGURE 6: Foam Lifts Glued Together to Form Rough Stern Shape

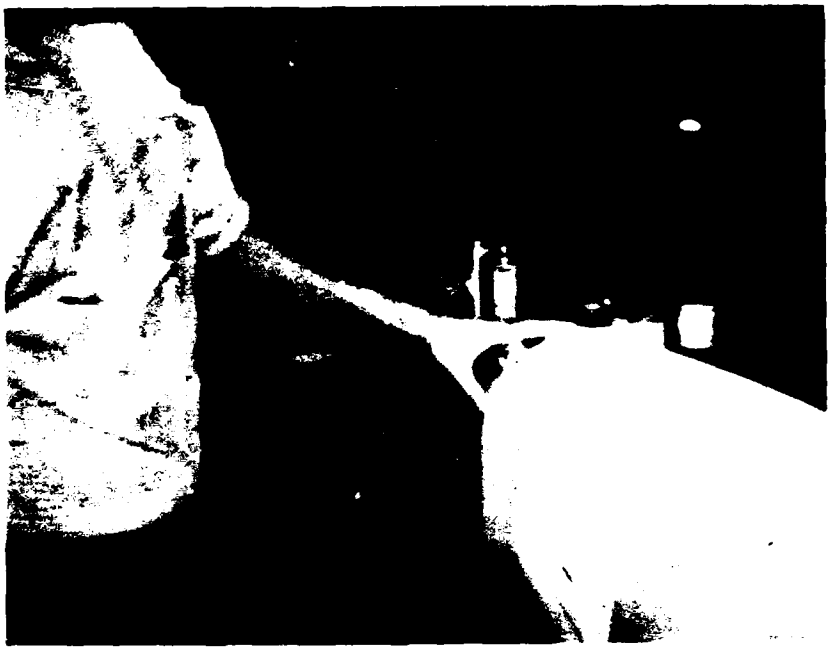

FIGURE 7: Final Model Shaping Using Station Templates

FIGURE 8: Model Being Cut Along Waterlines on the Numerically Controlled Milling Machine

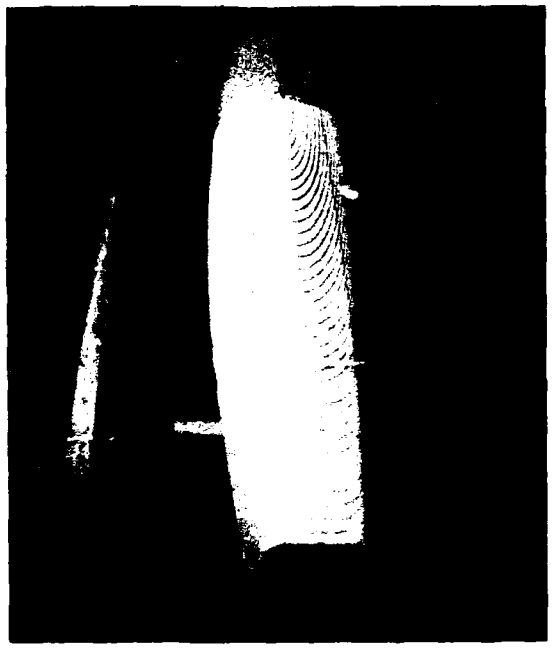

FIGURE 9: Milled Model Stern Awaiting Final Hand Fairing (as in Figure 7)

After final shaping, the individual sterns were aligned and affixed to the common forebody. The midhull joint was filled with body putty and faired. One coat of primer and one coat of enamel were sprayed over the model. The model was wet sanded after each coat to produce a smooth, wetting surface. Each model was gridded across the transom and for a distance of one foot forward of the transom to facilitate visualization of the local free surface flow in the vicinity of the transom.

EXPERIMENTAL TEST PROGRAM

All testing was conducted in the 380 foot towing tank at the Naval Academy Hydromechanics Laboratory. The International Towing Tank Conference (ITTC) description of this tank is shown as Figure 10. The same model dynamometry and signal conditioning equipment were used for all tests in order to achieve the highest possible consistency of acquired data. The dynamometer restrained the model in surge, roll, sway, and yaw. The fresh water depth for all tests was sixteen feet. Blockage was not considered a problem since the blockage area ratio was less than 0.0012. The model was towed from amidships for all test runs. Figure 11 is a photograph of the testing rig with a model attached.

INTERNATIONAL TOWING TANK CONFERENCE CATALOGUE OF FACILITIES

TOWING TANKS, SEAKEEPING AND MANOEUVRING BASINS

U. S. NAVAL ACADEMY HYDROMECHANICS LABORATORY — U.S.A.
ANNAPOLIS, MARYLAND 21402
TELEPHONE: (301) 267-3361

128m HIGH PERFORMANCE TOWING TANK (1979)

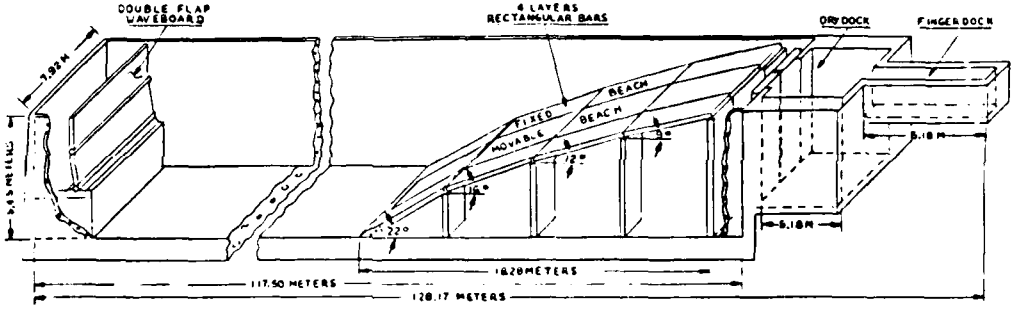

380 FOOT TANK AND WAVEMAKER

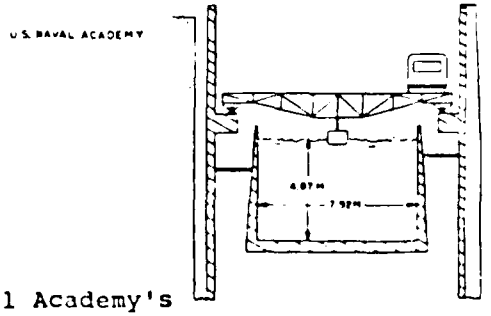

FIGURE 10: ITTC Description of the U.S. Naval Academy's 380 Foot Towing Tank

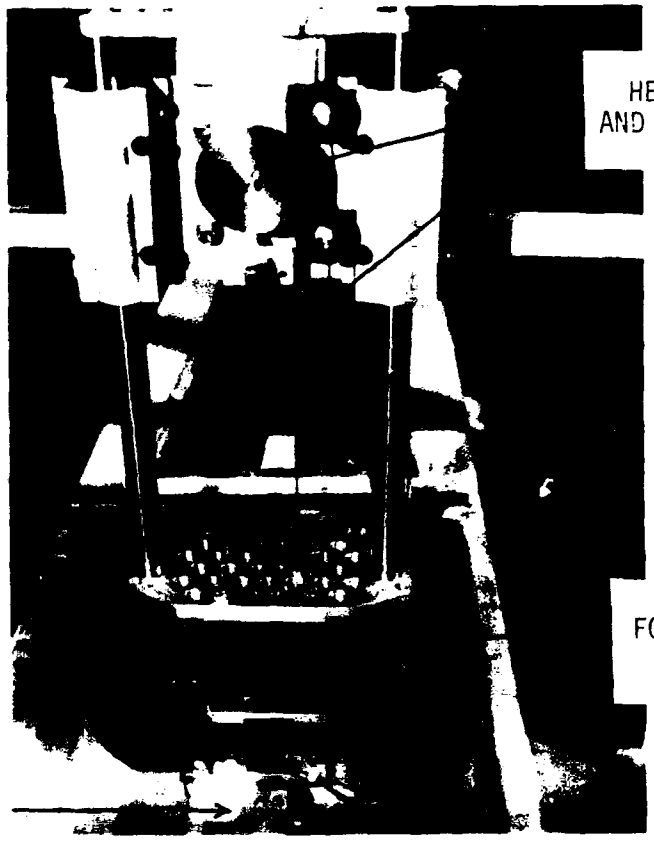

FIGURE 11: Towing Dynamometer Mounted in the Model

Turbulent flow stimulation was provided by studs placed parallel to, and aft of, the stem at a distance of 5% of the model length (L_{pp}). The studs were right circular cylinders having a diameter of 0.1 inches, a height of 0.1 inch, spaced every one inch around the model girth. Turbulence stimulation is necessary because the fluid flow about a ship's hull is turbulent. To achieve valid experimental results, the model must also operate in turbulent flow. Due to the much lower Reynold's numbers for models, the smoothness of the model surface, and the stillness of the water in the towing tank, some form of turbulence stimulator is needed to induce turbulent flow. The Reynold's number range for each model tested was from 3.91×10^6 to 1.17×10^7.

The models were tested in still water over a range of speeds from 4 to 12 ft/s at 0.5 ft/s intervals. These speeds corresponded to ship speeds ranging from 10 to 45 knots for a 408 foot long ship. Repeat points were run at 4.5, 8.0, and 11.5 ft/s for each model. C_{Tm} measurements differing more than one percent were cause to check the force block calibration and the setting of the signal conditioning unit. A wait time between test runs was necessary to allow the waves created by the previous run

to damp out. For consistency, runs were made every two minutes for low speed runs (less than 8.0 ft/s) and every three minutes for higher speed runs.

Model speed, running trim angle, sinkage at amidships, and resistance were recorded for each run. Running trim angle, sinkage, and resistance were measured with an inclinometer, rotary potentiometer, and variable reluctance force block (rated to 25 lbs.) respectively. All three transducers were calibrated before each test series and rezeroed between test runs as required. The resistance and sinkage transducers were calibrated in place for all tests to achieve consistently accurate results throughout the test program. All transducers calibrated linearly through their effective range.

Tests were conducted at two displacements for each hull. The hull was tested at the design displacement and with a displacement 20% greater than designed. The models were all ballasted in the same manner. The SHCP output (zero trim condition) was used to determine the proper displacements and wetted surface areas. The displacements were corrected for the towing tank water temperature at the time of testing. The models were ballasted to achieve

zero trim and heel. Video recordings were made of each run to observe characteristics of the fluid flow about the transom of each hull as a function of speed.

PRESENTATION OF EXPERIMENTAL MODEL DATA

A total of ten identical tests were run (5 hulls at 2 displacements each). The model data acquired for each test were plotted and faired by hand for all test cases. The curve faired through a given set of data represented the author's interpretation of the discrete data points. Plots of all measured data for all tests are included as Appendix A. Resistance was presented in the form of a nondimensional coefficient, C_{TM}. This coefficient is defined as:

$$C_{TM} = R_{TM}/(0.5 \times \rho \times Vm^2 \times S)$$

The measured running trim angle and rise/sinkage at amidships were combined to form the rise/sinkage at the forward and after perpendiculars using

$$\text{FP Rise} = Z_{\text{XX}} + 0.5*L_{pp}*\text{SIN}(\tau)$$

$$\text{AP Rise} = Z_{\text{XX}} - 0.5*L_{pp}*\text{SIN}(\tau)$$

As an example of the results of single test, Figures 12 and 13 are presented. Measured discrete data are shown by plot symbols, while the curves represent the continuous trends against speed for the indicated

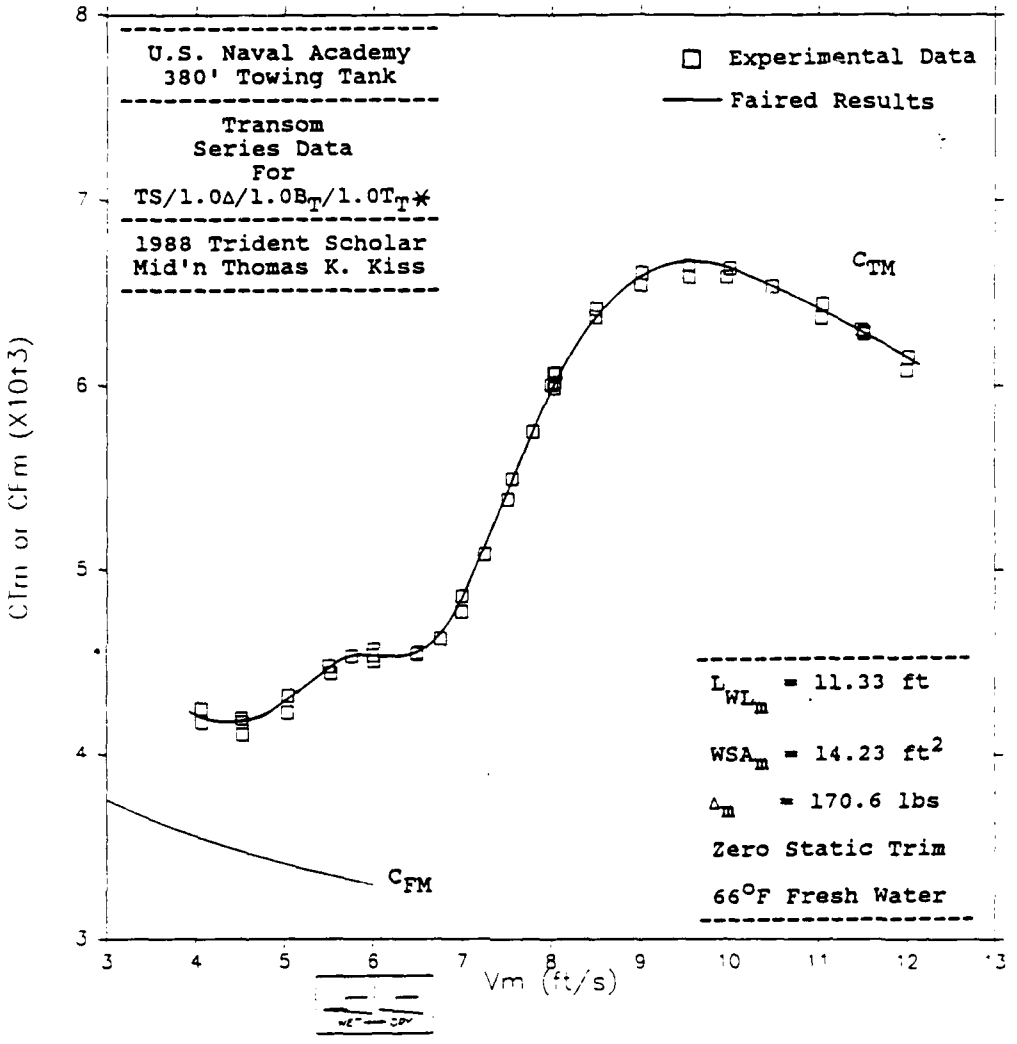

FIGURE 12: Example Plot of Measured Resistance Data with Faired Curve

* MODEL DESIGNATION

TS/1.0Δ/1.0B_T/1.0T_T

- TS: transom series
- 1.0Δ: displacement w/r design
- 1.0B_T: beam w/r baseline
- 1.0T_T: draft w/r design

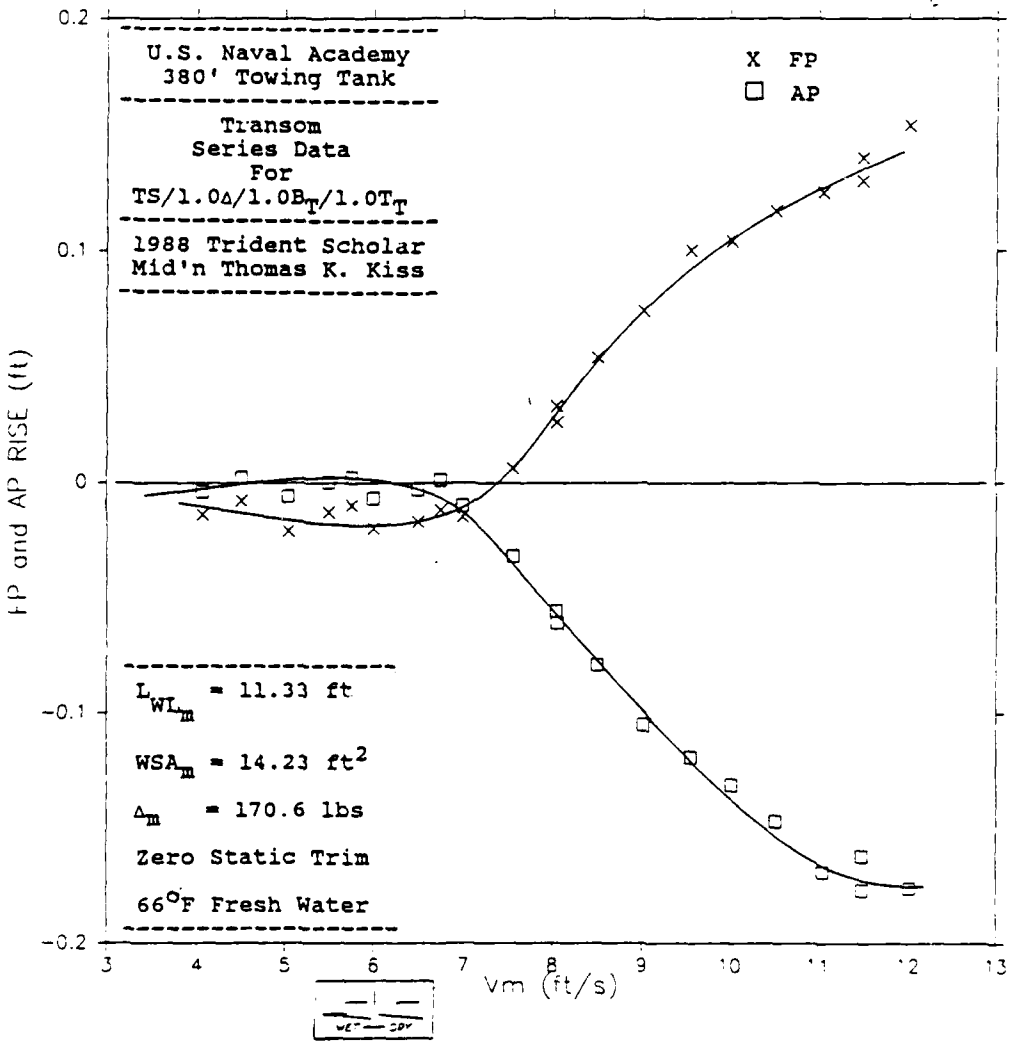

FIGURE 13: Example Plot of Rise at the Perpendiculars with Faired Curves

dependent variables. When developing such curves, careful attention was paid to the interrelation of the phenomena being considered. Humps and hollows in the resistance coefficient curve can usually be correlated with changes in the attitude of the model as indicated in the FP rise/AP rise curves. The corresponding plots for the other nine test conditions are presented in Appendix A. It should also be noted that, because of the systematic variation of the hull forms tested, the data plots could be expected to be similar; i.e., all faired curves were developed with the other test conditions in mind.

The video tapes of the flow near the transom for each run were reviewed to ascertain the speed at which the water separated cleanly from the hull at the transom, the "transom ventilation speed." Table IV contains the transom ventilation speeds for the design displacement hulls as well as the transom-draft-based Froude Number,

$$F_{NT} = Vm/ (g * T_T)^{0.5}$$

proposed by Saunders.[3] Saunders suggested that F_{NT} should have an approximate value of 5.0. The speed at which transom ventilation occurs is indicated on Figures 12 and 13 as well as on all figures in Appendix A.

In an attempt to understand the reasons for the difference in the maximum resistance coefficients for the different transom sterns, the video tapes for all tests

TABLE IV

TRANSOM VENTILATION SPEEDS (FT/S)

	BASELINE	DEEP DRAFT	SHALLOW DRAFT	WIDE BEAM	NARROW BEAM
TRANSOM VENTILATION SPEED (FT/S)	6.0	6.0	6.0	6.0	6.5
F_{NT}	4.75	4.12	5.18	4.75	5.14

were reviewed. Figure 14 shows how the water surface was deformed in the vicinity of the transom by the moving hull at speeds above separation.

EXPERIMENTAL DATA ANALYSIS

Figure 15 is a plot of the faired curves of C_{TM} vs. model speed, Vm, for the design displacement hulls with different transom draft variations. Figure 16 is the corresponding plot for the transom beam variations. To clarify the effects on calm water resistance of transom geometry further, the faired experimental data summarized in Figures 15 and 16 have been cross plotted at discrete speeds (Froude Numbers) against the transom geometry ratios, B_T/B_X and T_T/T_X, which represent the normalized independent geometrical variables for this study. Figure 17 shows a very gradual change in resistance at six discrete Froude Numbers as a function of the transom draft to maximum draft ratio, T_T/T_X. Similarly, Figure 18 shows slight variations of resistance at the same discrete Froude Numbers as a function of the transom beam to maximum beam ratio, B_T/B_X. Figure 19 is a composite plot of the wave trace near the transom for the three

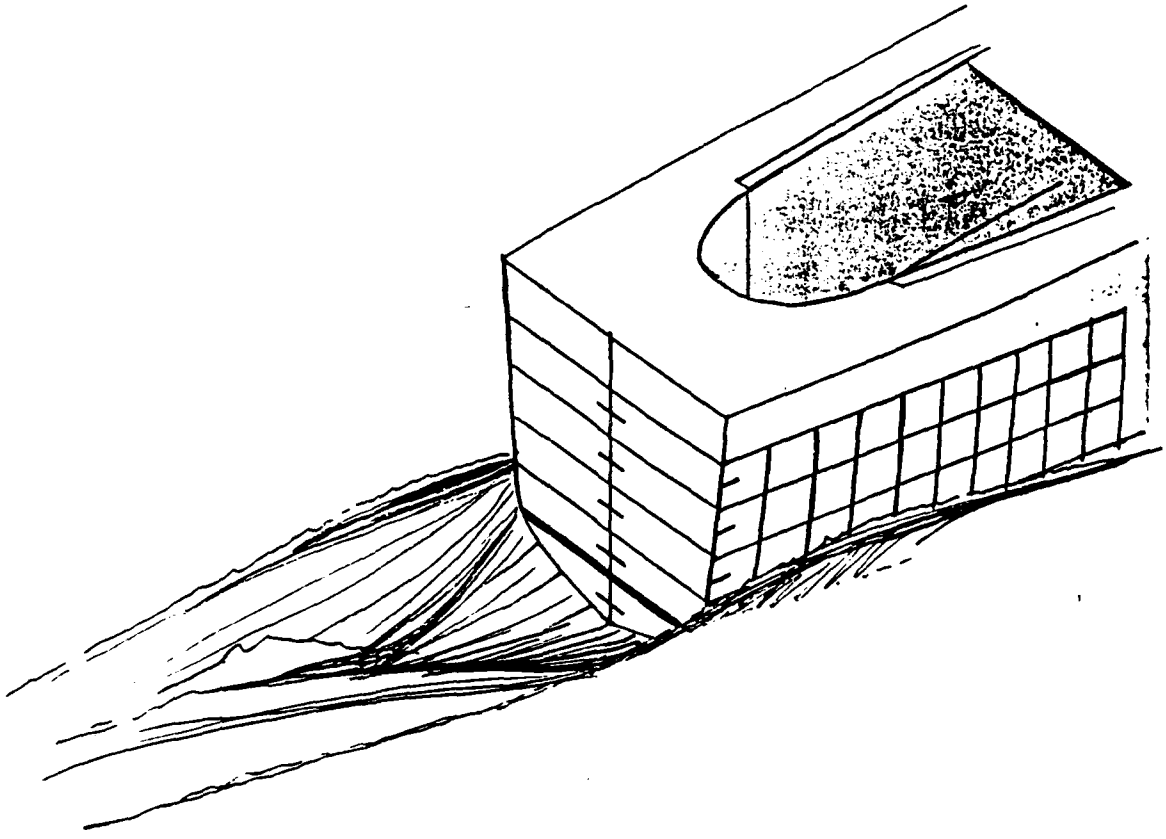

FIGURE 14: Isometric Sketch of Transom Flow After Separation

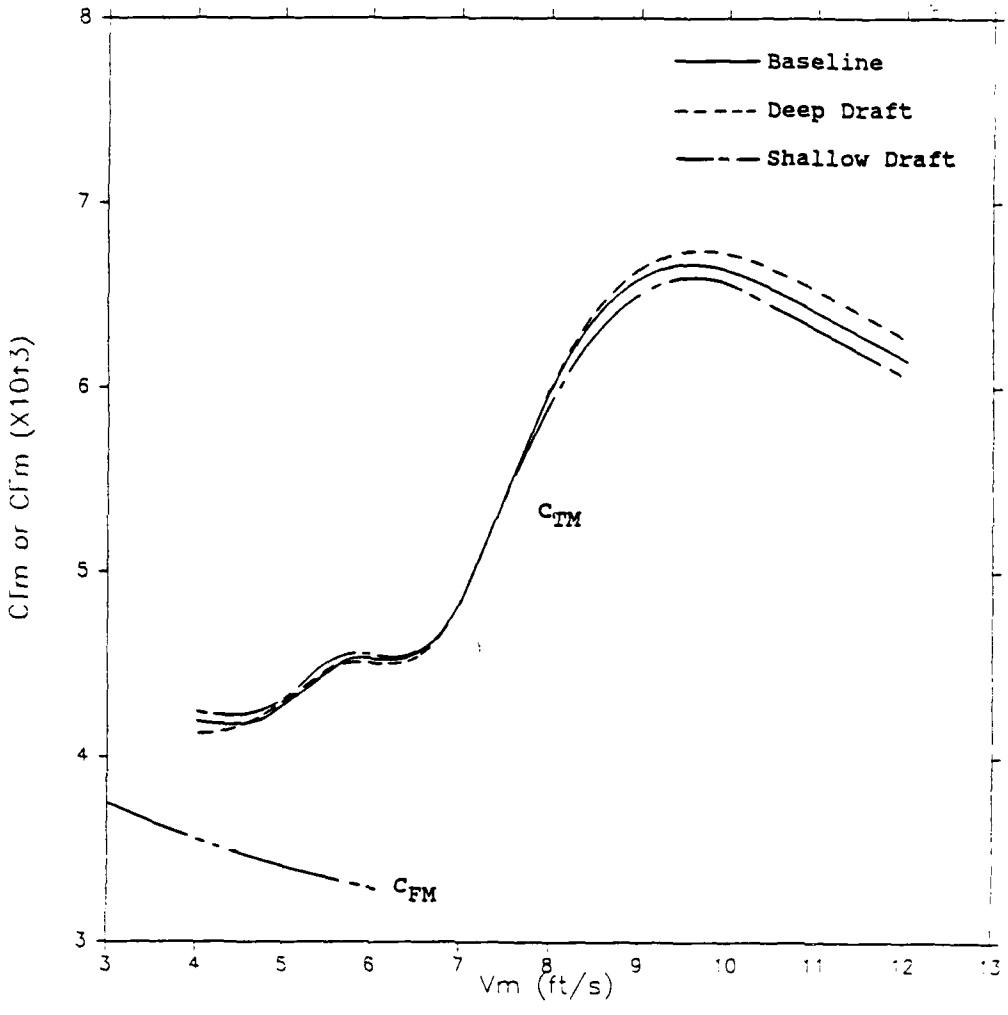

FIGURE 15: Faired Curves of Total Model Resistance Coefficient for the Draft Variation Series at Design Displacement

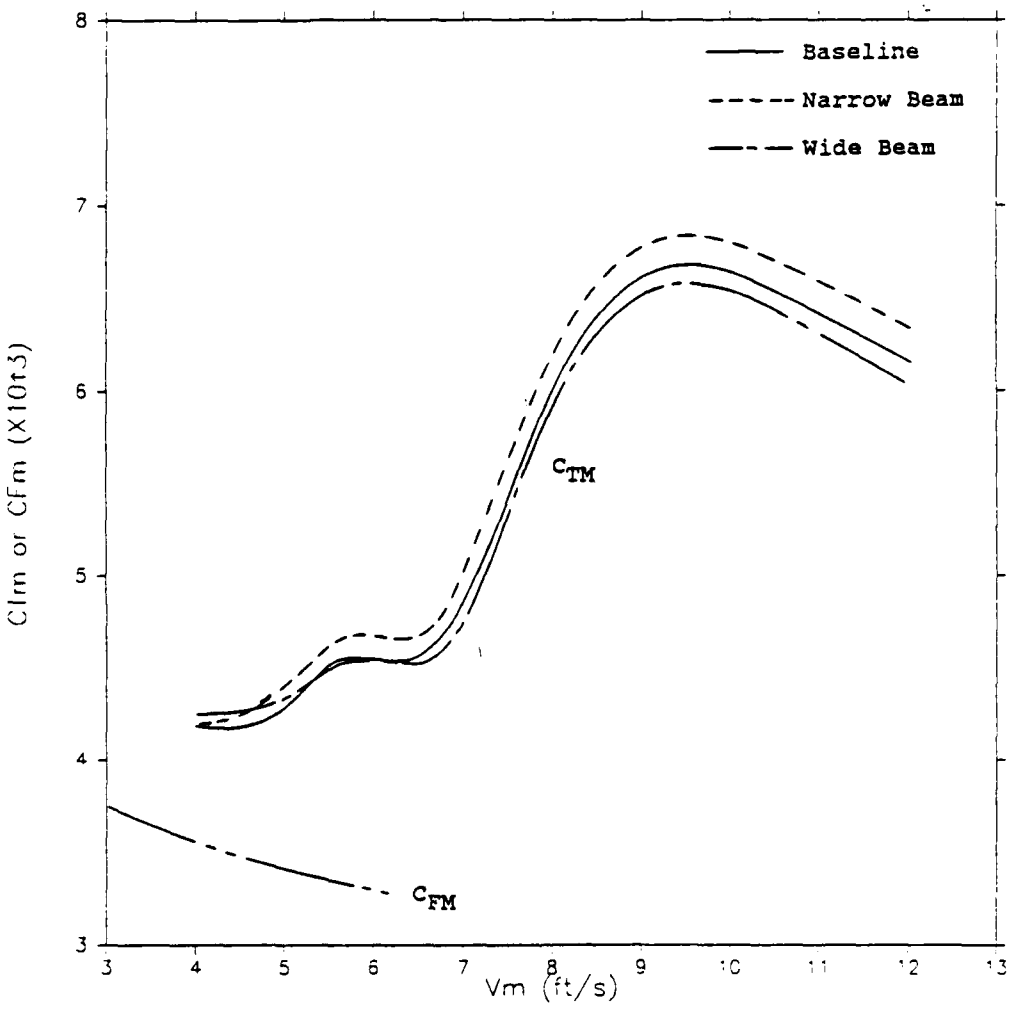

FIGURE 16: **Faired Curves of Total Model Resistance Coefficient for the Beam Variation Series at Design Displacement**

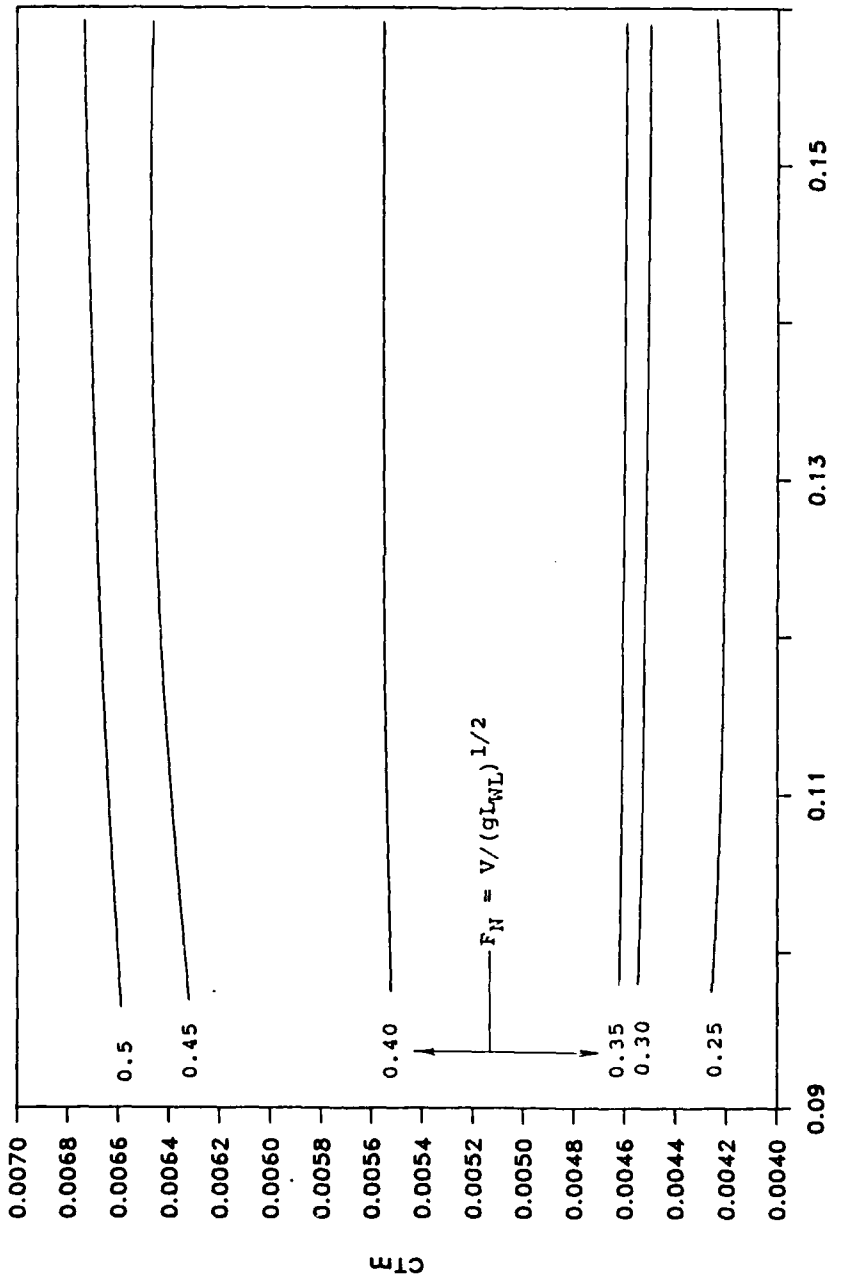

FIGURE 17: Crossplot of Total Model Resistance Coefficient Versus Draft Ratio at Discrete Froude Numbers (Design Displacement)

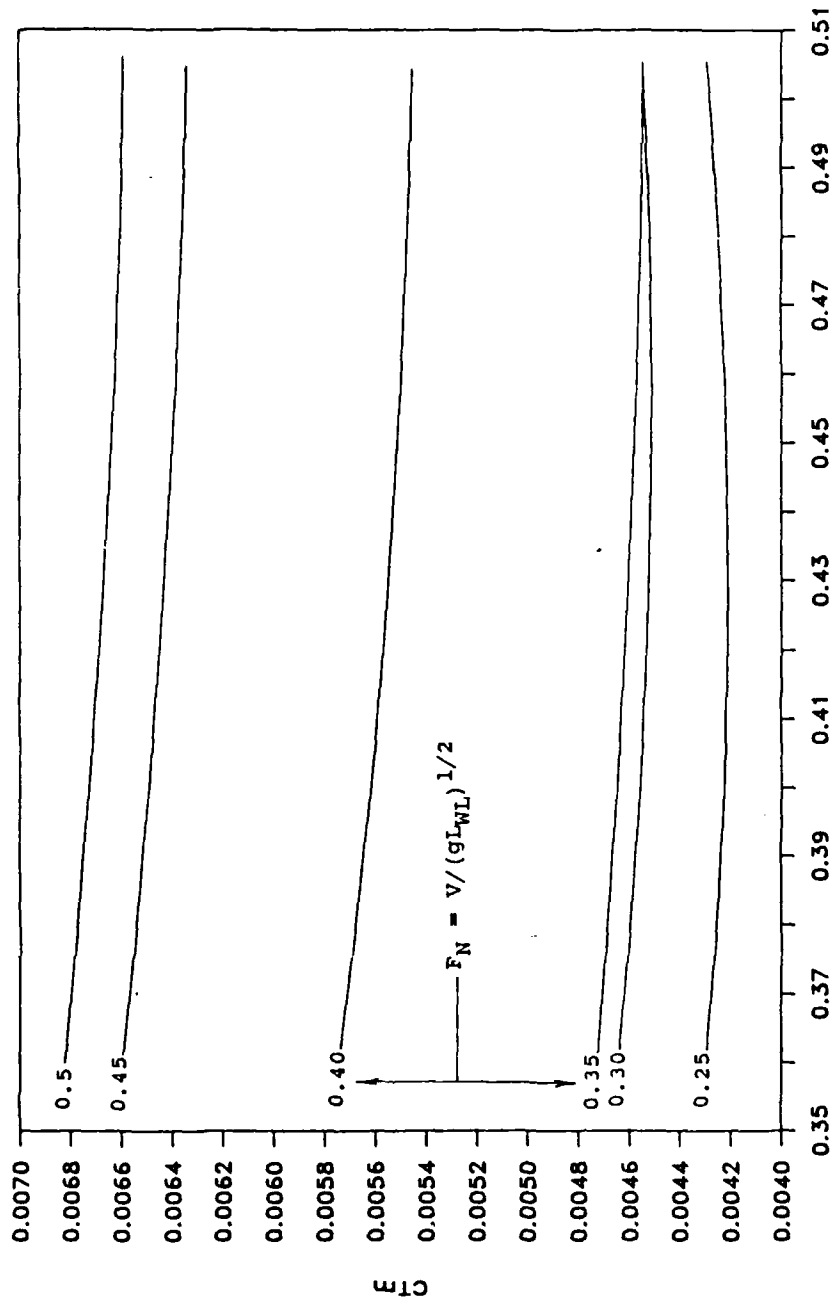

FIGURE 18: Crossplot of Total Model Resistance Coefficient Versus Beam Ratio at Discrete Froude Numbers (Design Displacement)

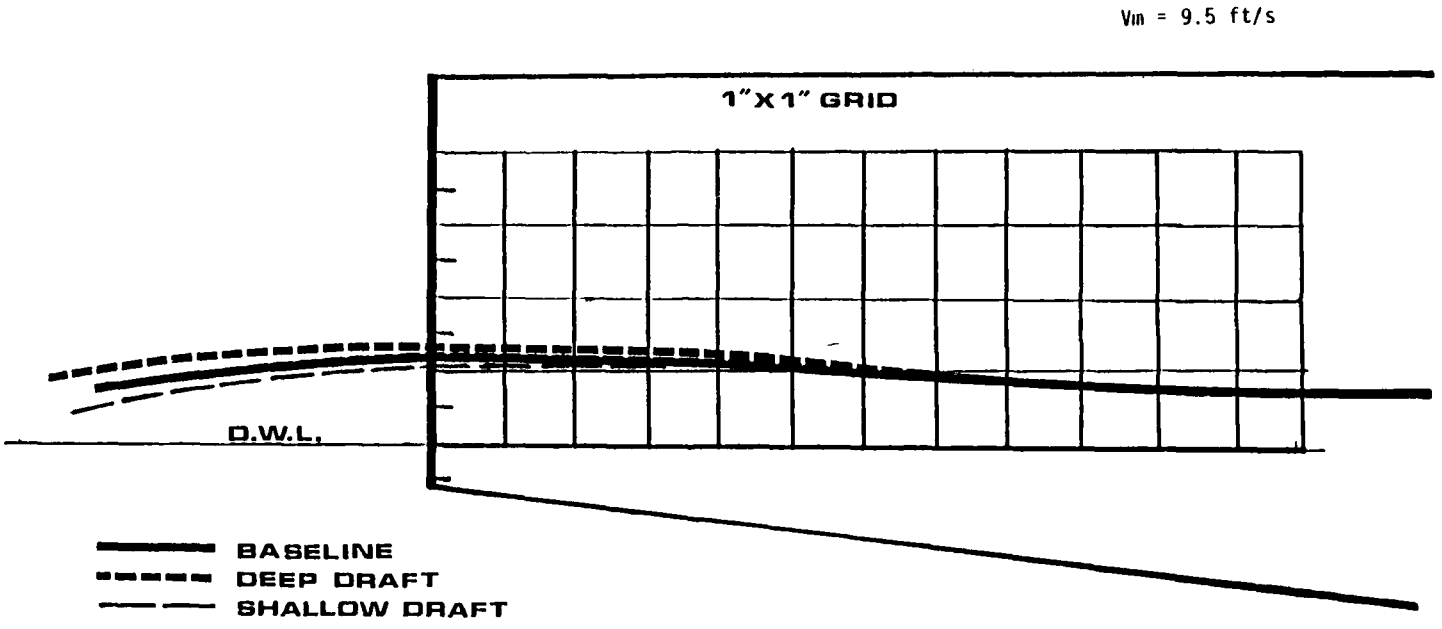

FIGURE 19: Transom Flow Approaching Transom - Draft Variations

hulls having varying transom drafts. Figure 20 is the corresponding set of wave traces for the beam varied series.

The same procedures were used to evaluate the hulls with a displacement 20% greater than the design condition. Figures 21 through 24 present data for the these hulls in the same format as used for the design displacement variations.

ANALYTICAL ANALYSIS

The calm water resistance characteristics of the five systematically varied hulls in the design condition were analyzed using two computer flowcodes. The first, the Ship Resistance Prediction Method (SRPM), is installed on a Hewlett Packard workstation at the U.S. Naval Academy's Hydromechanics Laboratory. It was run for each hull at the design displacement for six discrete Froude numbers. The second flow code is XYZ Free Surface. This program was used extensively by Wilson and Thomason to examine the effects of transom geometry on ship resistance. Their report concluded with an interpolation scheme designed to predict the change in resistance from one hull to another with transom geometry being the only

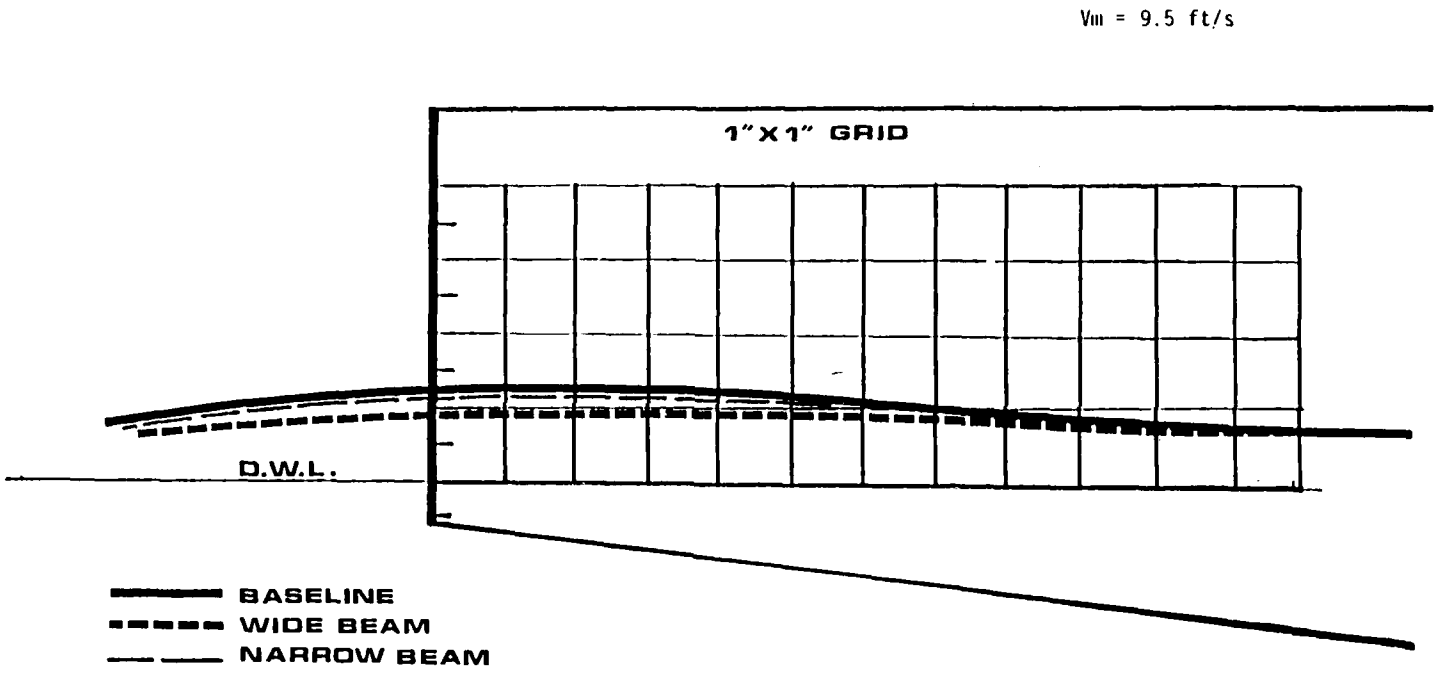

FIGURE 20: Transom Flow Approaching Transom - Beam Variations

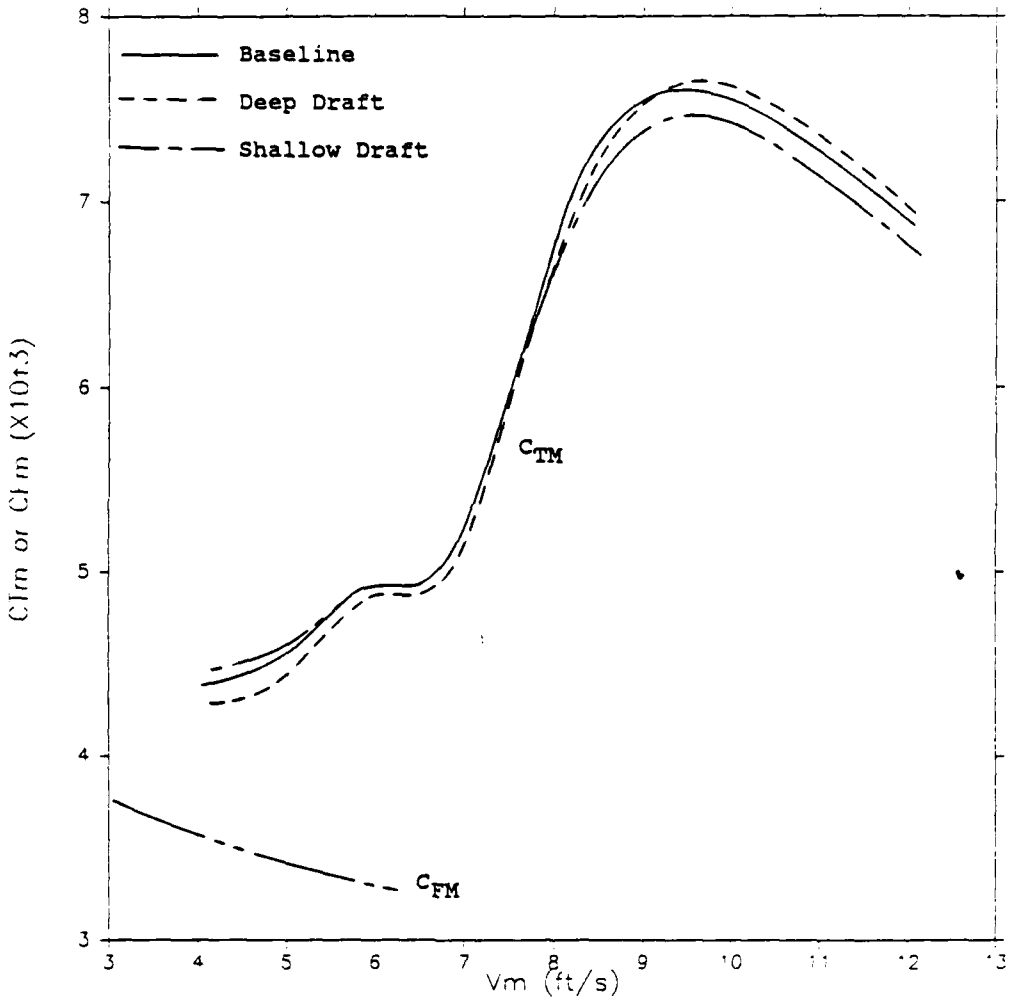

FIGURE 21: Faired Curves of Total Model Resistance Coefficient for the Draft Variation Series at Heavy Displacement

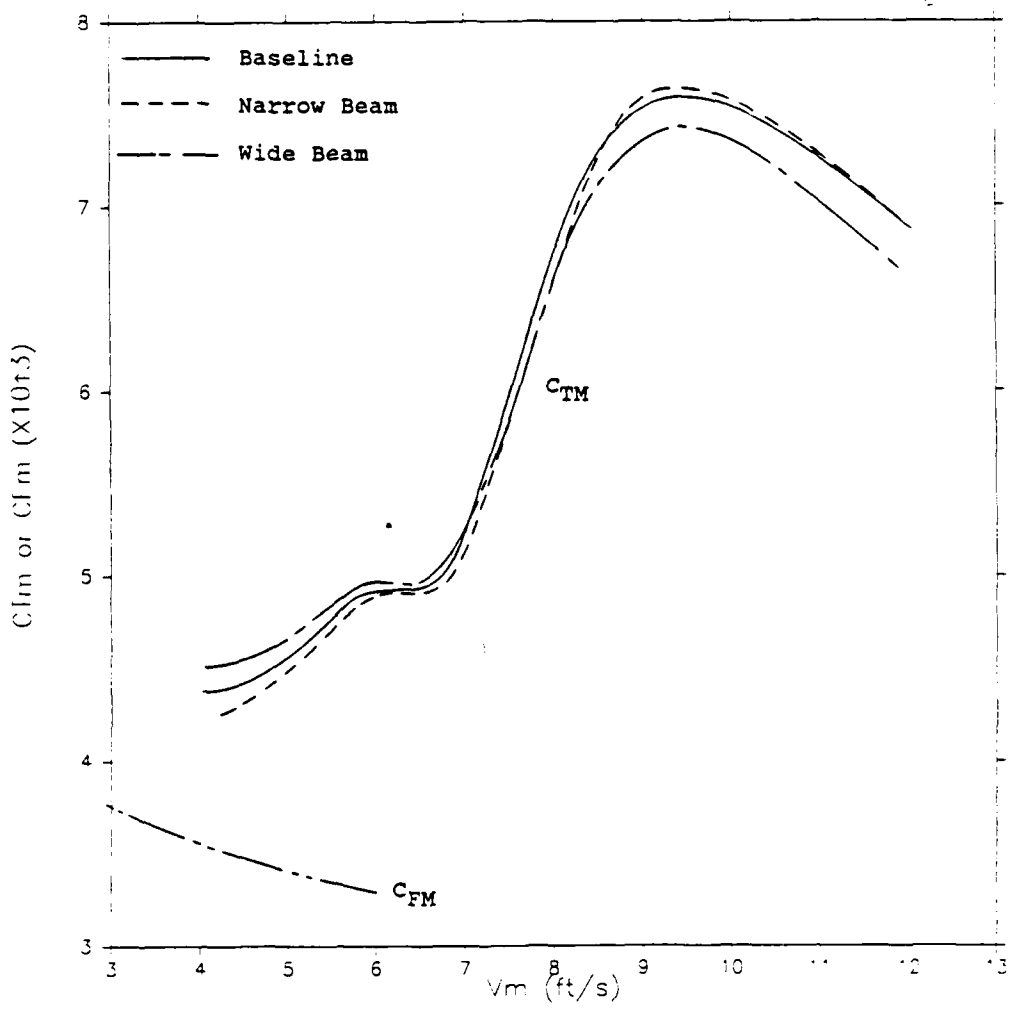

FIGURE 22: Faired Curves of Total Model Resistance Coefficient for the Beam Variation Series at Heavy Displacement

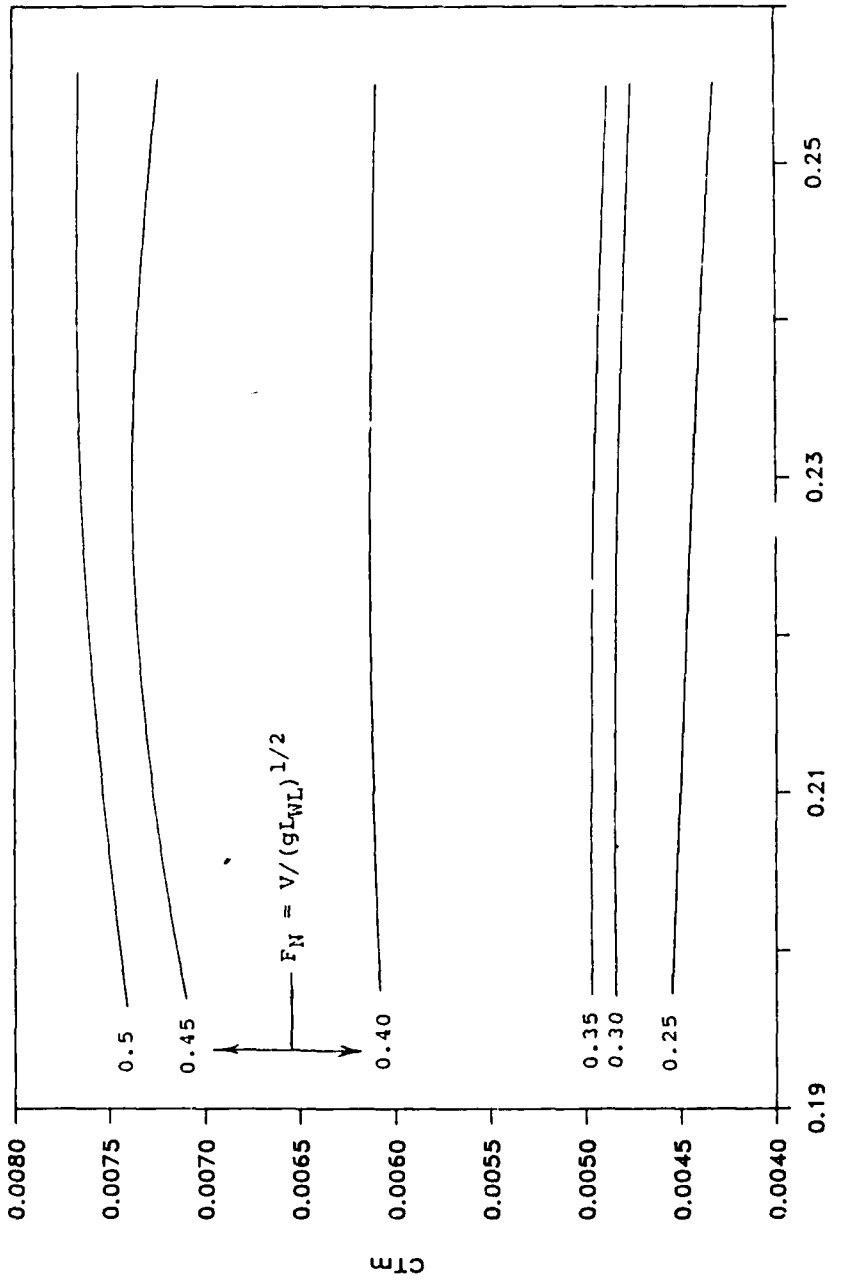

FIGURE 23: Crossplot of Total Model Resistance Coefficient Versus Draft Ratio at Discrete Froude Numbers (Heavy Displacement)

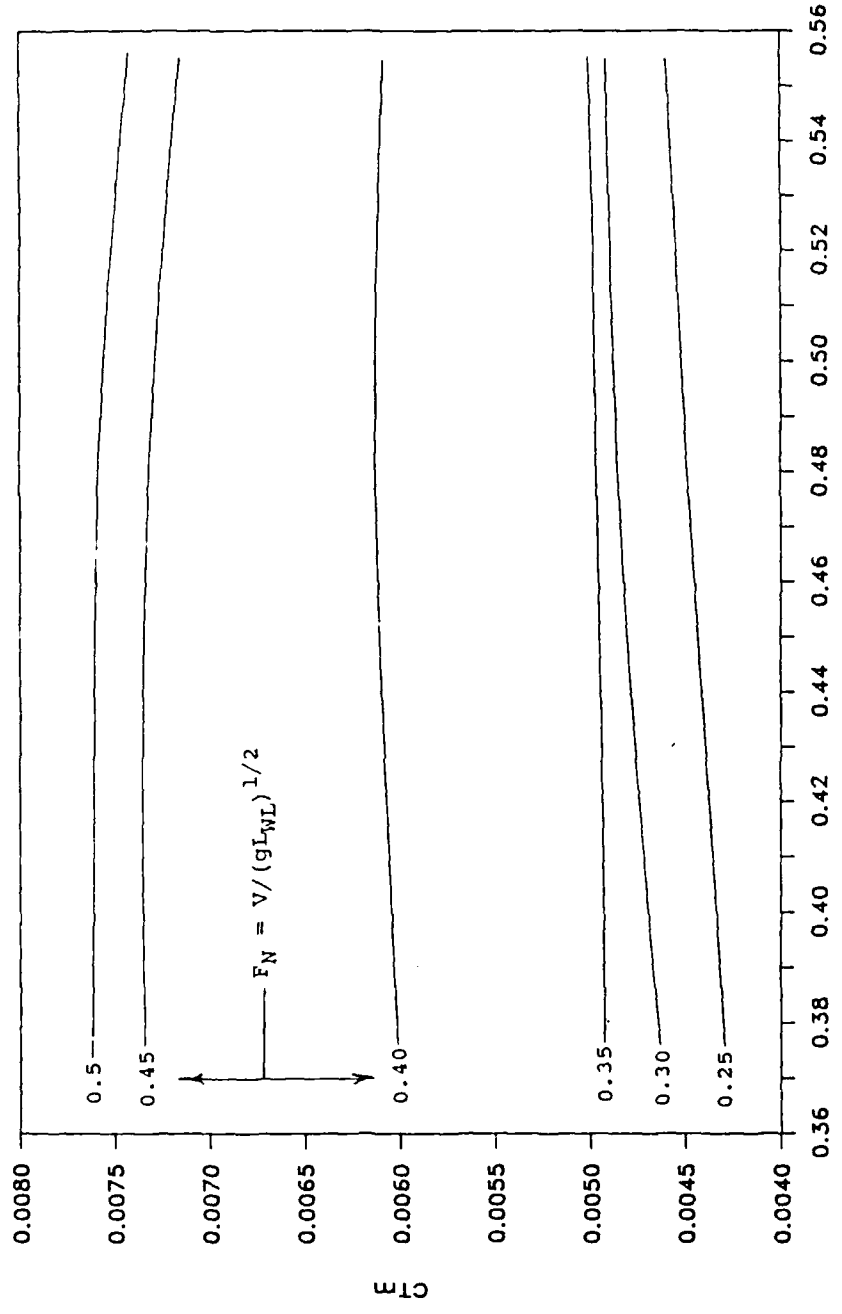

FIGURE 24: Crossplot of Total Model Resistance Coefficient Versus Beam Ratio at Discrete Froude Numbers (Heavy Displacement)

major difference between hulls. This interpolation scheme was used to evaluate the five hulls of the present series at their design displacements.

These flow codes both assume that the ship is moving at a constant velocity in an initially undisturbed ideal fluid of infinite depth. The resulting mathematical problem requires the solution of a second order, partial differential equation (Laplace's equation) everywhere in the fluid. Boundary conditions must be satisfied at the fluid/air interface and on the hull surface itself. The differences between these two flow codes lie in how the boundary conditions and the velocity potential are approximated. SRPM uses zeroth-order slender ship wave resistance theory to calculate resistance. Zeroth-order slender ship theory uses the approximate surface of the ship as the body boundary condition and applies a linear free-surface boundary condition. XYZFS also applies a linear free-surface boundary condition but the body boundary condition is solved exactly. The initial velocity potential for the zeroth-order theory is a uniform stream of fluid without the presence of the ship. XYZFS's initial velocity potential includes the ship's double body in an infinite uniform stream. The double body is a mirror image of a ship's underwater hull about its design waterline. Because of differences in the

boundary condition assumptions, SRPM cannot predict sinkage and trim while XYZFS can. This requires that a sinkage and trim file be input to SRPM. Faired experimental sinkage and trim data for the FFG-7 were used for the SRPM evaluations.

For both flow codes, the subject hull must be defined by a series of quadrilateral or triangular panels before it can be evaluated. FASTSHIP defines each hull form with panels which are acceptable input for SRPM. The panelization process for XYZFS is considerably more complicated. The process must be done by hand and requires several days of work by an experienced user. Another advantage of SRPM is that it requires less computer memory and executes much faster than XYZFS.

Both flow codes compute wave resistance only. To this an empirically determined form resistance (based upon experimental results) must be added to arrive at residuary resistance before any comparison with experimental results or ship powering estimates can be made. For SRPM, a constant form resistance coefficient of 0.0005, based on earlier FFG-7 experimental analyses, was assumed. For XYZFS, a form resistance coefficient is calculated based upon the various geometric dimensions of the hull in question. Sample flow code results for SRPM are tabulated in Appendix B.

COMPARISON OF EXPERIMENTAL AND ANALYTICAL METHODS FOR SHIP POWERING PREDICTION

Because the goal of any model analysis, be it experimental or analytical, is to predict full scale ship performance, it was decided to expand both experimental and analytical data to the same 408 foot hypothetical prototype ship size before making any comparisons. Table V contains the principal dimensions of the hypothetical frigate for which powering performance were estimated. The values in Table V were expanded from the parameters and ratios given earlier in Tables II and III. Froude scaling was employed in both the experimental and analytical predictions. For both, the 1957 ITTC model-ship correlation line with a correlation allowance of 0.0005 was used.

Figure 25 is a plot of the baseline hull's effective horsepower, EHP, versus ship speed, V_S. The solid smooth curve is based on the model test data shown earlier in Figure 12. The flow code predictions are shown as discrete points. On such a scale, the flow code results appear reasonably close (within +/- 10 percent) to the experimental prediction. The dashed line is a Taylor Standard Series[9] estimate for a cruiser sterned form having the same C_p, B_X/T_X, and $\triangle$ as the hullform whose experimental results were expanded to obtain the solid

TABLE V: PROTOTYPE SHIP DIMENSIONS

Constant Parameters

L_{PP}= 408 FT BEAM= 45.58 FT. DRAFT= 15 FT

Design Displacement Parameters

	BASELINE	DEEP DRAFT	SHALLOW DRAFT	WIDE BEAM	NARROW BEAM
$\triangle$ LTSW	3652.4	3666.8	3637.9	3638.9	3661.7
A_T (FT^2)	26.40	26.68	26.37	26.40	26.61
A_X (FT^2)	516	516	516	516	516
T_T (FT)	1.78	2.37	1.50	2.37	2.37
B_T (FT)	19.62	19.56	19.70	22.90	16.32
S (FT^2)	18,440	18,468	18,504	18,503	18,457
LCG (FT AFT ⋈)	3.02	3.36	3.06	2.99	3.33

Design Displacement + 20% Parameters

	BASELINE	DEEP DRAFT	SHALLOW DRAFT	WIDE BEAM	NARROW BEAM
$\triangle$ LTSW	4383.0	4400.2	4365.4	4366.6	4394.0
A_T (FT^2)	66.28	67.15	65.47	72.66	59.86
A_X (FT^2)	602	602	602	602	602
T_T (FT)	3.67	4.26	3.38	3.65	3.69
B_T (FT)	21.84	21.84	21.84	25.42	17.58
S (FT^2)	20,052	20,083	20,112	20,102	20,072
LCG (FT AFT ⋈)	5.99	6.31	5.98	6.20	6.02

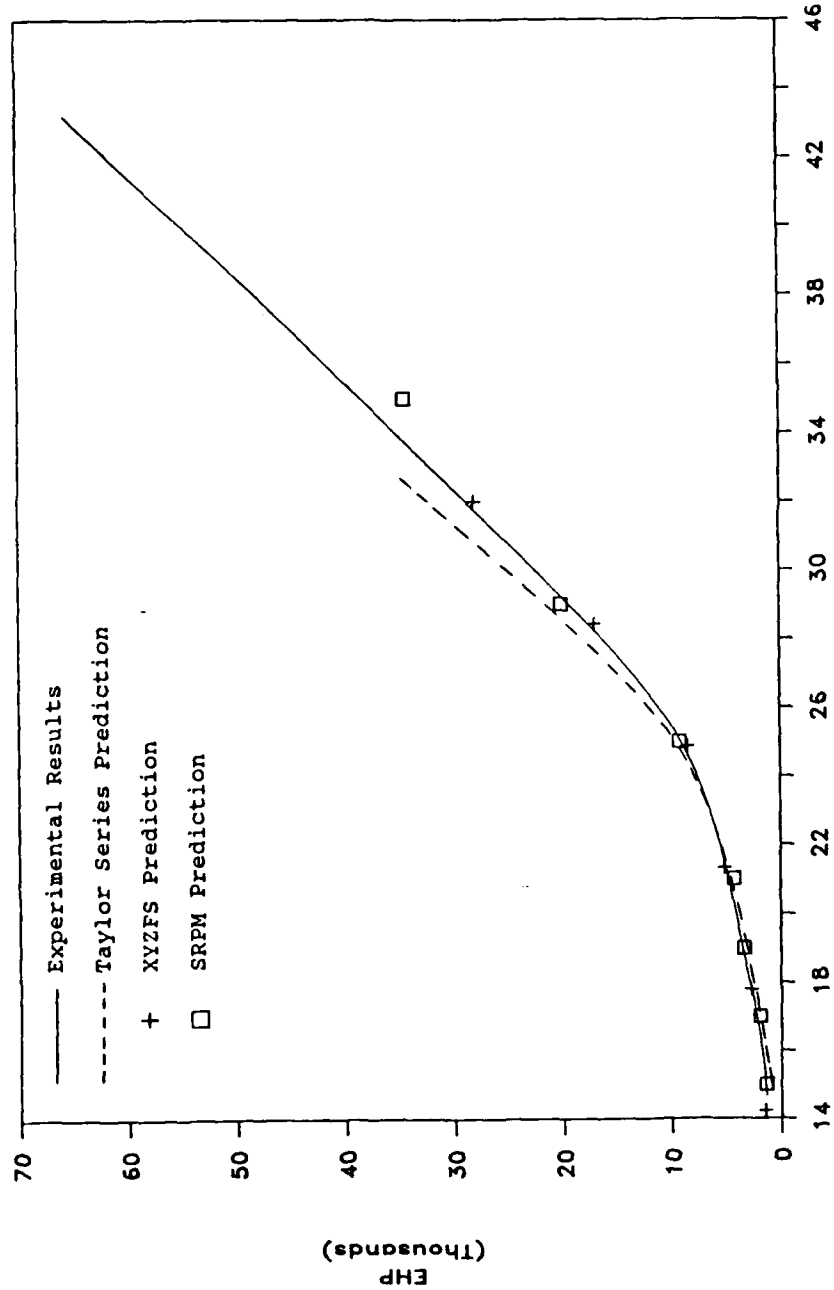

FIGURE 25: Effective Horsepower Trends for a 408 Foot Baseline Hull Predicted by Various Means

curve. As was expected, at the high end of the speed range, the cruiser stern shape became increasingly inferior to the transom stern shape as far as resistance is concerned. At 32 knots for example, the cruiser sterned hull requires 11.6 percent more EHP than the transom sterned hull. The two curves became coincident at about 23 knots. Below 22 knots, the cruiser stern hull exhibits lower EHP than the transom stern hull.

To show clearly the relatively small changes in EHP due to the systematic transom shape variations, a "percent difference from baseline values" format was developed. For Figures 26 and 27, the ordinate has the form:

$$\% \text{ Difference in EHP} = ((EHP - EHP_{BASELINE})/EHP_{BASELINE}) \times 100$$

Figure 26 shows the effect of transom draft variation while Figure 27 shows the effect of transom beam over the speed range for the standard (design) displacement. The continuous curves shown in Figures 26 and 27 represent the experimental predictions of the effects of transom draft and beam on EHP. These figures show clear, but not dramatically large, differences in EHP throughout the entire speed range tested due to transom geometry differences. The most significant trends

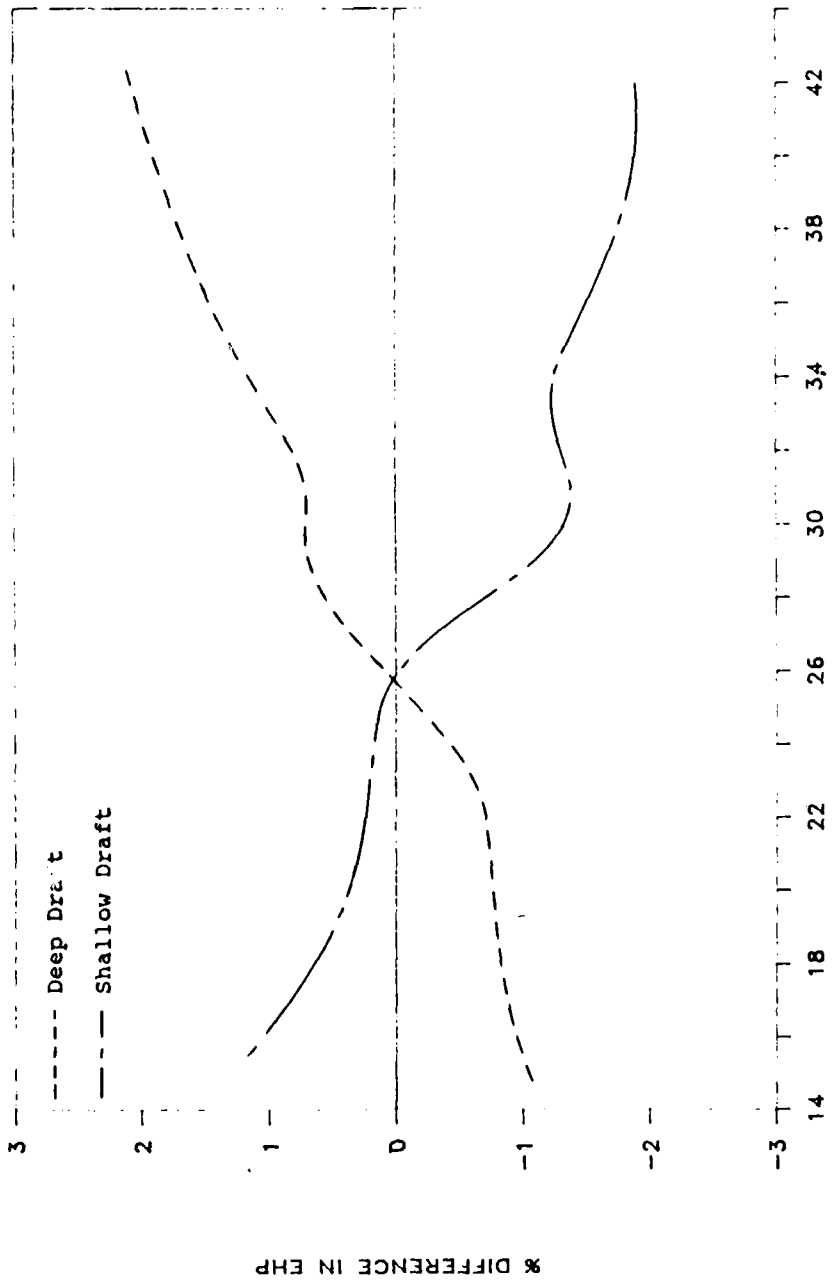

FIGURE 26: Percent Horsepower Differences for the Draft Variation Series - Experimental Results

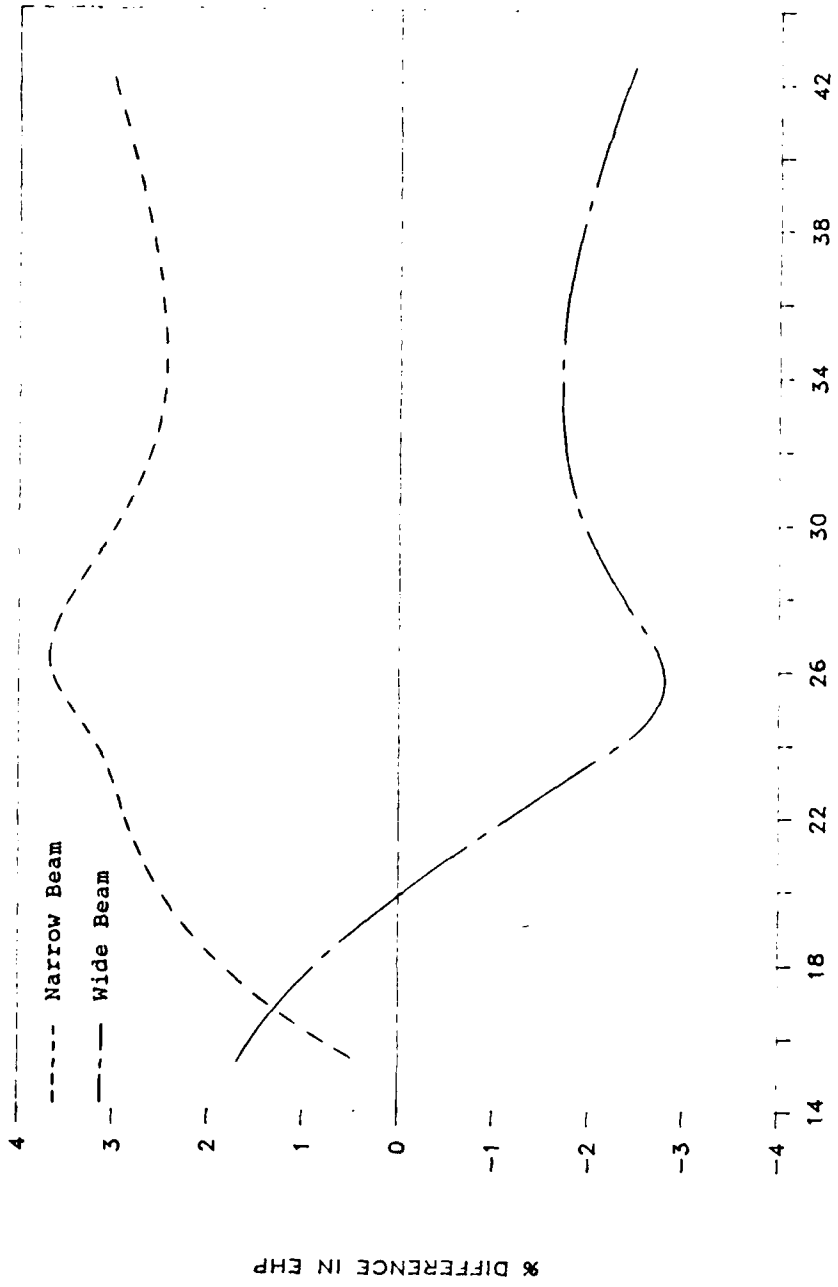

FIGURE 27: Percent Horsepower Differences for the Beam Variation Series - Experimental Results

shown are those for speeds greater than 20 knots. At the low speed end of the plot, the high speed trends tend to reverse, but it must be remembered that the differences represent a few percent of a much smaller horsepower (see Figure 25) than at higher speeds. A 2 percent difference in EHP at 16 knots represents about 37 horsepower, while a 2 percent difference at 25 knots represents about 186 horsepower.

To compare the flow code predictions with the experimental predictions just described, Figures 28 through 33 are presented. In every figure, the faired experimental curves of Figures 26 and 27 are repeated to facilitate comparison. Figures 28 and 29 show the XYZFS predictions as discrete plot symbols. In contrast to the apparently good agreement in Figure 25, the lack of correlation with the faired curves indicates to the author that the XYZFS flow code is not sufficiently sensitive to discern the effects of small changes in transom geometry. While this may seem to contradict the work of Hoyle et al[10], it must be remembered that the bulb geometry changes investigated by Midshipman Hoyle were at the extreme bow whereas the transom geometry variations were at the stern where greater viscous flow effects must certainly exist. The other flow code predictions fared no better.

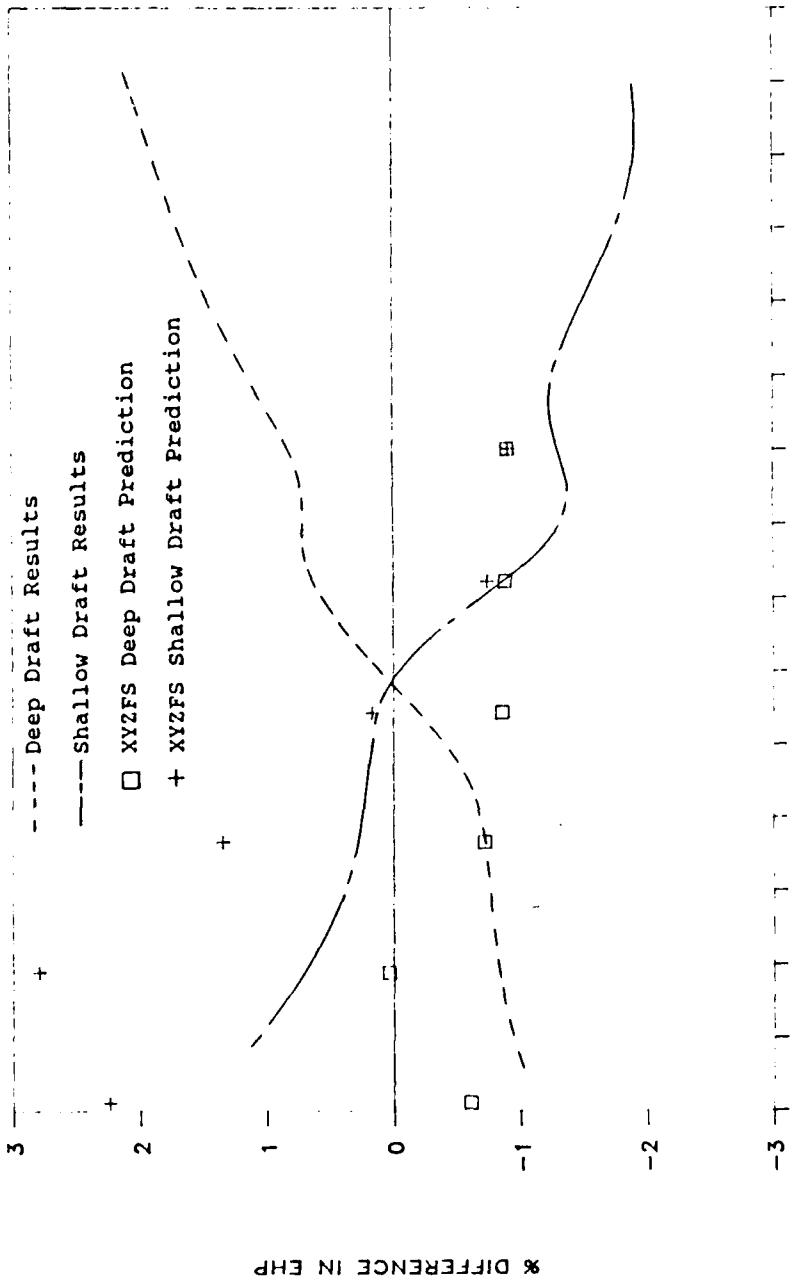

FIGURE 28: Percent Horsepower Differences for the Draft Variation Series - XYZFS/Experimental Comparison

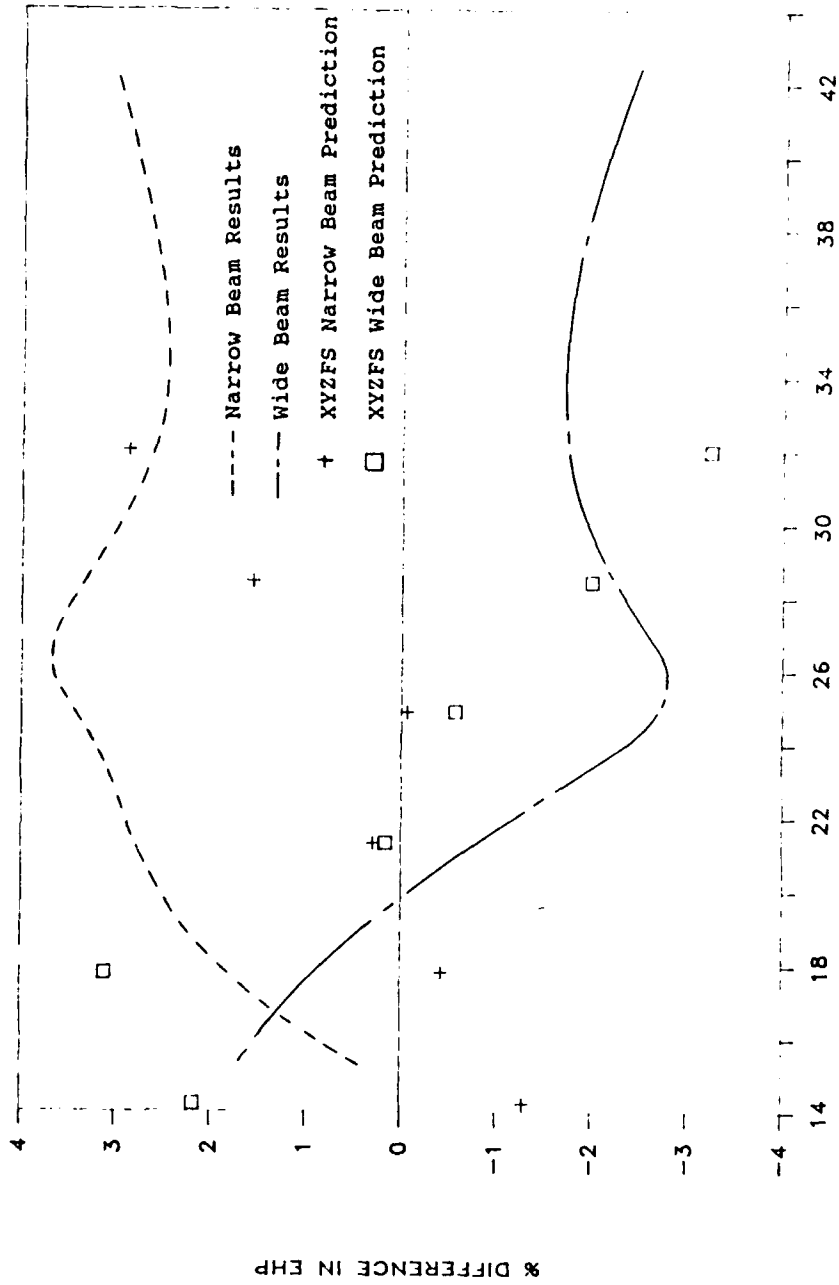

FIGURE 29: Percent Horsepower Differences for the Beam Variation Series - XYZFS/Experimental Comparison

Figure 30 and 31 show the discrete points computed by the interpolation method of Wilson et al[5]. Recalling that Wilson's work was based on XYZFS, it is not surprising that the agreement with the experimental trends is similarly poor. Figures 32 and 33 show the experimental curves from Figures 26 and 27 plotted with the discrete points computed by SRPM.

A very rough Prohaska form factor analysis[11] was performed on the data for each hull form configuration. Although the results must be considered approximate, since the number of data points acquired at extreme low speeds was very small, the form factors for the different transoms were found to differ by as much as 2 percent. While such results must be validated by more extensive experimentation at Froude numbers between 0.1 and 0.2, the tentative conclusion is that much of the difference in resistance among the forms tested could be attributed to form resistance phenomena rather than to wavemaking resistance. This conclusion supports the earlier statement of the greater viscous flow influence for geometric changes at or near the stern of the ship. Figures 34 and 35 show the effects of transom draft and transom beam respectively for the heavier displacement condition. Only experimental trends are shown.

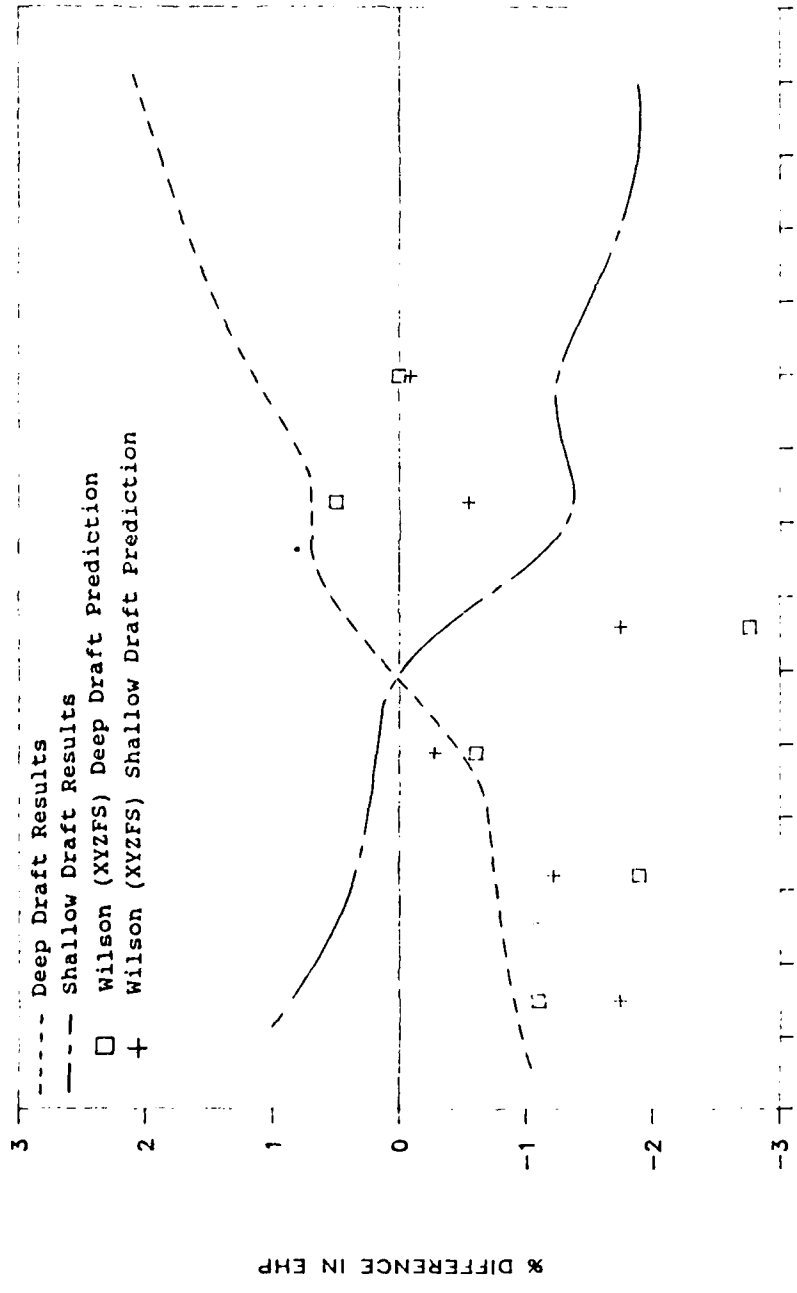

FIGURE 30: Percent Horsepower Differences for the Draft Variation Series - Wilson's Interpolation Method/Experimental Comparison

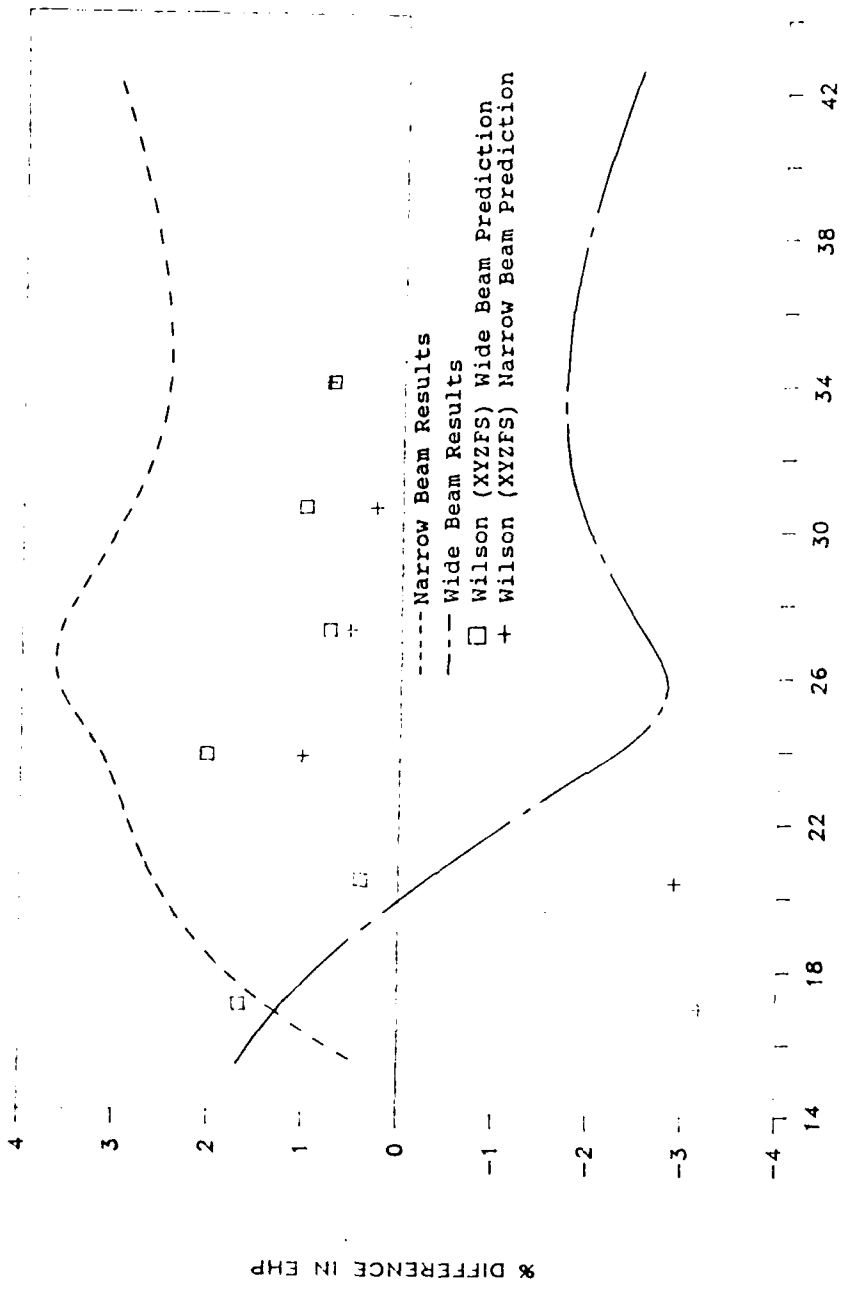

FIGURE 31: Percent Horsepower Differences for the Beam Variation Series - Wilson's Interpolation Method/Experimental Comparison

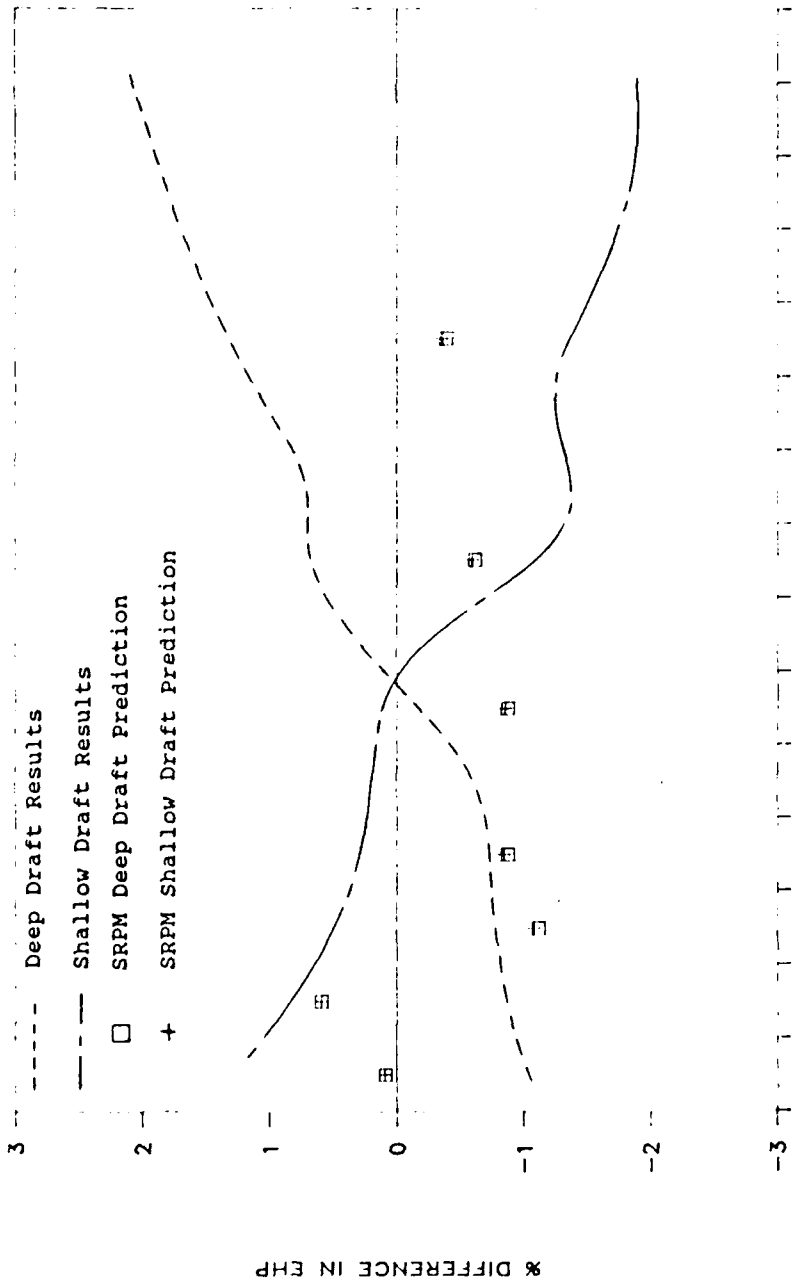

FIGURE 32: Percent Horsepower Differences for the Draft Variation Series - SRPM/Experimental Comparison

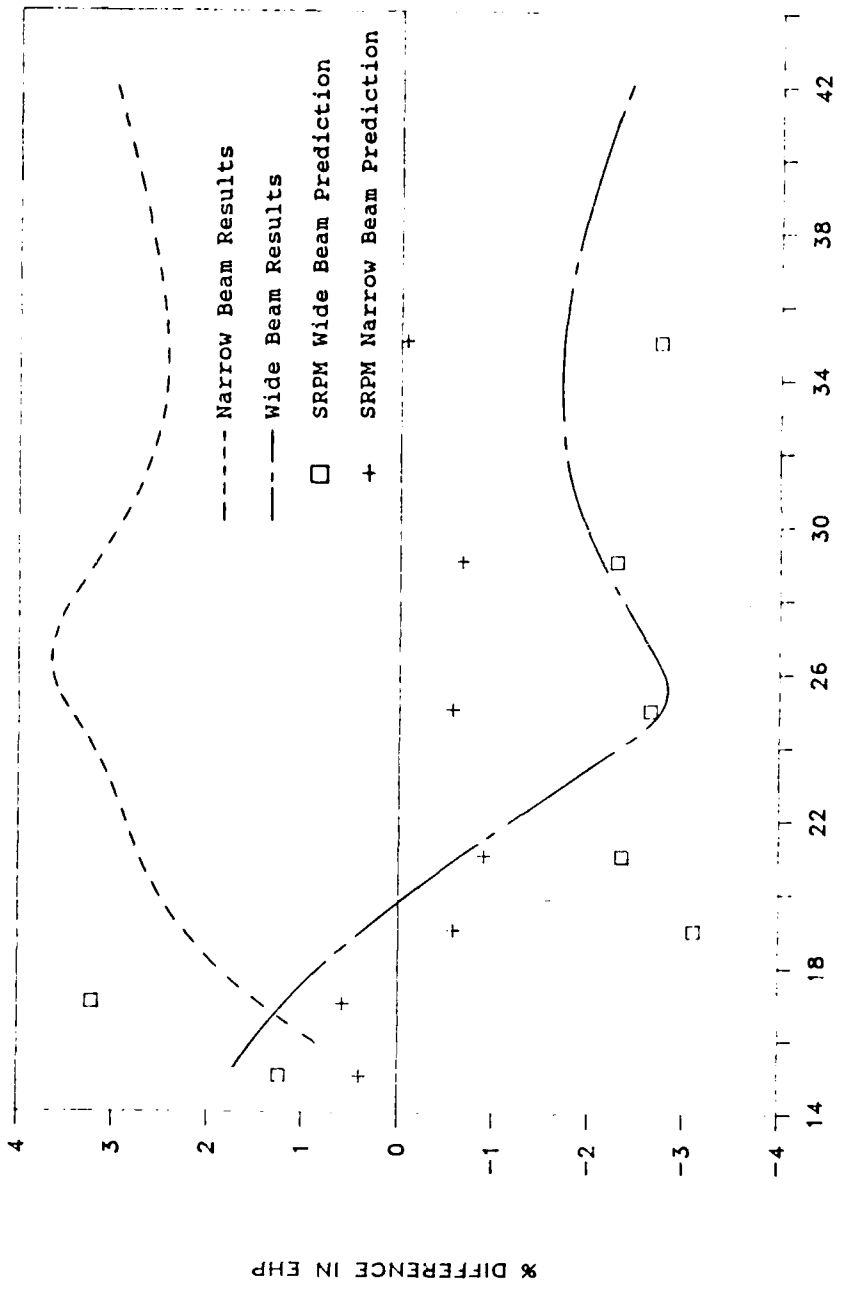

FIGURE 33: Percent Horsepower Differences for the Beam Variation Series - SRPM/Experimental Comparison

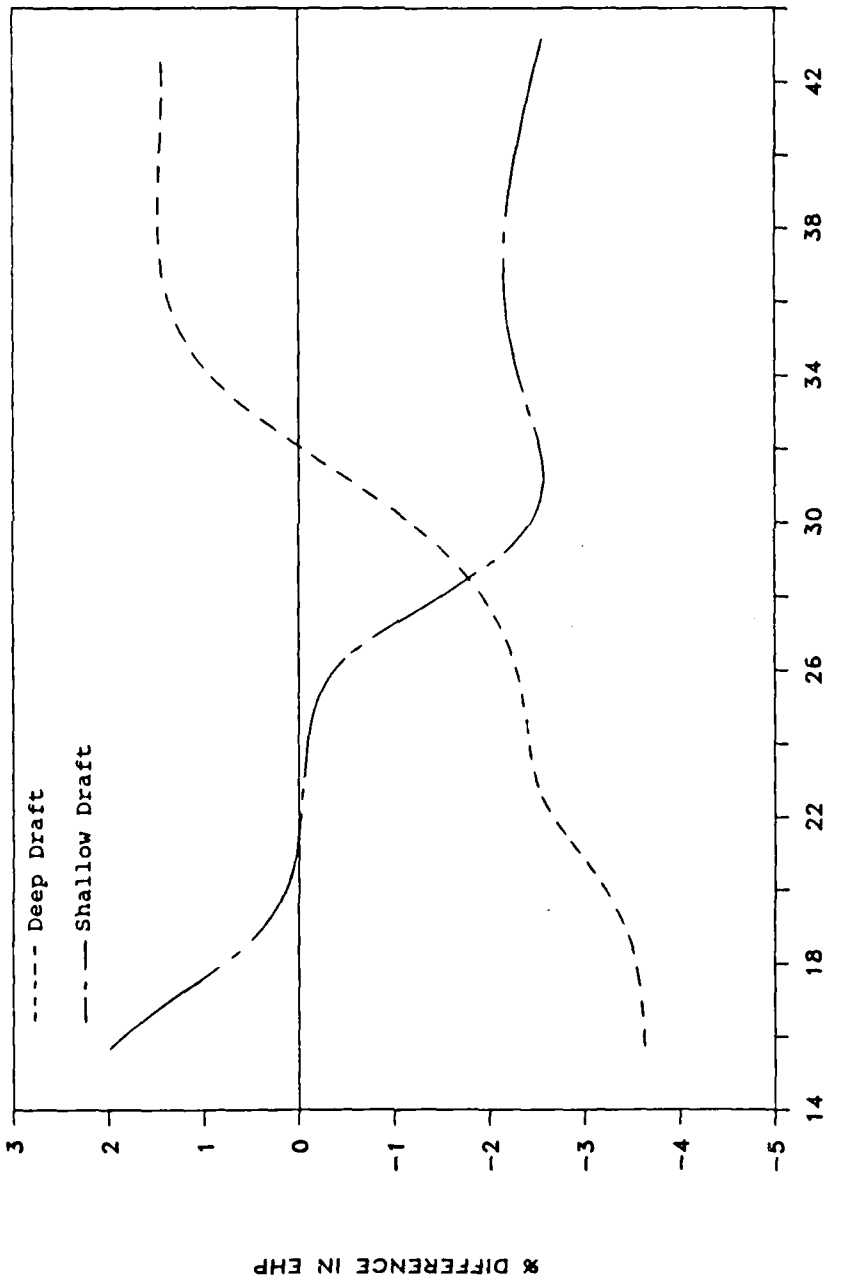

FIGURE 34: Percent Horsepower Differences for the Draft Variation Series - Heavy Displacement

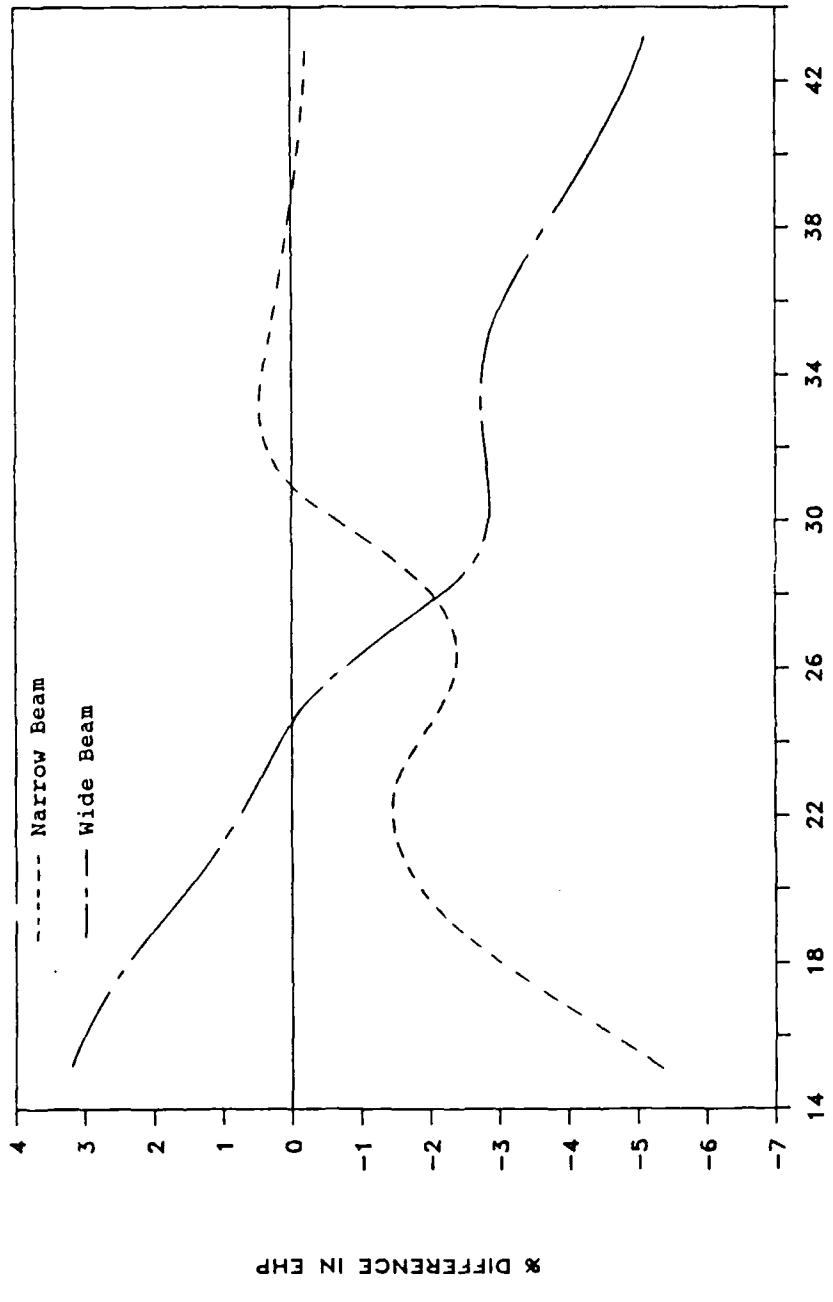

FIGURE 35: Percent Horsepower Differences for the Beam Variation Series - Heavy Displacement

CONCLUSIONS

Relatively small changes in transom geometry have been shown to cause small but measurable changes in a ship's calm water EHP. Experimental data indicate that:

(1) For a fixed transom sectional area, beam, and displacement:

a) A deep transom causes up to a 2 percent increase in EHP at high speeds above a Froude number of 0.38. At low speeds, below a Froude number of 0.38, the deep transom shows a marginal advantage in EHP of as much as 1 percent.

b) A shallow transom causes up to a 2 percent decrease in EHP at high speeds above a Froude number of 0.38. At low speeds, below a Froude number of 0.38, the shallow transom shows an addition to EHP of as much as 2 percent.

(2) For a fixed transom sectional area, transom draft, and displacement:

a) a wide transom causes up to a 3 percent decrease in EHP at high speeds above a Froude number of 0.29. At low speed, below a Froude number of 0.29, the wide transom shows an increase to EHP by as much as 1.75 percent.

b) a narrow transom cause an increase in EHP throughout the entire tested speed range.

(3) While the wide, shallow transom offers the least resistance in the higher speed range, there is no clear best configuration at low speeds.

(4) At high speeds, the hull that trims the most tends to have the highest resistance. This is especially true with the beam variation series. For the draft variation series, no significant trim difference was observed.

(5) When displacement is increased 20% above a nominal design condition the relative order of the transom variations remains but the resistance (and thus EHP) increases 21 percent.

(6) The narrow beam transom, which exhibited the highest resistance - especially at higher speeds - clearly caused the greatest surface wave disturbance in the towing tank.

(7) The transom ventilation speed is relatively insensitive to transom beam and draft variations at a fixed transom area ratio, A_T/A_X. Saunders' rule-of-thumb Froude number tends to predict transom ventilation at slightly lower speeds.

While one hypothetical ship size was chosen for illustrative purposes, the model data included can be expanded using conventional Froude scaling techniques to any reasonable ship size typical of frigates, destroyers, or cruisers.

Flow codes do not appear sensitive enough to discern properly the effects of small transom geometry changes. However, they are able to approximate ship resistance and could be used for preliminary design powering estimates.

SUGGESTIONS FOR FUTURE RESEARCH

The present systematic series should be expanded to include immersed transom areas greater and lesser than the area used in this project. These extensions should use the same rationale as developed in this project. Both beam and draft should be varied while holding immersed transom area constant. This would allow examination of the effect of varying immersed transom area on ship resistance. In addition, this would verify the results of the present study concerning the effects of transom beam and draft. Further series should also focus on the effects of concave and convex buttock lines and waterlines on resistance.

Modifications to the basic transom shape should also be examined. A transom with rapidly increasing beam above the waterline (i.e., flare) should be tested to see if the resistance benefits of medium beam transom at low speeds can be combined with the resistance benefits of wide beam transoms at high speeds. A systematic stern

wedge series should also be designed and tested on the five hulls designed in this project. Eventually, the effects of transom geometry studied in calm water should be quantified similarly in various ambient wave conditions representative of real ocean operation. Both motions and added resistance should be studied.

ACKNOWLEDGMENTS

The author of this Trident Scholar Report wishes to gratefully acknowledge the assistance of the following people:

Dr. Chu Chen of Naval Sea Systems Command for analyzing the transom series using XYZ Free Surface.

Mr. Tom Price of the U.S. Naval Academy Technical Support Department for the production of the sterns tested in this project.

Mr. John Hill and the entire staff of the Naval Academy Hydromechanics Laboratory for their assistance in all phases of this project.

And most importantly, Dr. Roger Compton who served as the Trident Scholar Advisor for this project.

REFERENCES

1. "Test of Transom Sterns on Destroyers," United States Experimental Experimental Model Basin Report 339, November 1932.

2. Gillmer, Thomas C., "Tank Tests of Several Transom-Stern Configurations on Destroyer Escort Type Hulls," United States Naval Academy Hydromechanics Laboratory Report E-3, December 1961.

3. Saunders, Capt. Harold E., USN (ret.), Hydrodynamics in Ship Design, The Society of Naval Architects and Marine Engineers, New York, 1957. (Volume II pp. 530-531)

4. Jenkins, D., Nagle, T., and O'Dea, J., "Flow Characteristics of a Transom Stern Ship," David Taylor Naval Ship Research and Development Center Report 81/057, September 1981.

5. Thomason, T.P., Wilson, M.B., "Study of Transom Stern Ship Hull Form and Resistance," David Taylor Naval Ship Research and Development Center Report 85/072, April 1986.

6. Principles of Naval Architecture, The Society of Naval Architects and Marine Engineers, New York, 1967. (pp. 341-364)

7. Eggers, K.W.H., Sharma, S.D., and Ward, L.W., "An Assessment of Some Experimental Methods for Determining the Wavemaking Characteristics of a Ship Form," Transactions of the Society of Naval Architects and Marine Engineers, 1967.

8. Dawson, C.W., "A Practical Computer Method for Solving Ship-Wave Problems," Proceedings of the Second International Conference in Numerical Ship Hydrodynamics, September 1977. (pp. 30-38)

9. Gertler, M., "A Reanalysis of the Original Test Data For the Taylor Standard Series," David W. Taylor Model Basin Report 806, March 1954.

10. Cheng, B.H., Hays, B., Hoyle, J.W., Johnson, B., and Nehrling, B., "A Bulbous Bow Design Methodology for High-Speed Ships," Transactions of the Society of Naval Architects and Marine Engineers, 1986.

11. Harvald, S. A., Resistance and Propulsion of Ships, Wiley-Interscience Ocean Engineering Series, New York, 1983. (pp. 101-103)

APPENDIX A

TRANSOM SERIES MEASURED

DATA PLOTS WITH FAIRED CURVES

NOTE: HULL FORMS ARE IDENTIFIED AS FOLLOWS:

$$TS/\underline{a}\,\Delta/\underline{b}\,B_T/\underline{c}\,T_T$$

WHERE a = MULTIPLIER FOR DISPLACEMENT

b = MULTIPLIER FOR TRANSOM BEAM

c = MULTIPLIER FOR TRANSOM DRAFT

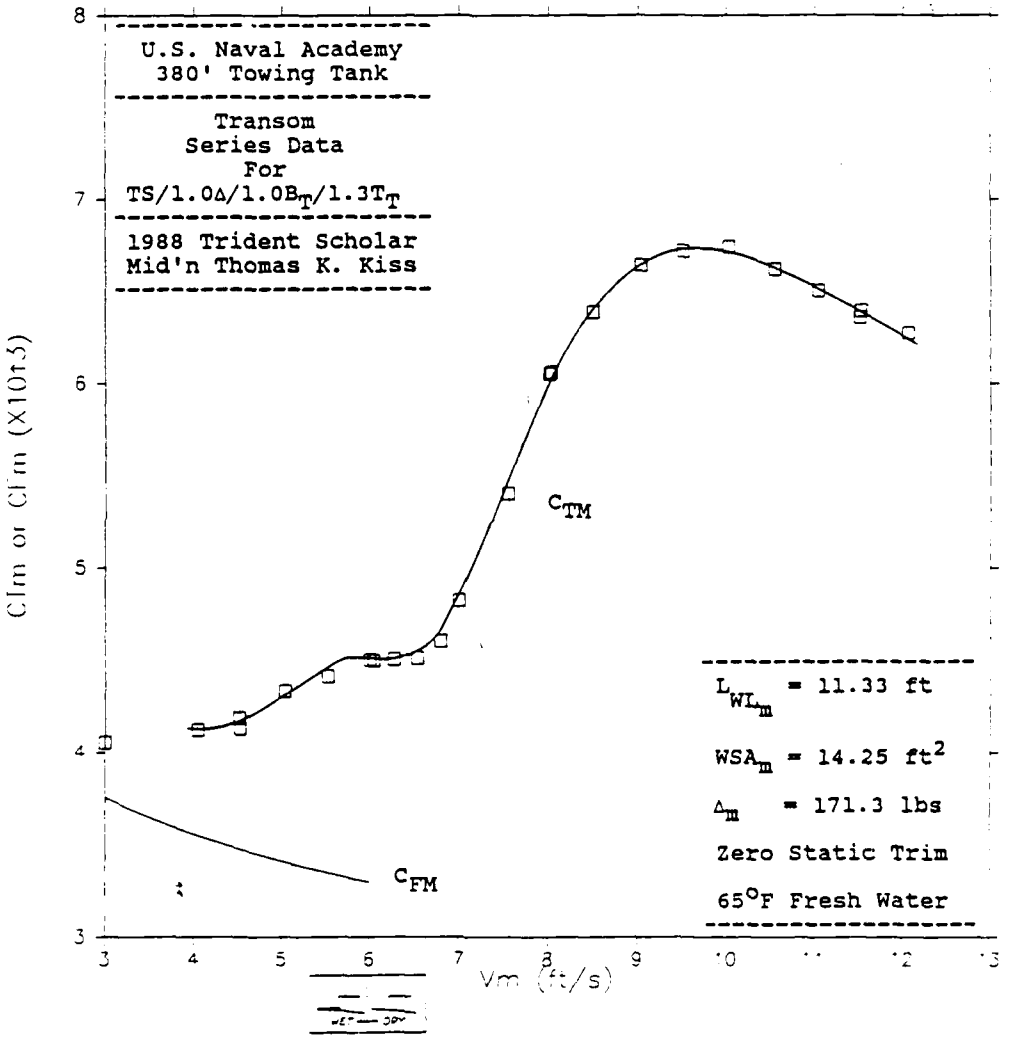
U.S. Naval Academy
380' Towing Tank
Transom
Series Data
For
TS/1.0Δ/1.0B_T/1.3T_T
1988 Trident Scholar
Mid'n Thomas K. Kiss
C_TM
C_FM
L_WL_m = 11.33 ft
WSA_m = 14.25 ft^2
Δ_m = 171.3 lbs
Zero Static Trim
65°F Fresh Water
Cfm or Cfm (X10f3)
Vm (ft/s)
8
7
6
5
4
3
3
4
5
6
7
8
9
10
11
12
13

FIGURE A1

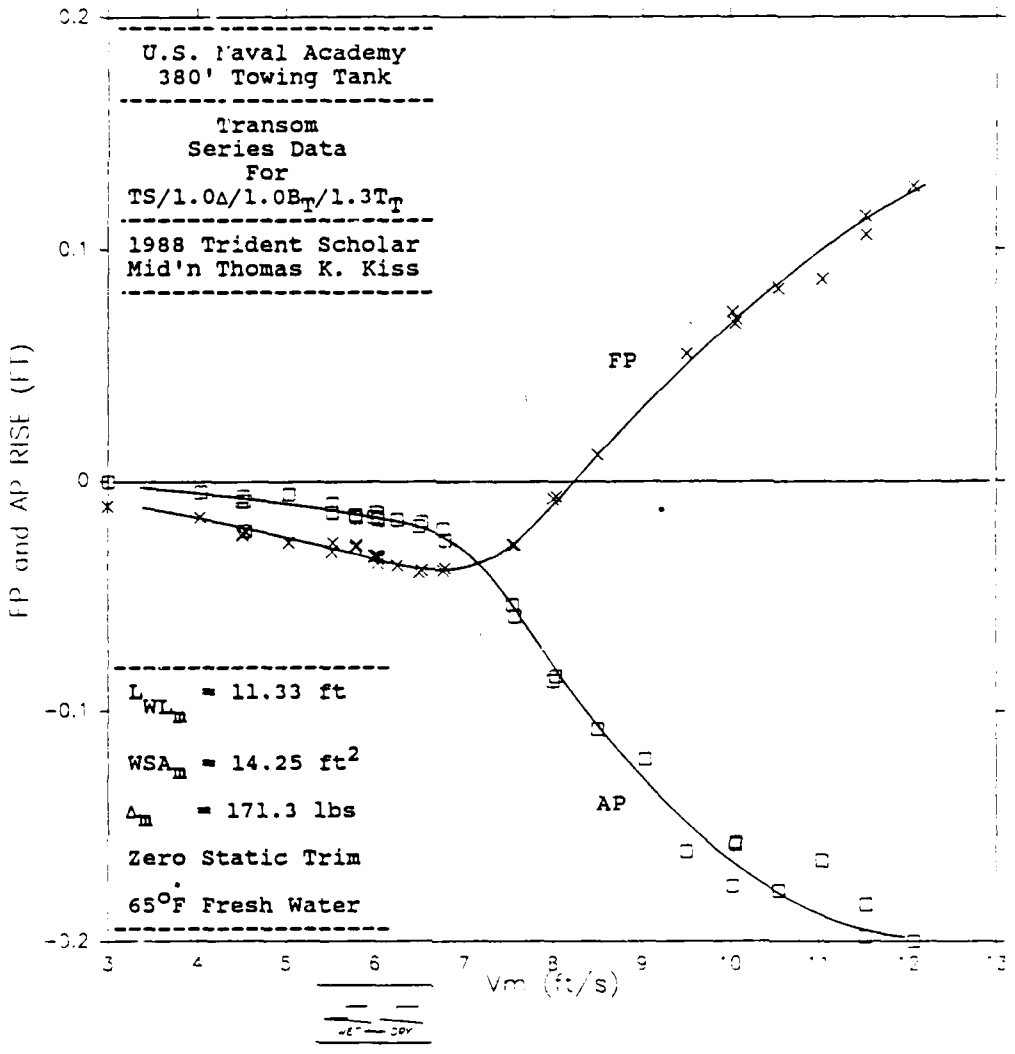
U.S. Naval Academy
380' Towing Tank
Transom
Series Data
For
TS/1.0Δ/1.0B_T/1.3T_T
1988 Trident Scholar
Mid'n Thomas K. Kiss
FP
AP
L_WLm = 11.33 ft
WSA_m = 14.25 ft²
Δ_m = 171.3 lbs
Zero Static Trim
65°F Fresh Water
FP and AP RISE (FT)
Vm (ft/s)
0.2
0.1
0
-0.1
-0.2
3
4
5
6
7
8
9
10
11
12
13

FIGURE A2

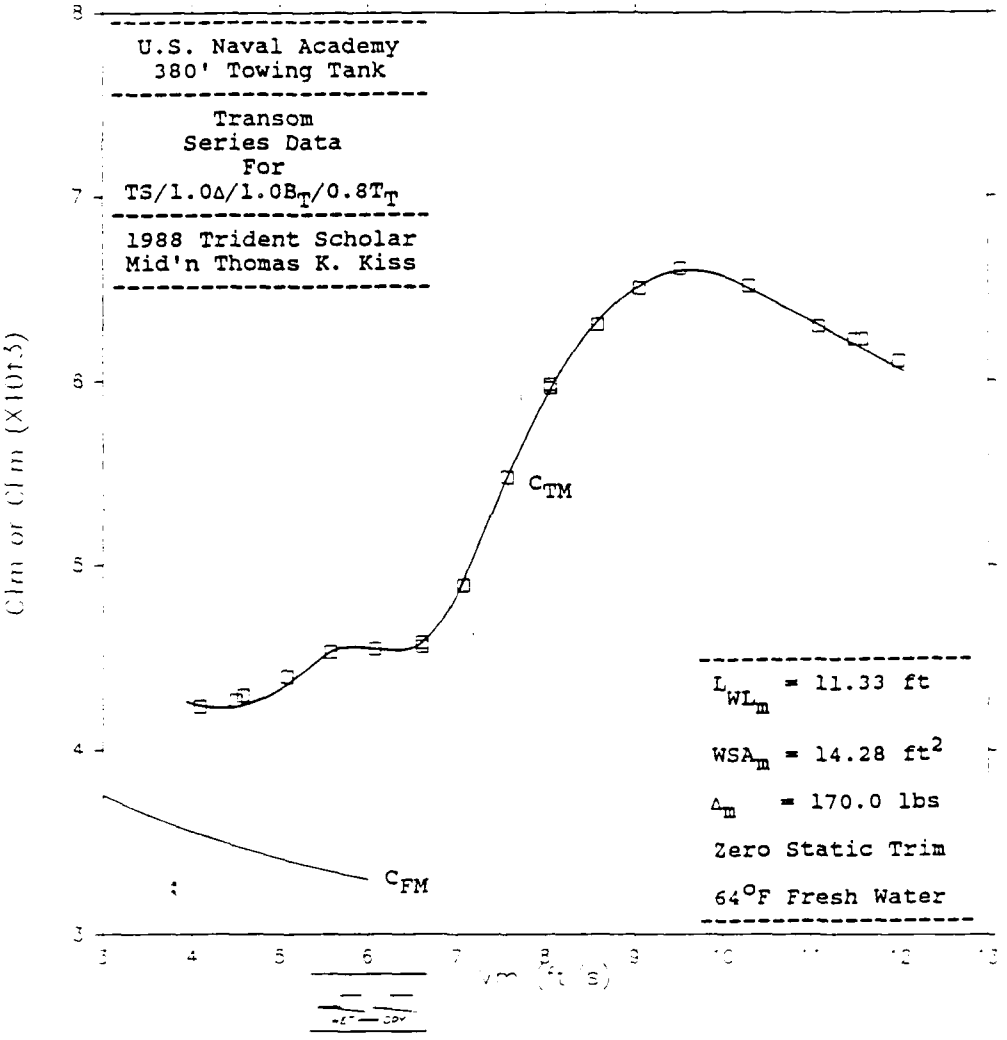
U.S. Naval Academy
380' Towing Tank
Transom
Series Data
For
TS/1.0Δ/1.0B_T/0.8T_T
1988 Trident Scholar
Mid'n Thomas K. Kiss
C_TM
C_FM
L_WLm = 11.33 ft
WSA_m = 14.28 ft²
Δ_m = 170.0 lbs
Zero Static Trim
64°F Fresh Water
Clm or Cfm (X10f3)
Vm (ft/s)

FIGURE A3

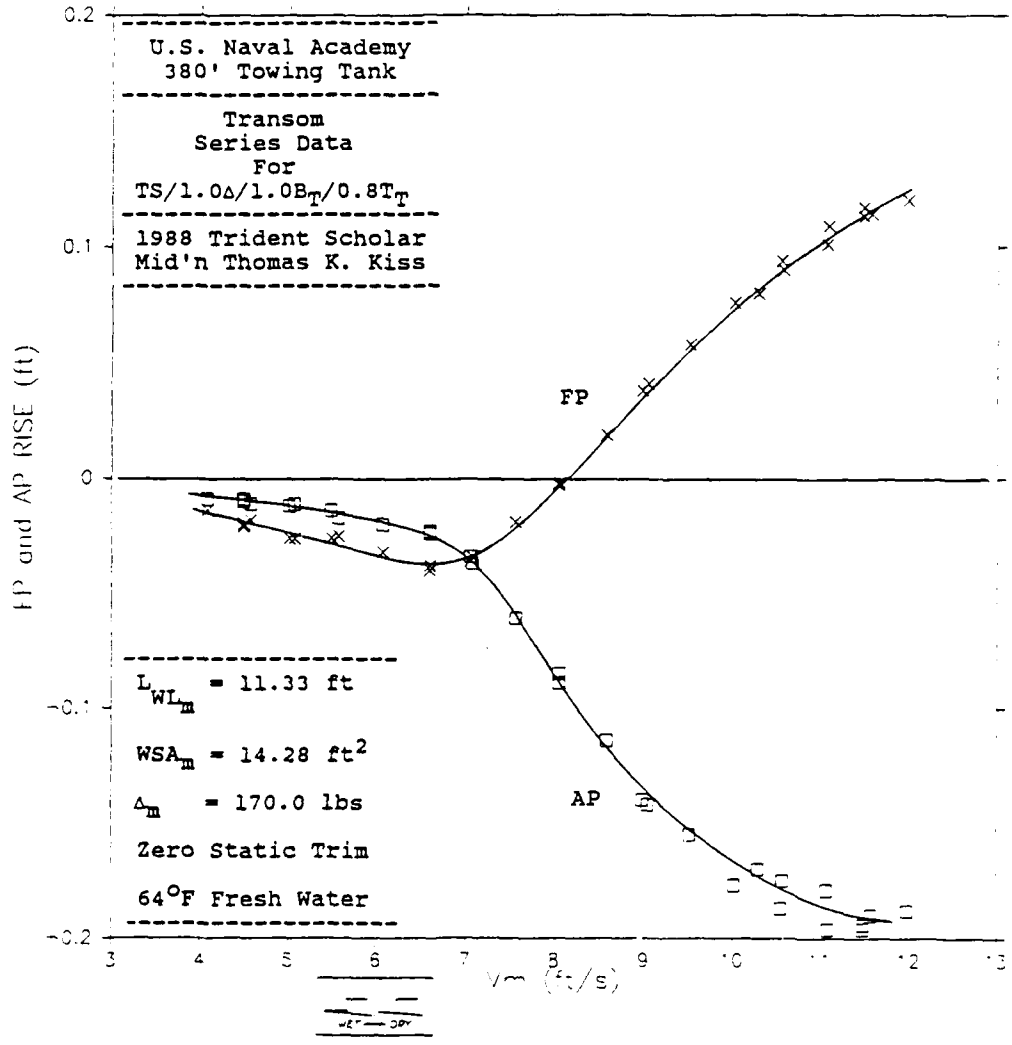
U.S. Naval Academy
380' Towing Tank
Transom
Series Data
For
TS/1.0Δ/1.0B_T/0.8T_T
1988 Trident Scholar
Mid'n Thomas K. Kiss
FP
AP
L_WL_m = 11.33 ft
WSA_m = 14.28 ft^2
Δ_m = 170.0 lbs
Zero Static Trim
64°F Fresh Water
FP and AP RISE (ft)
0.2
0.1
0
-0.1
-0.2
3
4
5
6
7
8
9
10
12
13

FIGURE A4

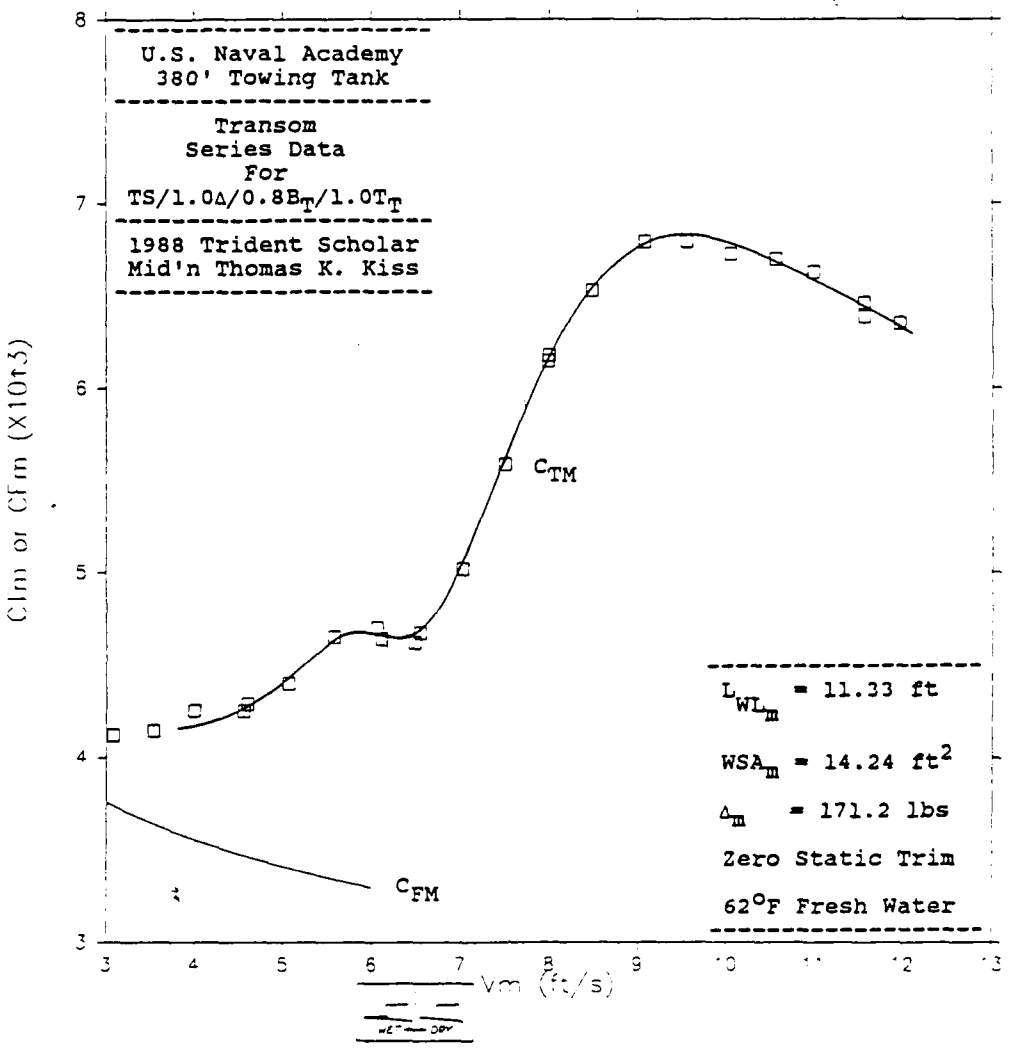
U.S. Naval Academy
380' Towing Tank
Transom
Series Data
For
TS/1.0Δ/0.8B_T/1.0T_T
1988 Trident Scholar
Mid'n Thomas K. Kiss
C_TM
C_FM
L_WLm = 11.33 ft
WSA_m = 14.24 ft²
Δ_m = 171.2 lbs
Zero Static Trim
62°F Fresh Water
Clm or Cfm (X10t3)
Vm (ft/s)
8
7
6
5
4
3
3
4
5
6
7
8
9
10
11
12
13

FIGURE A5

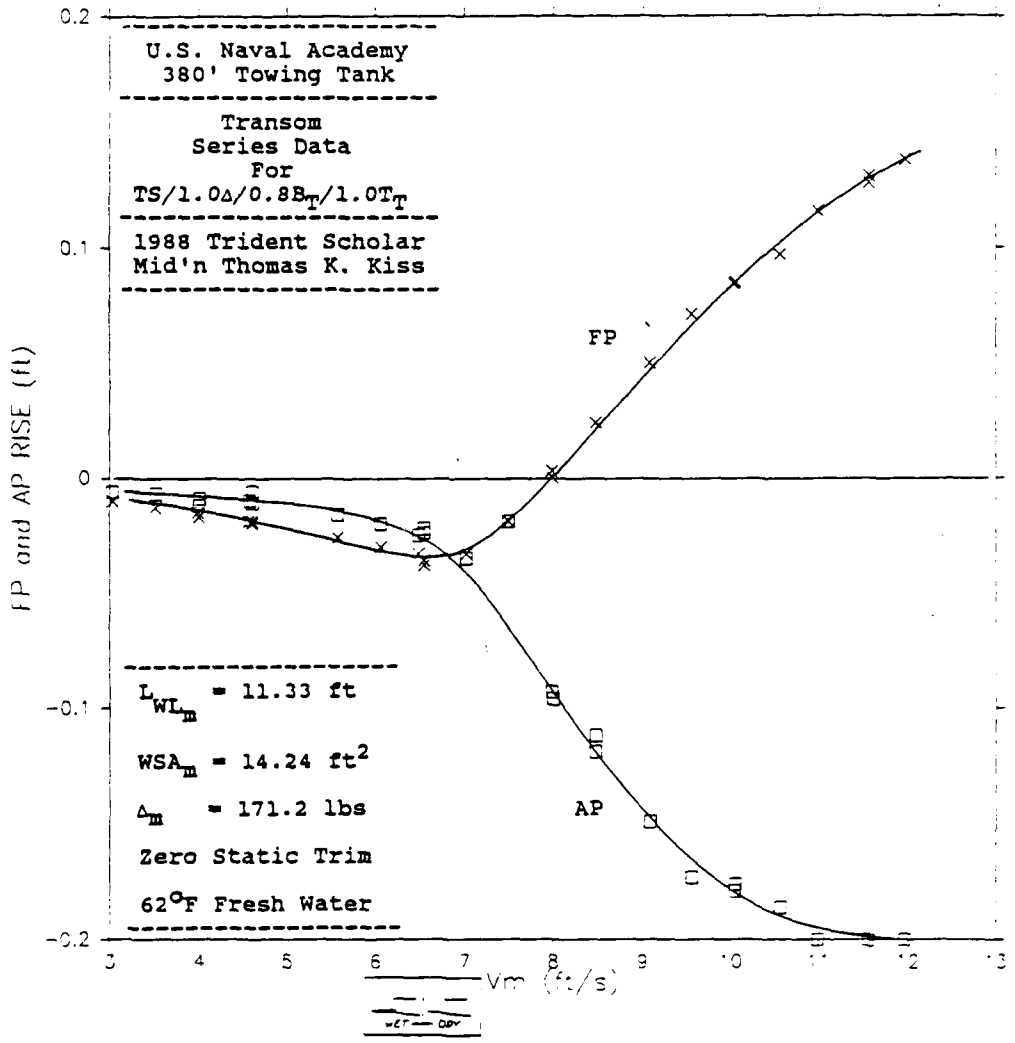
U.S. Naval Academy
380' Towing Tank
Transom
Series Data
For
TS/1.0Δ/0.8B_T/1.0T_T
1988 Trident Scholar
Mid'n Thomas K. Kiss
FP
AP
L_WL_m = 11.33 ft
WSA_m = 14.24 ft²
Δ_m = 171.2 lbs
Zero Static Trim
62°F Fresh Water
FP and AP RISE (ft)
Vm (ft/s)
0.2
0.1
0
-0.1
-0.2
3
4
5
6
7
8
9
10
11
12
13
WET
DRY

FIGURE A6

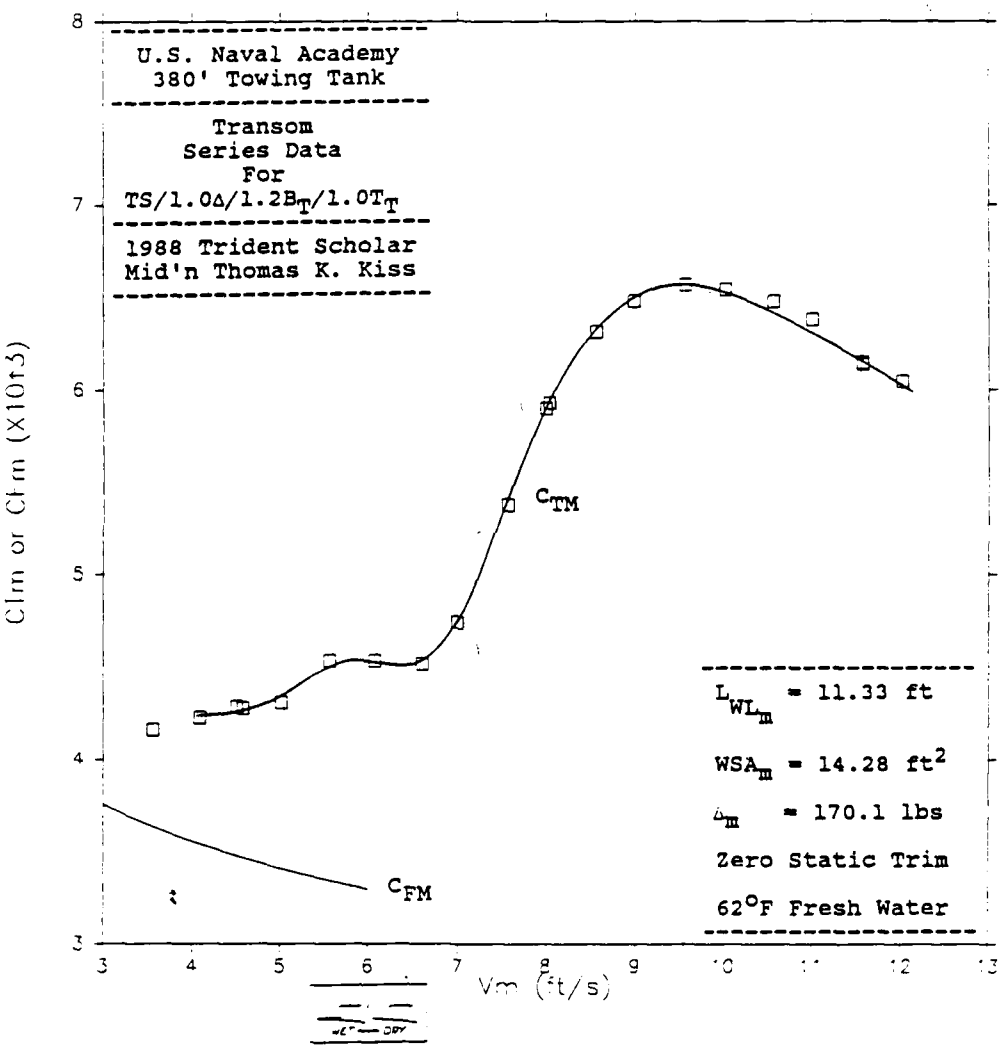
U.S. Naval Academy
380' Towing Tank
Transom
Series Data
For
TS/1.0Δ/1.2B_T/1.0T_T
1988 Trident Scholar
Mid'n Thomas K. Kiss
C_TM
C_FM
L_WLm = 11.33 ft
WSA_m = 14.28 ft²
Δ_m = 170.1 lbs
Zero Static Trim
62°F Fresh Water
Clm or Cfm (X10t3)
Vm (ft/s)
8
7
6
5
4
3
3
4
5
6
7
8
9
10
11
12
13

FIGURE A7

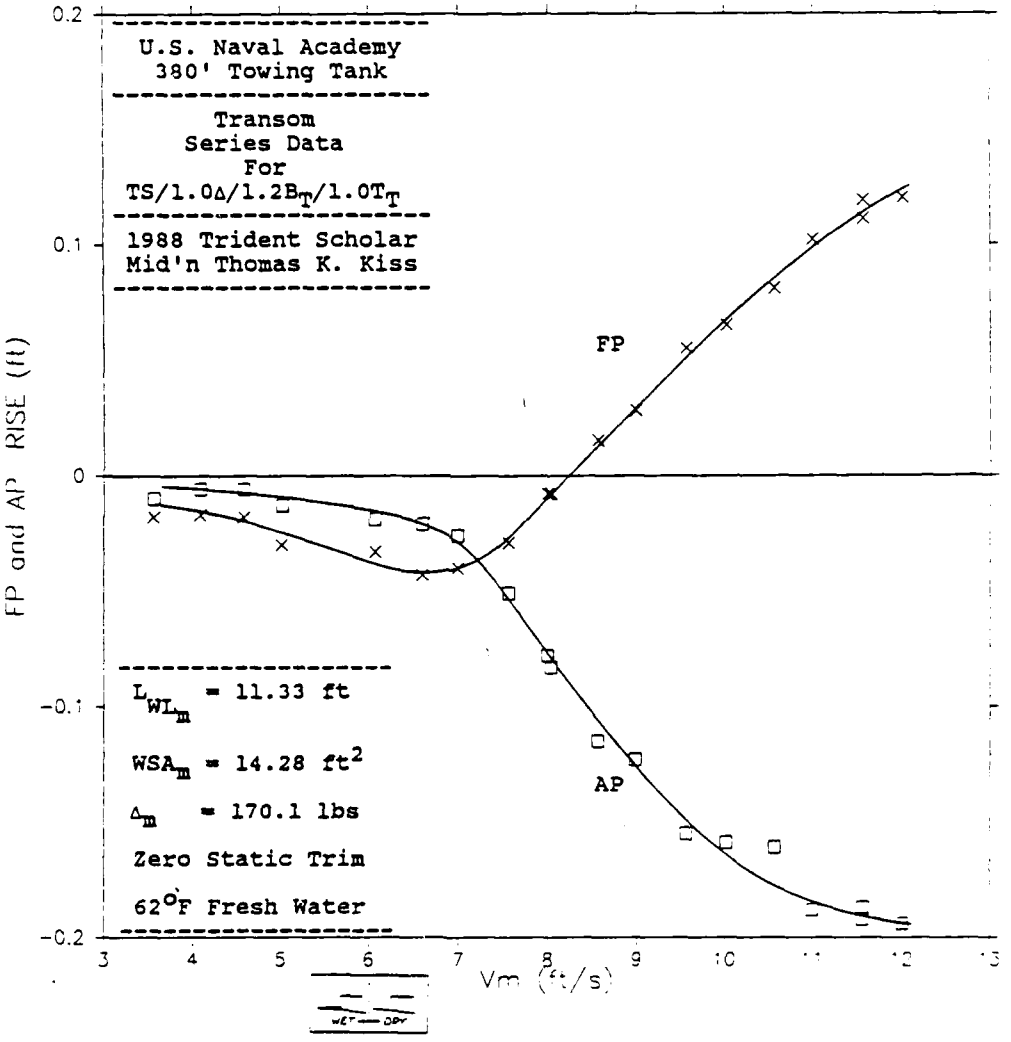
U.S. Naval Academy
380' Towing Tank
Transom
Series Data
For
TS/1.0Δ/1.2B_T/1.0T_T
1988 Trident Scholar
Mid'n Thomas K. Kiss
FP
AP
L_WL_m = 11.33 ft
WSA_m = 14.28 ft^2
Δ_m = 170.1 lbs
Zero Static Trim
62°F Fresh Water
FP and AP RISE (ft)
Vm (ft/s)
0.2
0.1
0
-0.1
-0.2
3
4
5
6
7
8
9
10
11
12
13
WET
DRY

FIGURE A8

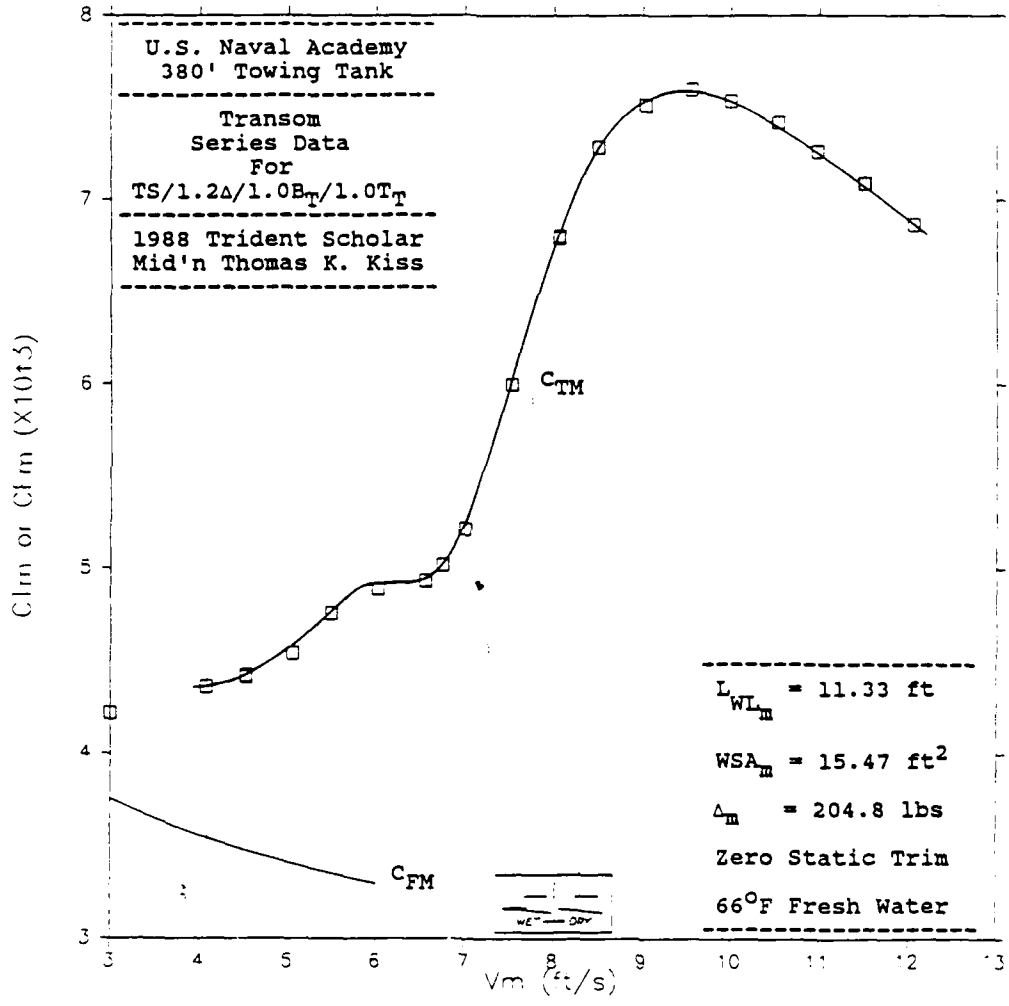
U.S. Naval Academy
380' Towing Tank
Transom
Series Data
For
TS/1.2Δ/1.0B_T/1.0T_T
1988 Trident Scholar
Mid'n Thomas K. Kiss
C_TM
C_FM
L_WL_m = 11.33 ft
WSA_m = 15.47 ft²
Δ_m = 204.8 lbs
Zero Static Trim
66°F Fresh Water
WET
DRY
Cfm or Ctm (X10t3)
Vm (ft/s)
8
7
6
5
4
3
3
4
5
6
7
8
9
10
11
12
13

FIGURE A9

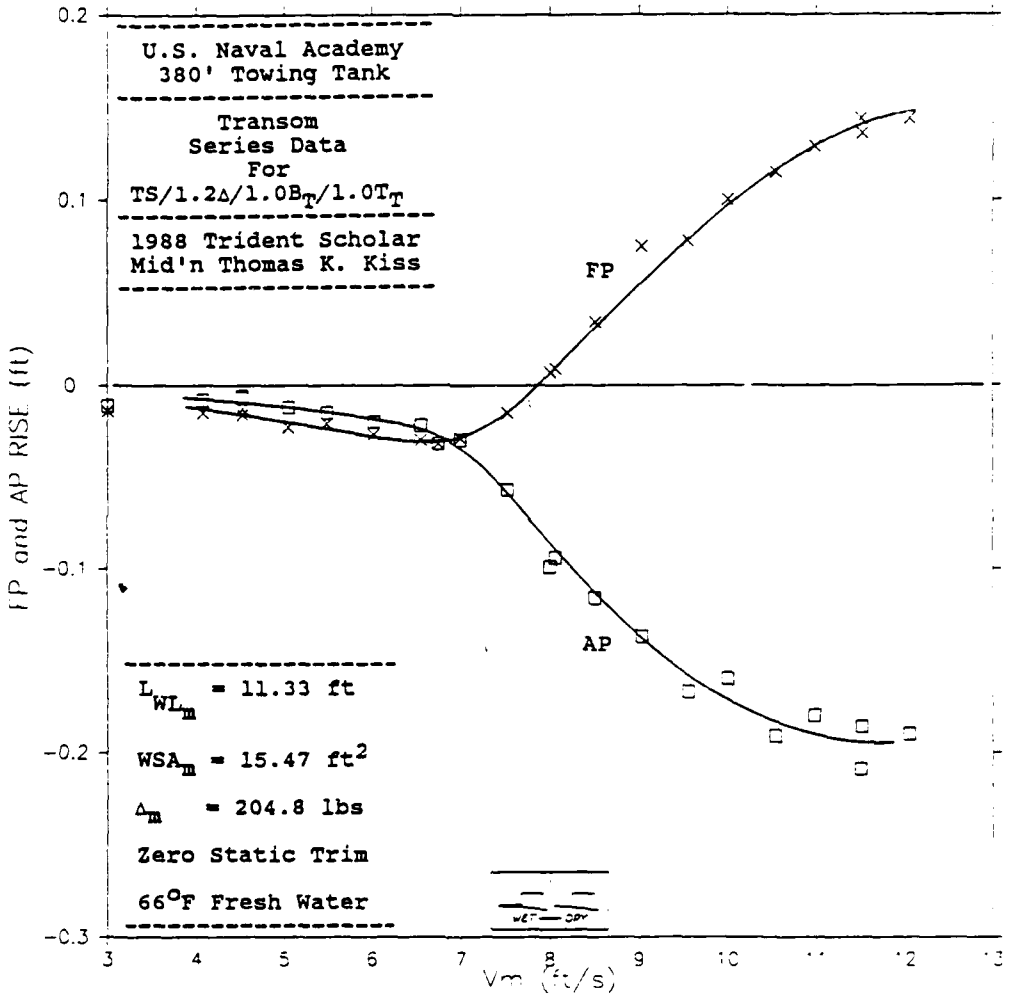
U.S. Naval Academy
380' Towing Tank
Transom
Series Data
For
TS/1.2Δ/1.0B_T/1.0T_T
1988 Trident Scholar
Mid'n Thomas K. Kiss
FP
AP
L_WLm = 11.33 ft
WSA_m = 15.47 ft²
Δ_m = 204.8 lbs
Zero Static Trim
66°F Fresh Water
FP and AP RISE (ft)
Vm (ft/s)
0.2
0.1
0
-0.1
-0.2
-0.3
3
4
5
6
7
8
9
10
11
12
13

FIGURE A10

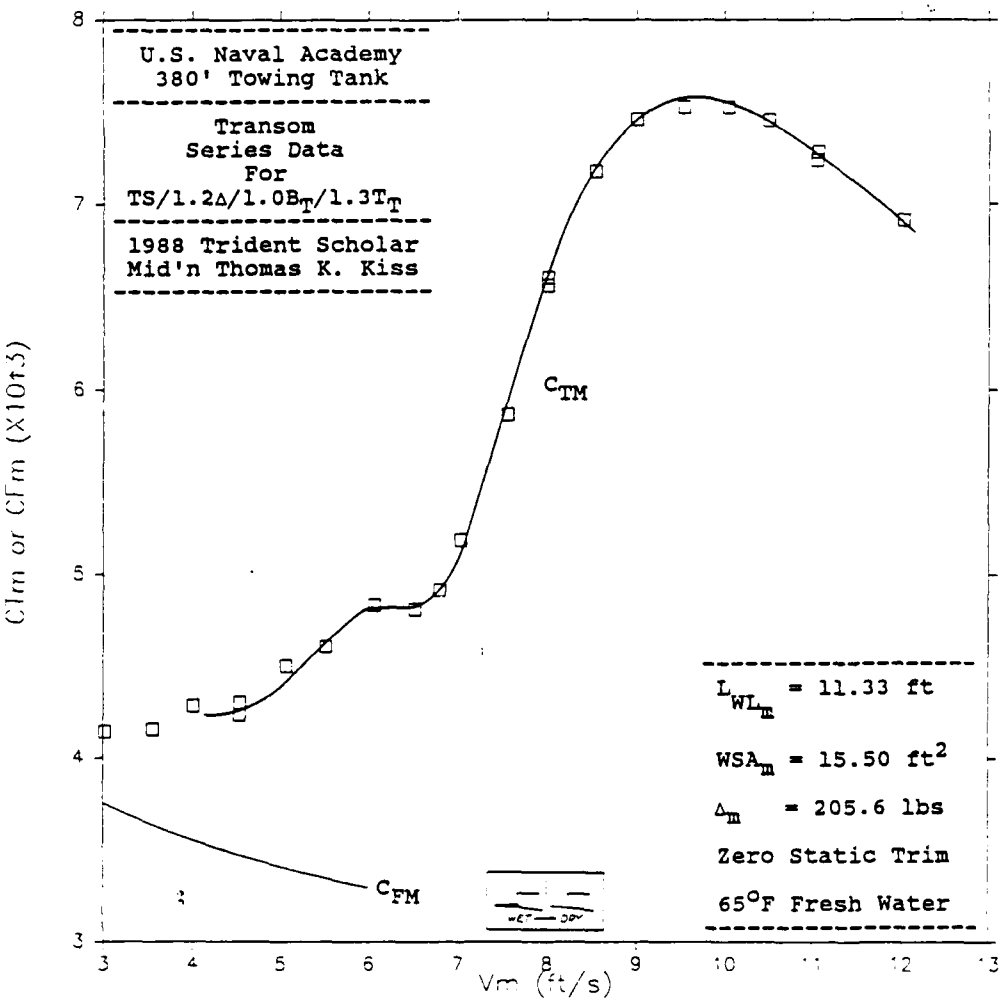
U.S. Naval Academy
380' Towing Tank
Transom
Series Data
For
TS/1.2Δ/1.0B_T/1.3T_T
1988 Trident Scholar
Mid'n Thomas K. Kiss
C_TM
C_FM
L_WL_m = 11.33 ft
WSA_m = 15.50 ft^2
Δ_m = 205.6 lbs
Zero Static Trim
65°F Fresh Water
Vm (ft/s)
3
4
5
6
7
8
9
10
11
12
13

FIGURE A11

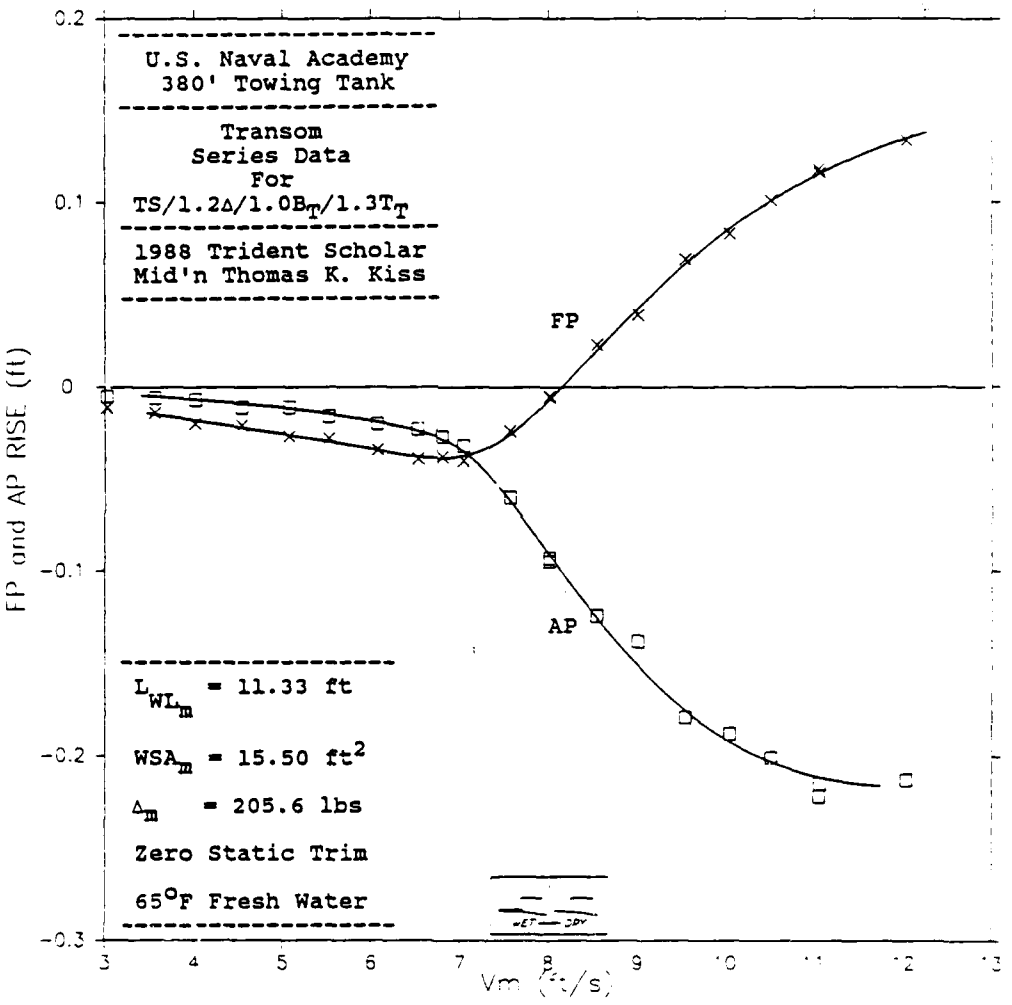
U.S. Naval Academy
380' Towing Tank
Transom
Series Data
For
TS/1.2Δ/1.0B_T/1.3T_T
1988 Trident Scholar
Mid'n Thomas K. Kiss
FP
AP
L_WL_m = 11.33 ft
WSA_m = 15.50 ft²
Δ_m = 205.6 lbs
Zero Static Trim
65°F Fresh Water
FP and AP RISE (ft)
Vm (ft/s)
0.2
0.1
0
-0.1
-0.2
-0.3
3
4
5
6
7
8
9
10
11
12
13

FIGURE A12

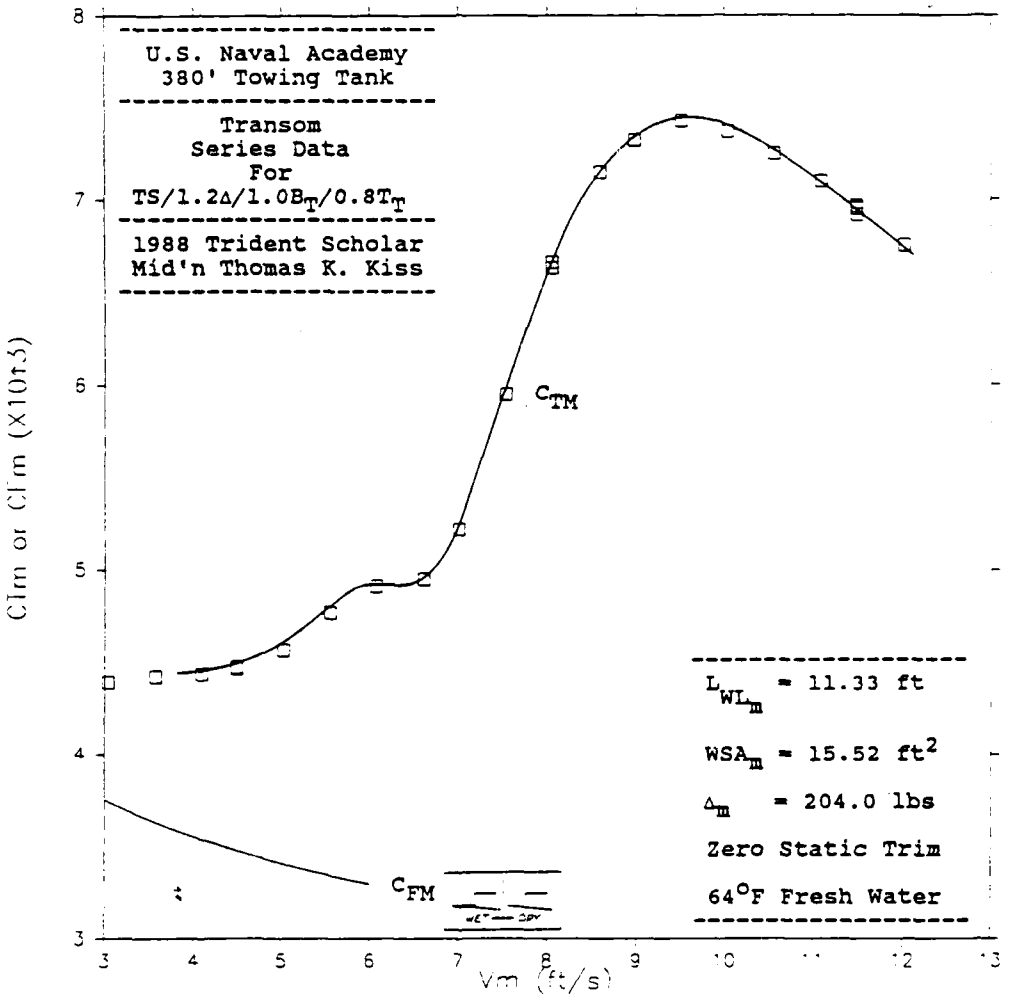
U.S. Naval Academy
380' Towing Tank
Transom
Series Data
For
TS/1.2Δ/1.0B_T/0.8T_T
1988 Trident Scholar
Mid'n Thomas K. Kiss
C_TM
C_FM
L_WL_m = 11.33 ft
WSA_m = 15.52 ft²
Δ_m = 204.0 lbs
Zero Static Trim
64°F Fresh Water
Clm or Clm (X10t3)
Vm (ft/s)
8
7
6
5
4
3
3
4
5
6
7
8
9
10
11
12
13

FIGURE A13

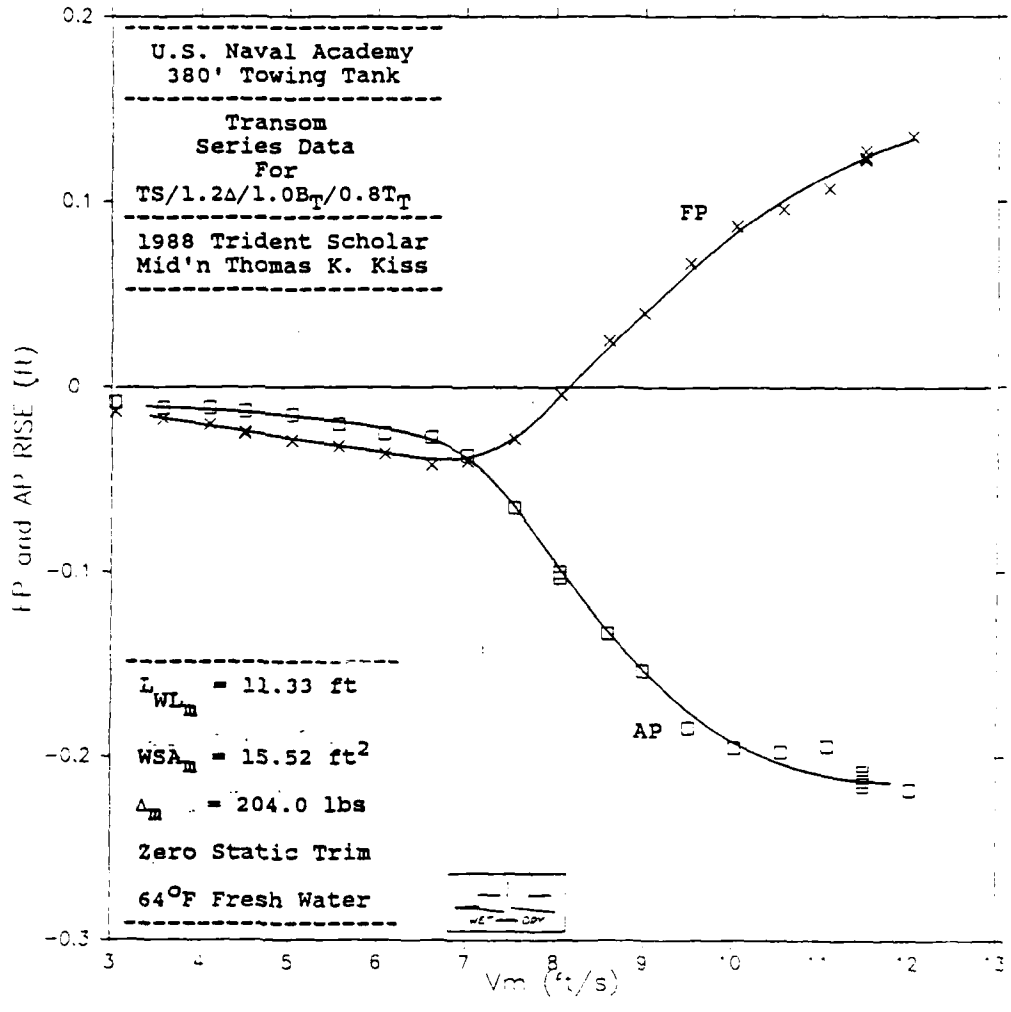
U.S. Naval Academy
380' Towing Tank
Transom
Series Data
For
TS/1.2Δ/1.0B_T/0.8T_T
1988 Trident Scholar
Mid'n Thomas K. Kiss
L_WL_m = 11.33 ft
WSA_m = 15.52 ft²
Δ_m = 204.0 lbs
Zero Static Trim
64°F Fresh Water
FP
AP
FP and AP RISE (ft)
Vm (ft/s)
0.2
0.1
0
-0.1
-0.2
-0.3
3
5
6
7
8
9

FIGURE A14

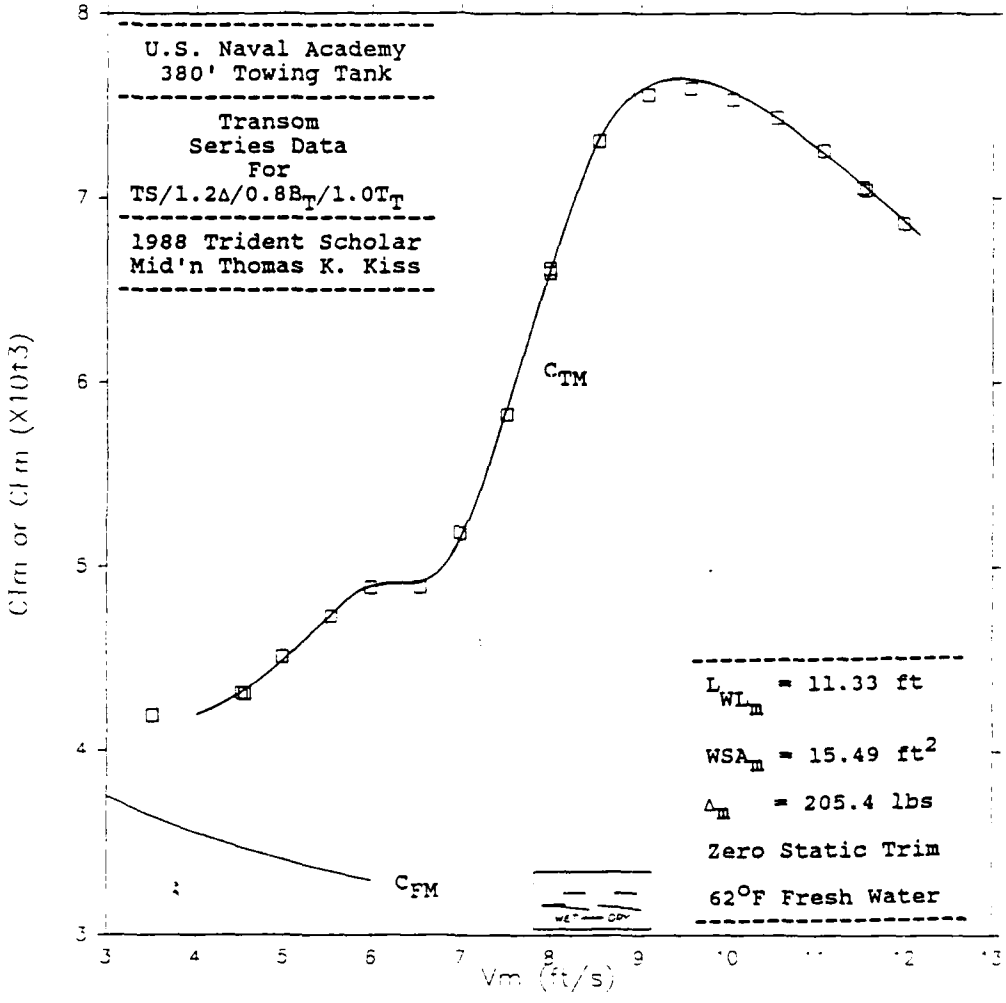
U.S. Naval Academy
380' Towing Tank
Transom
Series Data
For
TS/1.2Δ/0.8B_T/1.0T_T
1988 Trident Scholar
Mid'n Thomas K. Kiss
C_TM
C_FM
L_WL_m = 11.33 ft
WSA_m = 15.49 ft²
Δ_m = 205.4 lbs
Zero Static Trim
62°F Fresh Water
Clm or Cl m (X10t3)
Vm (ft/s)
8
7
6
5
4
3
3
4
5
6
7
8
9
10
12
13

FIGURE A15

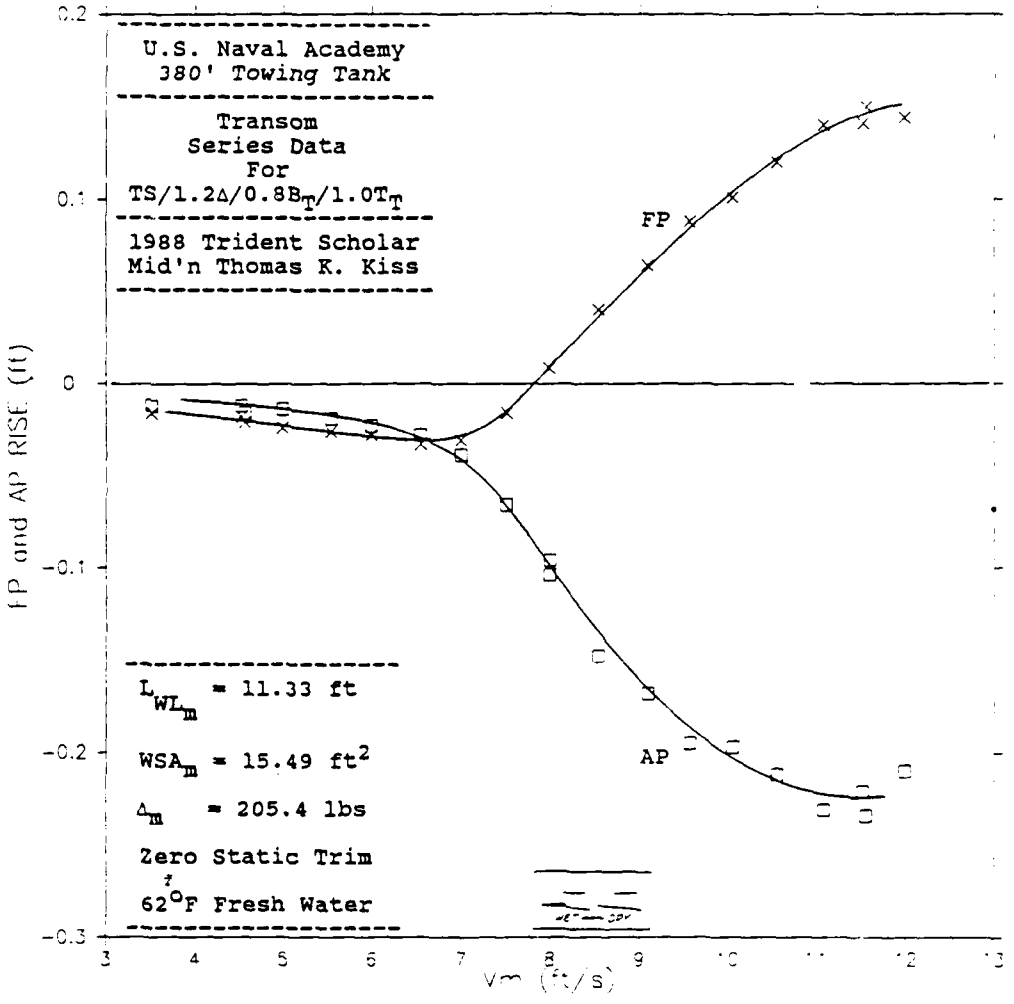
U.S. Naval Academy
380' Towing Tank
Transom
Series Data
For
TS/1.2Δ/0.8B_T/1.0T_T
1988 Trident Scholar
Mid'n Thomas K. Kiss
L_WLm = 11.33 ft
WSA_m = 15.49 ft²
Δ_m = 205.4 lbs
Zero Static Trim
62°F Fresh Water
FP
AP
FP and AP RISE (ft)
Vm (ft/s)
0.2
0.1
0
-0.1
-0.2
-0.3
3
4
5
6
7
8
9
10
11
12
13

FIGURE A16

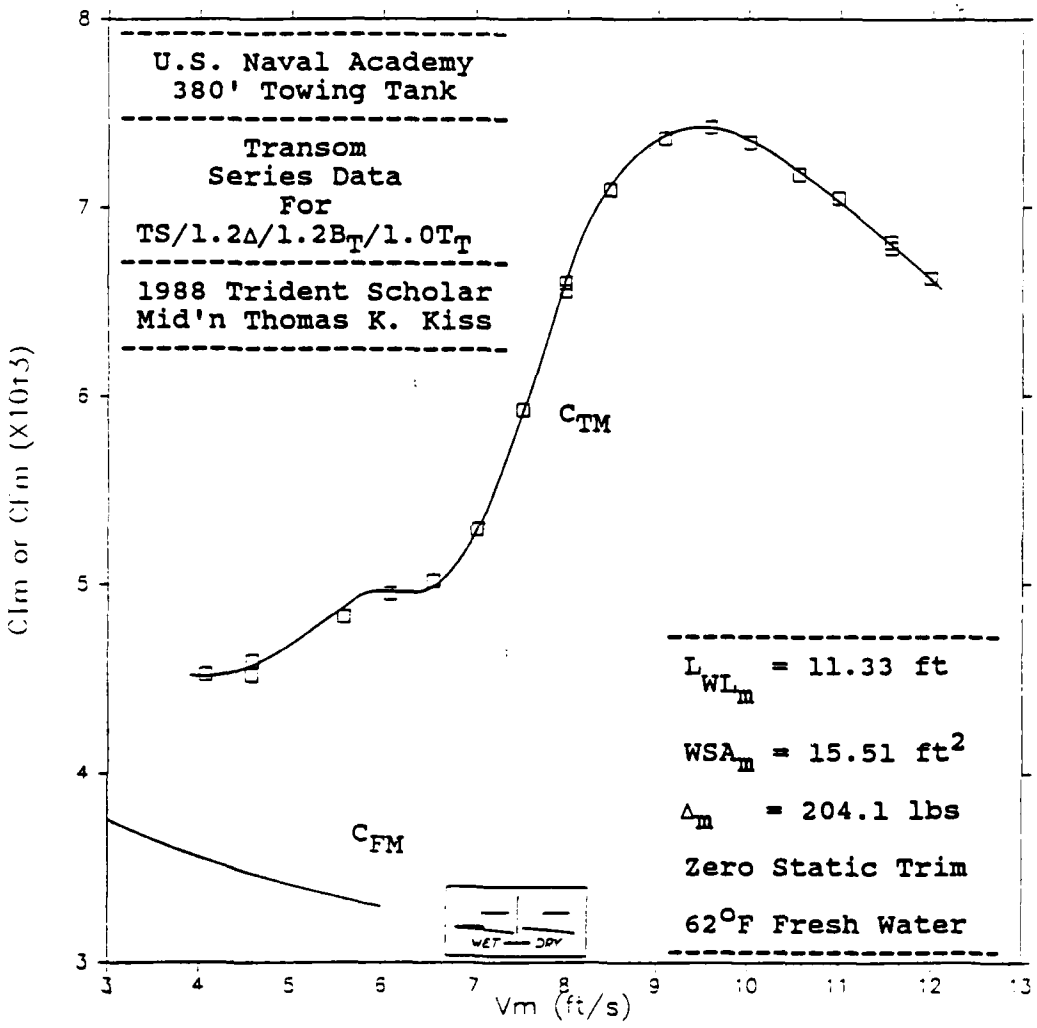
U.S. Naval Academy
380' Towing Tank
Transom
Series Data
For
TS/1.2Δ/1.2B_T/1.0T_T
1988 Trident Scholar
Mid'n Thomas K. Kiss
C_TM
C_FM
L_WL_m = 11.33 ft
WSA_m = 15.51 ft^2
Δ_m = 204.1 lbs
Zero Static Trim
62°F Fresh Water
WET
DRY
Clm or Cfm (X10t5)
Vm (ft/s)
8
7
6
5
4
3
3
4
5
6
7
8
9
10
11
12
13

FIGURE A17

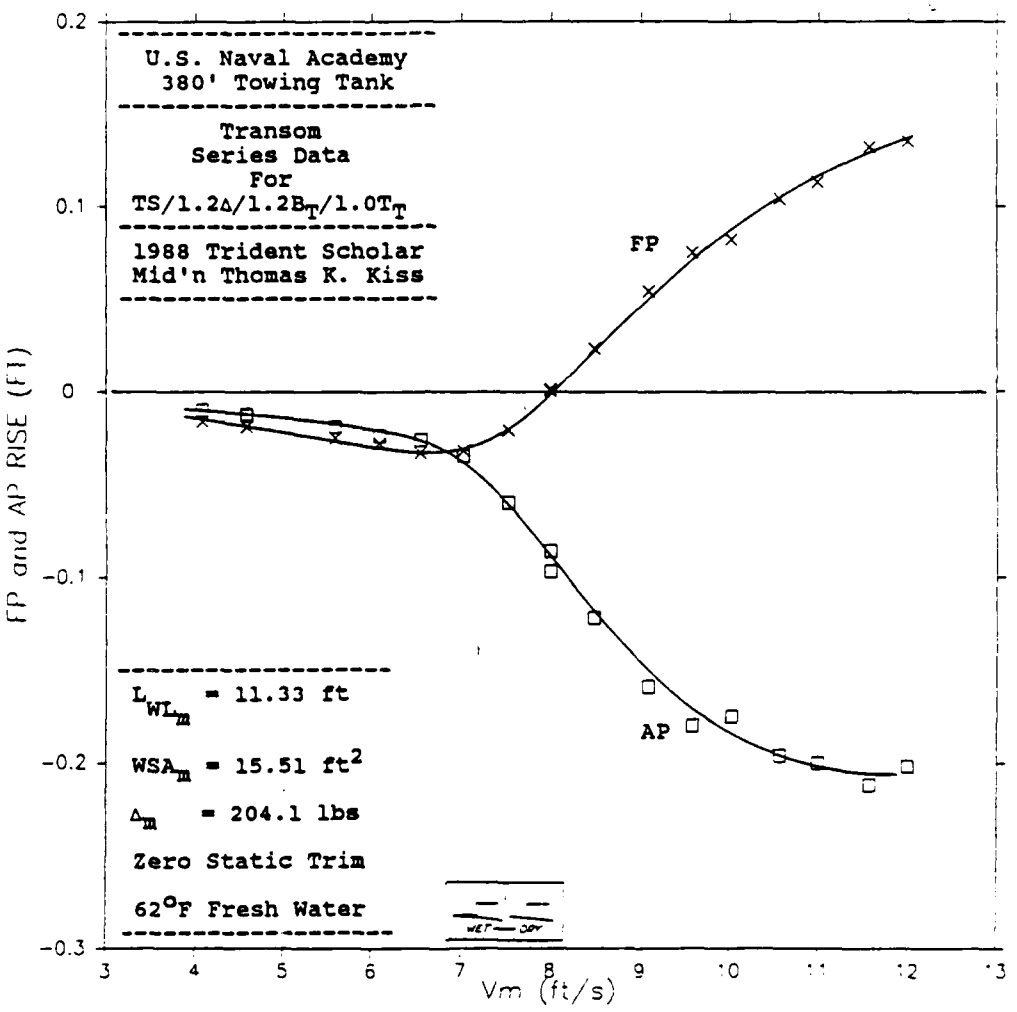
U.S. Naval Academy
380' Towing Tank
Transom
Series Data
For
TS/1.2Δ/1.2B_T/1.0T_T
1988 Trident Scholar
Mid'n Thomas K. Kiss
L_WL_m = 11.33 ft
WSA_m = 15.51 ft²
Δ_m = 204.1 lbs
Zero Static Trim
62°F Fresh Water
FP
AP
FP and AP RISE (FT)
Vm (ft/s)
0.2
0.1
0
-0.1
-0.2
-0.3
3
4
5
6
7
8
9
10
11
12
13

FIGURE A18

APPENDIX B

SAMPLE FLOW CODE RESULTS

```
   SSSSSSS     RRRRRRRR      PPPPPPPP     MM          MM
 SS            RR      RR    PP      PP   MMM        MMM
 SS            RR      RR    PP      PP   MMMM      MMMM
   SSSSSSS     RRRRRRRR      PPPPPPPP     MM MM    MM MM
         SS    RR    RR      PP           MM  MM MM  MM
         SS    RR     RR     PP           MM   MMM   MM
 SSSSSSSS      RR      RR    PP           MM    M    MM
```

SRPM - SHIP RESISTANCE PREDICTION METHOD
VERSION 1.10 - JANUARY 30, 1987

>>>>>>> RESISTANCE DATA PRINTOUT <<<<<<<<

Resistance run title :
FFG BASELINE TRANSOM
Today's date : Wed Jan 13 11:17:25 1988~H

----- USER-DEFINED RESISTANCE CALCULATION PARAMETERS -----

Ship Geometry data input file	=ffg1.pan
Units in the Geometry data file	=METRIC
Dynamic Sinkage and Trim data file	=ftrm.trm
Static (zero speed) sinkage	= .00000E+00 ,feet
Static (zero speed) trim angle	= .00000E+00 ,degrees
Residuary resist. calculation method	=CALC. FORM DRAG: CR = CW + CFD
Correlation Allowance	= .50000E-03

----- GEOMETRIC PROPERTIES FOR THE SPECIFIED STATIC SINKAGE AND TRIM -----

The following dimensions are in ENGLISH units

Maximum length	= .40858E+03	Waterline length	= .40858E+03
Maximum beam	= .45574E+02	Waterline beam	= .45574E+02
Maximum draft	= .15014E+02	Displaced volume	= .12641E+06
Wetted surface	= .18392E+05	Waterplane area	= .13316E+05
X-coordinate of FP	= -.19897E+02	LCF aft of FP	= .20458E+03
Longitudinal second moment of waterplane area			= .12948E+09

------- CALCULATED RESISTANCE AND POWERING DATA ------

Froude Number	Speed, knots	Speed, feet/sec	LWL, feet	CW	CR
.1768	12.000	20.268	.40889E+03	.32110E-03	.42156E-03
.2210	15.000	25.335	.40902E+03	.37260E-03	.47093E-03
.2504	17.000	28.713	.40917E+03	.34382E-03	.44100E-03
.2799	19.000	32.091	.40936E+03	.96558E-03	.10618E-02
.3094	21.000	35.469	.40954E+03	.80602E-03	.90131E-03
.3683	25.000	42.225	.40969E+03	.16311E-02	.17249E-02
.4272	29.000	48.981	.40866E+03	.31076E-02	.32002E-02
.5156	35.000	59.115	.40705E+03	.30247E-02	.31157E-02

Froude Number	Speed, knots	Speed, feet/sec	CF	CT	RW, pounds

.1768	12.000	20.268	.16036E-02	.25251E-02	.24145E+04
.2210	15.000	25.335	.15591E-02	.25300E-02	.43776E+04
.2504	17.000	28.713	.15349E-02	.24759E-02	.51885E+04
.2799	19.000	32.091	.15139E-02	.30757E-02	.18202E+05
.3094	21.000	35.469	.14954E-02	.28967E-02	.18561E+05
.3683	25.000	42.225	.14639E-02	.36888E-02	.53232E+05
.4272	29.000	48.981	.14379E-02	.51381E-02	.13647E+06
.5156	35.000	59.115	.14059E-02	.50217E-02	.19348E+06

Froude Number	Speed, knots	Speed, feet/sec	RR pounds	RF pounds	RT, pounds
.1768	12.000	20.268	.31698E+04	.12058E+05	.18987E+05
.2210	15.000	25.335	.55329E+04	.18317E+05	.29725E+05
.2504	17.000	28.713	.66550E+04	.23163E+05	.37364E+05
.2799	19.000	32.091	.20015E+05	.28538E+05	.57978E+05
.3094	21.000	35.469	.20755E+05	.34436E+05	.66705E+05
.3683	25.000	42.225	.56293E+05	.47776E+05	.12039E+06
.4272	29.000	48.981	.14053E+06	.63145E+05	.22564E+06
.5156	35.000	59.115	.19930E+06	.89932E+05	.32122E+06

Froude Number	Speed, knots	Speed, feet/sec	EHP, horsepower	V L**.5	RR DEL
.1768	12.000	20.268	.69969E+03	.59367E+00	.87705E+00
.2210	15.000	25.335	.13692E+04	.74209E+00	.15309E+01
.2504	17.000	28.713	.19506E+04	.84103E+00	.18414E+01
.2799	19.000	32.091	.33828E+04	.93998E+00	.55378E+01
.3094	21.000	35.469	.43017E+04	.10389E+01	.57427E+01
.3683	25.000	42.225	.92424E+04	.12368E+01	.15576E+02
.4272	29.000	48.981	.20094E+05	.14347E+01	.38884E+02
.5156	35.000	59.115	.34525E+05	.17315E+01	.55144E+02